

COMPREHENSIVE INVESTIGATION OF BIOACTIVE STEROIDAL ALKALOIDS
IN *VERATRUM CALIFORNICUM*

by

Matthew West Turner



A dissertation

submitted in partial fulfillment

of the requirements for the degree of

Doctor of Philosophy in Biomolecular Sciences

Boise State University

December 2019

© 2019

Matthew West Turner

ALL RIGHTS RESERVED

BOISE STATE UNIVERSITY GRADUATE COLLEGE

DEFENSE COMMITTEE AND FINAL READING APPROVALS

of the dissertation submitted by

Matthew West Turner

Dissertation Title: Comprehensive Investigation of Bioactive Steroidal Alkaloids in
Veratrum californicum

Date of Final Oral Examination: 01 October 2019

The following individuals read and discussed the dissertation submitted by student Matthew West Turner, and they evaluated the student's presentation and response to questions during the final oral examination. They found that the student passed the final oral examination.

Owen M. McDougal, Ph.D.	Chair, Supervisory Committee
Julia T. Oxford, Ph.D.	Member, Supervisory Committee
Daniel Fologea, Ph.D.	Member, Supervisory Committee
Xinzhu Pu, Ph.D.	Member, Supervisory Committee

The final reading approval of the dissertation was granted by Owen M. McDougal, Ph.D., Chair of the Supervisory Committee. The dissertation was approved by the Graduate College.

DEDICATION

This dissertation is dedicated to my beloved wife Lindsey, and to my daughter Matilda. Lindsey, thank you for your support, love, and encouragement. Matilda, you are my heart's darling.

ACKNOWLEDGMENTS

This work was made possible by the monumental effort put forth by those that came before me and those that worked with me to make the progress described in this dissertation. I wish to acknowledge the literature review, initial extraction methods, meticulously detailed record keeping, and plant harvest contribution made by Chris Chandler. Jared Mattos and Rob Cruz were instrumental to harvest plants and develop alkaloid extraction methods. Megan Rossi, Vannessa Campfield, Petr Malek, John French, Jordan Elwell, Ellie Hunt, Emily Wade, Nic Baughman, Jenny Fothergill, Anna Nielsen, Jessica Brookhouse, Ashton Bartlett, Katherine Ambrose, Susana Jiménez, and Drs. Ashley Fisher, Jeff Habig, Shin Pu, Matt King, and Joe Dumais provided the foundation upon which my work, progress, and achievement was made possible. I thank them for their time and effort that has resulted in six publications and has culminated with this dissertation. I would also like to acknowledge the valuable input provided by the members of my Supervisory Committee, Drs. Owen McDougal, Julia Oxford, Xinzhu Pu, and Daniel Fologea.

ABSTRACT

Veratrum californicum, commonly referred to as corn lily or Californian false hellebore, grows in high mountain meadows and produces bioactive steroidal alkaloids, including cyclopamine. Cyclopamine is a potent inhibitor of the Hedgehog (Hh) signaling pathway. Our lab has optimized methods to extract cyclopamine and related steroidal alkaloids from *V. californicum*, and implemented in-house Hh signaling bioactivity evaluation of these steroidal alkaloids using a Shh-Light II cell assay. A survey of extraction methods and solvents resulted in the identification of conditions most favorable for alkaloid extraction yield and antagonist activity in the Shh-Light II cell assay. The highest amount of bioactive cyclopamine was obtained by soaking *V. californicum* biomass in ethanol for 24 hr. with vigorous stirring. The extraction protocol was effective for isolating additional alkaloids beyond cyclopamine, some of which have been reported in the literature prior and some that have not. In all cases, bioactivity screening was performed and new insights provided. Expansion of the extraction protocol for the investigation of detailed differences in alkaloid composition of *V. californicum* based on plant part, harvest location, and growth stage, provides a detailed assessment of alkaloids that have been characterized previously (cyclopamine, veratramine, muldamine and isorubijervine), and identifies at least six alkaloids that have not been previously characterized.

TABLE OF CONTENTS

DEDICATION	iv
ACKNOWLEDGMENTS	v
ABSTRACT	vi
LIST OF TABLES	x
LIST OF FIGURES	xi
LIST OF PICTURES.....	xiii
LIST OF ABBREVIATIONS.....	xiv
CHAPTER ONE: INTRODUCTION	1
1.1 The Hedgehog Signaling Pathway	1
1.2 Teratogenic Alkaloids in <i>Veratrum californicum</i> and Elucidation of Their Molecular Mechanism.....	5
1.3 The Hedgehog Signaling Pathway and Cancer.....	9
1.4 Overview of the Genus <i>Veratrum</i> and Biological Activity of <i>Veratrum</i> Alkaloids	14
CHAPTER TWO: CYCLOPAMINE BIOACTIVITY BY EXTRACTION METHOD FROM <i>VERATRUM CALIFORNICUM</i>	19
2.1 Foreword.....	19
2.2 Abstract.....	19
2.3 Introduction.....	20
2.4 Materials and Methods	22
2.4.1 Extraction of Cyclopamine.....	22

2.4.2. Purification, Quantification, and Qualitative Analysis of Cyclopamine from Extracts	24
2.4.3. Biological Activity of Purified Extracts.....	26
2.5 Results and Discussion	27
2.6 Conclusion	37
CHAPTER THREE: NATIVE <i>V. CALIFORNICUM</i> ALKALOID COMBINATIONS INDUCE DIFFERENTIAL INHIBITION OF SONIC HEDGEHOG SIGNALING.....	
3.1 Foreword.....	39
3.2 Abstract.....	40
3.3 Introduction.....	40
3.4 Results.....	43
3.4.1 Qualitative Comparison of <i>V. californicum</i> Alkaloids by Plant Part	43
3.4.2 Quantitative Analysis of <i>V. californicum</i> Alkaloids.....	47
3.4.3 Bioactivity Evaluation of Combined Standards and Plant Extracts .	48
3.5 Discussion.....	51
3.6 Materials and Methods	54
3.6.1 Chemicals and Solvents	54
3.6.2 Sample Extraction and Preparation	54
3.6.3 Alkaloid Quantification.....	55
3.6.4 Alkaloid Identification	56
3.6.5 Cell Culture	57
3.6.6 Biological Assays	57
CHAPTER FOUR: STEROIDAL ALKALOID VARIATION IN <i>VERATRUM CALIFORNICUM</i> AS DETERMINED BY MODERN METHODS OF ANALYTICAL ANALYSIS.....	
	58

4.1	Foreword.....	58
4.2	Abstract.....	59
4.3	Introduction.....	59
4.4	Materials and Methods	63
	4.4.1 Materials.....	63
	4.4.2 Plant collection	64
	4.4.3 Biomass preparation	64
	4.4.4 Alkaloid extraction	64
	4.4.5 Alkaloid Quantification.....	65
	4.4.6 Alkaloid Identification	66
4.5	Results.....	67
	4.5.1 Root/rhizome alkaloid variation	70
	4.5.2 Aerial plant alkaloid variation.....	72
4.6	Discussion.....	72
4.7	Conclusion	76
	CHAPTER FIVE: PRELIMINARY DATA, FUTURE DIRECTIONS AND CONCLUSION	77
	REFERENCES.....	83

LIST OF TABLES

Table 1.	Comparison of extraction efficiency and corresponding bioactivity of cyclopamine. Recovery is reported as mg of alkaloid per g of biomass used.....	30
Table 2.	Alkaloid list extracted from <i>V. californicum</i> leaf, stem and root. Summary data of corresponding to the peaks identified in Figure 3.1 a-c.....	46
Table 3.	Quantification of cyclopamine, veratramine, muldamine and isorubijervine by plant part. Alkaloid quantities are reported as mg of alkaloid per g of plant biomass.....	47
Table 4.	Bioactivity treatment conditions for Shh-Light II cell assay.	49
Table 5.	Summary data corresponding to the peaks identified in Figure 4.1.....	68

LIST OF FIGURES

Figure 1.1	Reception of Hedgehog and initiation of signal transduction.....	3
Figure 1.2	Molecular structures of A) cyclopamine (11-deoxojervine) and B) jervine.. ..	7
Figure 1.3.	Cyclopamine binding to Smoothed receptor.	9
Figure 1.4.	Molecular structures of synthetic and natural Smo anatagonists.. ..	13
Figure 1.5.	Molecular skeletons of C-nor-D-homo and cyclopentanophenanthrene steroidal alkaloids.....	16
Figure 2.2.	Molecular structures of steroidal alkaloids present in <i>V. californicum</i>	29
Figure 2.3.	Direct comparison of MS and MS/MS of the acidic ethanol Soxhlet isolated product and veratramine standard.	31
Figure 2.4.	Effects of extract on Shh-stimulated Gli-responsive promoter in the Shh-Light II cell line.....	33
Figure 2.5.	Direct comparison of Shh-Light II cells treated with 1 μ M veratramine standard, compared to 1 μ M acid degraded product from acidic ethanol Soxhlet extraction.....	34
Figure 2.6.	Comparison of acidic ethanol Soxhlet extraction and supercritical fluid extraction spiked with cyclopamine standard.	36
Figure 2.7.	MS analysis of cyclopamine standards and collected from supercritical fluid extraction.	37
Figure 3.1.	Alkaloid chromatograms of <i>V. californicum</i> by plant part.. ..	44
Figure 3.2.	Mass spectra data showing the m/z, retention time and source for each alkaloid used to estimate molecular formulas listed in Table 2.....	45
Figure 3.3.	HPLC Comparison of ethanolic root extract with root standard mixture..	48

Figure 3.4.	Bioactivity data for cyclopamine alone, the alkaloid standard mixtures and the plant extracts at a) high concentration (0.5 μ M) and b) low concentration (0.1 μ M).....	50
Figure 4.1.	Chromatograms of alkaloids extracted from above-ground and below-ground <i>V. californicum</i> from two collection sites.....	67
Figure 4.2.	Quantification of alkaloids from both harvest sites for aerial and below ground <i>V. californicum</i>	69
Figure 4.3.	Mass spectra from the peaks identified from Figure 4.1 used to generate the data in Table 5.	70
Figure 5.1	Biological activity of individual steroidal alkaloids for Hh signaling inhibition.....	77
Figure 5.2.	Alkaloid chromatogram for biomass extracts from the root/rhizome of <i>V. californicum</i>	80
Figure 5.3.	Comparison of biological and chemical characteristics of cyclopamine and a potentially novel steroidal alkaloid.....	81

LIST OF PICTURES

- Picture 1. Graphical abstract for “Cycloamine bioactivity by extraction method from *Veratrum californicum*”19
- Picture 2. Graphical abstract for “Native *V. californicum* alkaloid combinations induce differential inhibition of Sonic hedgehog signaling”39
- Picture 3. Graphical abstract form “Steroidal alkaloid variation in *Veratrum californicum* as determined by modern methods of analytical analysis” ..58

LIST OF ABBREVIATIONS

Hh	Hedgehog
Shh	Sonic Hedgehog
Ihh	Indian Hedgehog
Dhh	Desert Hedgehog
Ptch	Patched
Smo	Smoothed
Gli	Glioma-associated oncogene
SUFU	Suppressor of fused homolog
MMP	Matrix metalloproteinase
BCC	Basal cell carcinoma
R _t	Retention Time
MS	Mass spectrometry
HPLC	High performance liquid chromatography
NMR	Nuclear magnetic resonance
CD	Circular dichroism
HSQC	Heteronuclear single quantum coherence
HMBC	Heteronuclear multiple bond correlation

CHAPTER ONE: INTRODUCTION

1.1 The Hedgehog Signaling Pathway

Christiane Nusslein-Volhard and Eric Wieschaus first identified the Hedgehog (Hh) signaling pathway during an investigation to survey genes that disrupt the larval body plan in *Drosophila*. The name hedgehog was ascribed based on the appearance of embryos with *Hh* mutations displaying disorganized, pointy, hair-like bristles similar to hedgehog spines [1]. Later, the *Drosophila Hh* gene was discovered to code for a secreted protein that directs pattern formation of adjacent cells [2-4]. The Hh signaling pathway is critical in embryonic development, and is essential for orchestrating cell specification and cell division required to form a functional organism [5,6]. Hh signaling is evolutionarily conserved, and in mammals is vital for the formation of various tissues including the neural tube, axial bone, hair, and teeth [7-9]. Hh signaling is inhibited in most adult tissues, but continues in discrete populations of cells within many adult mammalian tissues, presumably to control proliferation, specification, and cellular plasticity [10]. Continued Hh signaling activity in adults has been demonstrated in various organs, including the brain, skin, and prostate [11-13]. Additionally, Hh signaling plays a role in the proliferation and differentiation of germline stem cells in the gonads [14].

In mammals, the Hh signaling pathway consists of the secreted ligands Sonic hedgehog (Shh), Desert hedgehog (Dhh) and Indian hedgehog (Ihh); the 12-pass transmembrane protein receptor Patched (Ptch), the 7-pass transmembrane signal transducer Smoothed (Smo), and the Gli transcription factors (Gli1, Gli2, Gli3) [15].

Although the Hh ligand proteins all act as morphogens and have similar physiological effects, each Hh ligand performs specialized functions due to the spatial and temporal differences in their expression [16]. Shh is mostly expressed in the central nervous system, lungs, teeth, gut, and hair follicles [17-21]. Ihh is a key regulator of endochondral ossification and is expressed and secreted by prehypertrophic and early hypertrophic chondrocytes during bone formation [22]. Dhh is expressed mostly in the Sertoli cells in the gonads to aid in the proliferation and differentiation of germline stem cells [23]. The Hh ligand proteins are synthesized as precursors of about 45 kDa, that undergo extensive post-translational modifications, including self-cleavage in the endoplasmic reticulum, conjugation of cholesterol to the C-terminus, and N-terminal palmitoylation, after which they are released by the secreting cell and operate in paracrine or autocrine manner [10,24]. Both the palmitoylation and cholesterol modification limit the free mobility of the protein and result in association of Hh with sterol-rich microdomains in the membrane [25,26]. Once at the outer surface of the plasma membrane, dually lipid-modified Hh ligand is associated with the lipid bilayer as a monomer until it is released by one of four mechanisms: 1) The cholesterol-modified Hh monomer is released by the cooperative action of the transmembrane protein Dispatched and the secreted SCUBE2 protein 2) monomeric Hh can also self-associate to form large soluble multimers that are released from the membrane, 3) Hh oligomers can interact with the heparan sulphate chains of glypicans, which enables them to recruit lipophorin apolipoproteins and assemble into lipoprotein particles, or 4) Hh may be released at the surface of exovesicles [27].

In the absence of Hh ligands, Ptch prevents the translocation of Smo to the primary cilia, thereby inhibiting the nuclear localization of Gli and suppressing transcriptional activity. The exact mechanism of Ptch repression of Smo activity remains

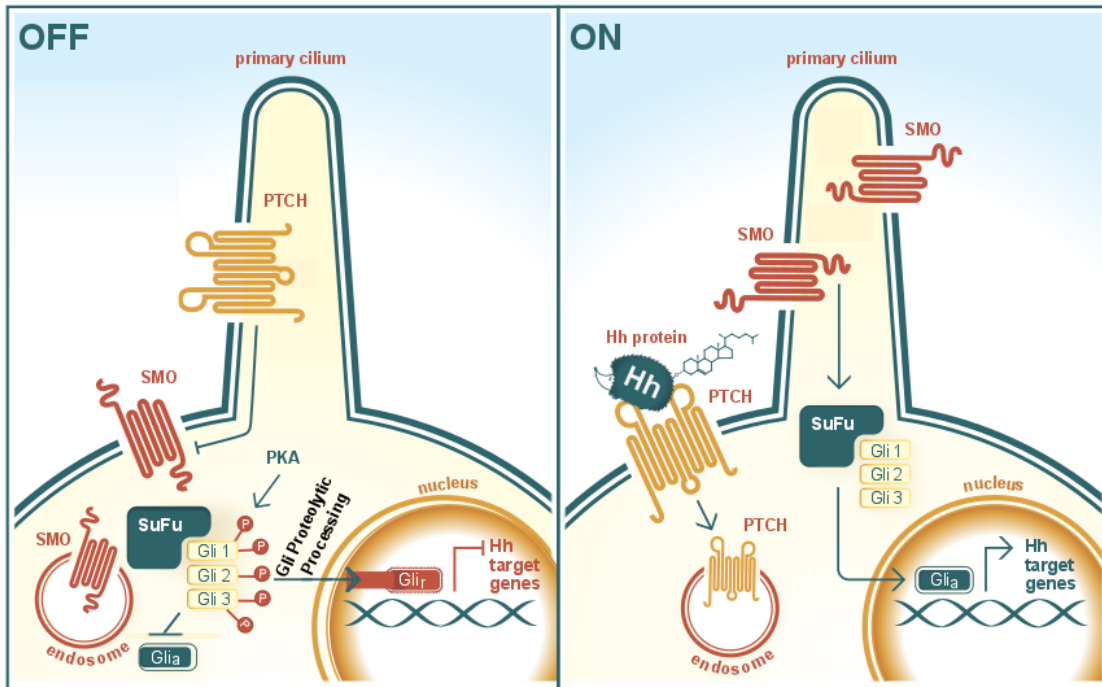


Figure 1.1 Reception of Hedgehog and initiation of signal transduction. In the “off” state, Ptch is enriched in the primary cilium where it inhibits Smo. In the absence of Hh, the GLI proteins are phosphorylated by PKA, leading to their proteolytic cleavage to generate the repressor forms. In the presence of Hh, Ptch exits the cilium. Smo is phosphorylated and transported to the cilium, where the activated Smo is anchored near the base of the cilium. The SuFu/Gli complex accumulates at the tip of the cilium, where the complex dissociates. Upon exiting the cilia, activated Gli proteins enter the nucleus to promote the transcription Hh target genes.

unclear. Upon binding of Hh ligands to Ptch, Smo suppression is abolished and downstream pathway activity proceeds, resulting in nuclear translocation and activation of Gli. More specifically, when a Hh ligand binds to Ptch, the inhibition of Smo is relieved, which disrupts the stability of the suppressor of fused (SuFu), kinesin family member 7 (Kif7), and Gli complex, resulting in the release and nuclear localization of the

Gli transcription factors [14]. In this process downstream of Smo inhibition alleviation, the Gli transcription factors mediate the Hh signal transduction. This canonical activation of Gli is depicted in **Figure 1.1**. The Gli transcription factors are bifunctional, and can activate or inhibit transcription [27]. In the absence of Hh ligand, Gli2 and Gli3 are phosphorylated by protein kinase A (PKA), glycogen synthase kinase 3 (GSK3), and casein kinase 1 (CK1), and undergo limited proteasomal degradation in which their C-terminal activator domain is cleaved by beta-transducin repeat containing protein (β -TRCP), which leads to the conversion into transcriptional repressors, entering the nucleus and repressing Hh target genes. In the canonical Hh signaling pathway, Gli transcriptional activators are formed only in response to Hh stimulation. Therefore, Hh signaling functions through modulating the balance between Gli repressors and activators. The cellular response of this repressor/activator ratio is diverse and context dependent, with different tissues displaying differential expression patterns of target genes in response to Hh ligands [28]. Additionally, some Hh signaling target genes require positive input from Gli activators to initiate transcription, while others are activated simply by removing the Gli repressor protein from the enhancer. Gli activators bind to GACCACCCA motif to regulate transcription of various genes, including *GLII*, *PTCH1*, *PTCH2*, *MYCN*, *HHIP1*, *CCND1*, *CCND2*, *BCL2*, *CFLAR*, *FOXF1*, *FOXL1*, *PRDM1*, *JAG2*, *GREM1*, and *FST* [29]. Hh signals are fine-tuned based on positive feedback loop via *GLII* and negative feedback loop via *PTCH1*, *PTCH2*, and *HHIP1*. Excessive positive feedback or collapsed negative feedback of Hh signaling due to epigenetic or genetic alterations leads to carcinogenesis. Hh signals induce cellular proliferation through upregulation of N-Myc, Cyclin D/E, and FOXM1. Hedgehog

signals directly upregulate *JAG2*, indirectly upregulate mesenchymal *BMP4* via *FOXF1* or *FOXL1*, and also upregulate *WNT2B* and *WNT5A*. Hedgehog signals induce stem cell markers *BMI1*, *LGR5*, *CD44*, and *CD133*, based on cross-talk with WNT and/or other signals. Hh signals upregulate *BCL2* and *CFLAR* to promote cellular survival, *SNAI1* (Snail), *SNAI2* (Slug), *ZEB1*, *ZEB2*, *TWIST2*, and *FOXC2* to promote epithelial-to-mesenchymal transition, and *PTH1H* (PTHrP) to promote osteolytic bone metastasis.

1.2 Teratogenic Alkaloids in *Veratrum californicum* and Elucidation of Their Molecular Mechanism

During the 1940's and 50's, sheep herders in southwestern and south-central Idaho observed that ewes that grazed in alpine ranges during summer months gave birth to lambs with a variety of craniofacial deformities. These deformities included cyclopia, a domed cranium, cleft palate, shortening of the upper jaw, malformation of the nose into a proboscis positioned above the eye, hydrocephalus, and holoprosencephaly, or the failure of the forebrain to sufficiently divide into the double lobes of the cerebral hemispheres, resulting in a single-lobed brain structure [30]. In 1954, sheep herders in Idaho contacted scientists at the Poisonous Plant Research Laboratory in Logan, UT, to request assistance in identifying the cause of the malformed lambs [30-32]. Controlled breeding experiments eliminated the possibility that the congenital anomaly was caused by genetic factors and potential environmental elements or the presence of poisonous plants were assumed to underlie the developmental anomalies. Field studies determined that deformities occurred in lambs from ewes that grazed in meadows above 6,000 feet in elevation, where *Veratrum californicum* is commonly observed to grow [30]. Controlled

feeding trials of *V. californicum* in sheep reproduced the deformities observed in the field and definitively validated the teratogenic role of *V. californicum* [33]. Efforts led by researchers Richard Keeler and Wayne Binns focused on *Veratrum* alkaloids as the causative agent, and they began to methodically test crude alkaloid fractions obtained from ethanol and benzene soaks of *V. californicum* for their teratogenic potential. Hydrophilic cevanine alkaloids were ruled out as the causative agent, and eventually Keeler and Binns narrowed their search to fractions containing an unidentified glycoside and alkamine, which they referred to as alkaloid X and alkaloid V, respectively [34,35]. Chemical investigation revealed alkaloid V to be 11-deoxojervine, first isolated by Masamune et al. from *V. grandiflorum* in 1965, while alkaloid X was determined to be its C-3 glycoside (see **Figure 1.2**) [36]. Keeler gave these compounds the trivial names cyclopamine and cycloposine because of their teratogenic manifestation [37,38]. Definitive feeding trials in both sheep and rabbits with purified alkaloids established that cyclopamine and cycloposine are responsible for the cyclopean-malformations [39,40]. Later, malformations in the heads of chicken embryos following exposure to cyclopamine and jervine demonstrated teratogenic activity in non-mammalian vertebrates [41].

To gain a mechanistic understanding of how the key chemical features that governed molecular teratogenicity of these compounds interfere with proper embryonic development, derivative compounds and structurally related alkaloids were investigated. For these studies, hamster models were used to limit the amount of material needed. Alkylation of the nitrogen with a bulky moiety, such as N-butyl in jervine significantly reduced the teratogenicity, whereas methylation and formylation retained the teratogenicity of the alkaloid,

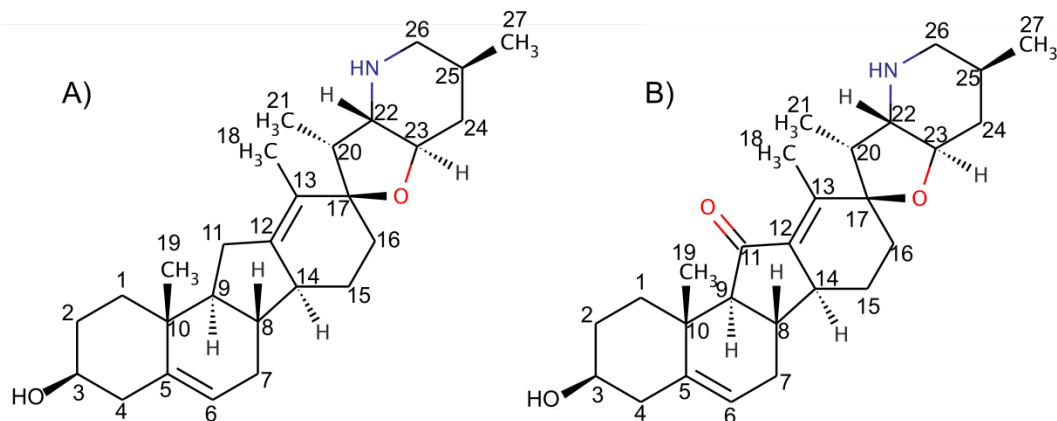


Figure 1.2 Molecular structures of A) cyclopamine (11-deoxojervine) and B) jervine. Structures of teratogenic steroidal alkaloids with atomic numbering system shown. For A), replacement of the hydroxyl group attached to C3 with glucosyl corresponds to cycloposine.

indicating that the steric and electrostatic state of the nitrogen atom is critical for functionality [42]. Additionally, acylation or oxidation of the hydroxyl group in jervine did not diminish biological activity, nor did hydrogenation of the C12-C13 double bond. Following these structure-activity studies, investigators hypothesized the mechanism of action to be interference of steroid hormone signaling in the developing embryo. This was a logical conclusion based on structural similarities between steroid hormones, and the C-nor-D-homosteroids to which cyclopamine and jervine belong. C-nor-D-homosteroids possess a steroid skeleton with an unusual 6-6-5-6 ring pattern, rather than cyclopentanophenanthrene skeleton which contains a 6-6-6-5 ring system characteristic of steroid hormones (see **Figure 1.5**). It would take several decades, and advances in other research fields to finally elucidate the enigmatic mechanism of these teratogenic compounds.

With the discovery of *Hh* in *Drosophila* by Nüsslein-Volhard and Wieschaus, and the subsequent identification of their vertebrate homologs, a key observation hinting

at a potential molecular mechanism for the teratogenic effect of cyclopamine was made by Chiang and Beachy while working with Shh knockout mice [43]. They were using this mouse model to study the role of the Shh secreted morphogen in vertebrate development. Shh^{-/-} mice displayed severe holoprosencephaly, extensive craniofacial deformities, including cyclopia and a proboscis consisting of fused nasal chambers at a location overlying the cyclopic eye. Based on the similarities in the developmental malformations produced by the Shh knockout in mice and those described decades prior from pregnant ewe consumption of *V. californicum*, it was speculated that cyclopamine and other alkaloids might act through inhibition of Hh signaling. Later, using chick neural plate explants, it was demonstrated that treatment with jervine recapitulated the Shh knockout mouse phenotype by inhibiting the response of target tissues to Shh protein [44]. This finding was corroborated shortly thereafter in chick embryos treated with cyclopamine, and it was determined that cyclopamine-induced teratogenesis is due to direct antagonism of Shh signal transduction [45]. Ultimately, it was determined using photoaffinity and fluorescent derivatives, that cyclopamine inhibits Hh signaling by binding to and blocking Smo [46]. These data were later corroborated by crystallographic analyses of the Smo/cyclopamine complex, in which cyclopamine was observed to bind to the internal heptahelical fold of Smo, rather than the extracellular domain of the cytoplasmic C-terminus [47]. The Smo/cyclopamine complex is shown in **Figure 1.3**. Smo is a G protein-coupled receptor that contains an extracellular domain composed of a cysteine-rich domain and a linker domain, a seven-transmembrane helical domain and an intracellular carboxy-terminal domain. Cyclopamine binds near to the entrance into a long and narrow cavity inside the receptor.

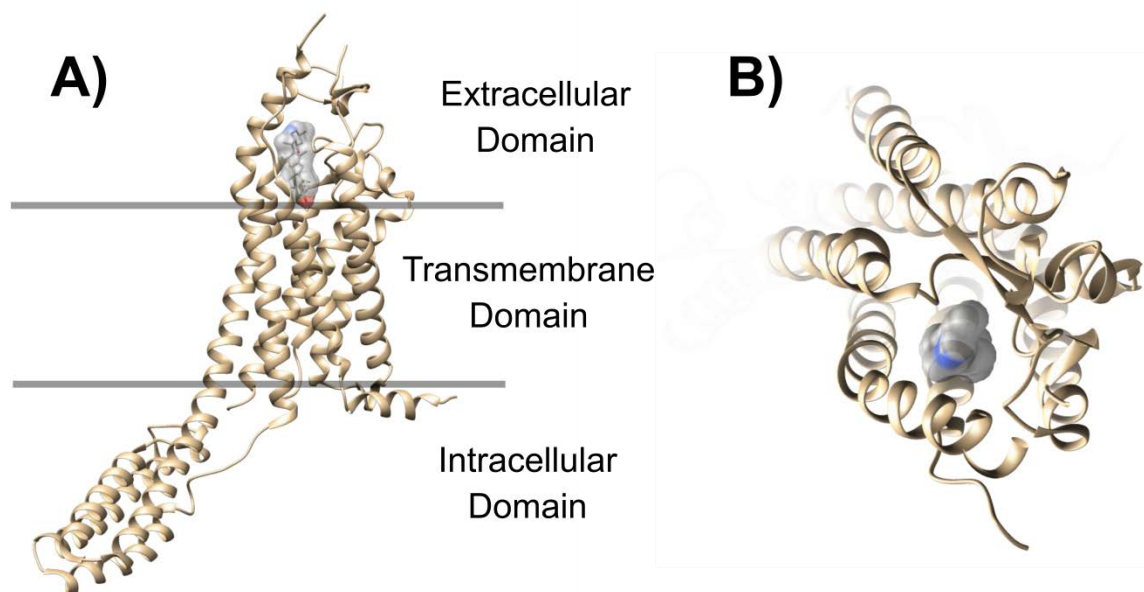


Figure 1.3. Cyclopamine binding to Smoothed receptor. (A) Receptor model of Smoothed shown as a tan cartoon with cyclopamine shown to bind as a space-filled model. The extracellular, transmembrane and intracellular domains of Smo are indicated. Horizontal lines indicate membrane boundaries. Cyclopamine binds near to the entrance into a long and narrow cavity inside the receptor. (B) Top view Smo receptor with cyclopamine bound to the cavity near the transmembrane domain.

Cyclopamine was the first small molecule known to specifically inhibit the Hh pathway, and has been widely used to study Hh signaling. Cyclopamine has also played an important role in the development of Smo antagonists as therapeutic agents, as Hh pathway activation not only controls tissue patterning but also contributes to oncogenesis.

1.3 The Hedgehog Signaling Pathway and Cancer

Abnormal activation of Hh signaling has been implicated in many cancer types including gastrointestinal, bladder and ovarian carcinomas, lung cancer, and hematological malignancies [48-55]. Aberrant Hh signaling also plays an important role in cancer proliferation and invasiveness. Several molecular mechanisms in the aberrant

activation of Hh signaling in human cancers have been identified. These include 1) ligand-independent activation due to loss-of-function mutations in *Ptch1* or *SUFU* that inactivate the suppression of Hh signaling, or gain-of-function mutations that enhance the activity of Smo or Gli, 2) ligand-dependent activation through tumor expression of Hh ligands acting in a autocrine or juxtacrine manner, and 3) paracrine ligand-dependent activation where Hh ligands are secreted by tumor cells turning on Hh signaling in the surrounding tissues [56].

Depending upon tissue type, abnormal Hh signaling contributes to the progression of specific cancers differentially [57]. In the case of basal cell carcinoma and medulloblastoma, mutations in the Hh pathway initiate tumorigenesis [58,59]. In some cancers, including colon and pancreatic, Hh signaling does not initiate tumorigenesis but contributes to the growth of the tumor [60,61]. Finally, for many cancers including lymphoma, lung and prostate, Hh signaling has been implicated but the exact role of the pathway on progression of these diseases remains enigmatic [57]. In gallbladder cancer, it has been demonstrated that Hh signaling promotes invasiveness through degradation of collagen IV via upregulation of MMP-2 and MMP-9 collagenases [62]. Degradation of collagen IV in the basement membrane is required for invasion into adjacent blood or lymphatic vessels. Inhibition of Smo in gallbladder cancer cells was shown to decrease cell invasiveness and inhibit epithelial-mesenchymal transitions. Therefore, suppression of Smo and Hh signaling was identified as a potential therapeutic strategy for this cancer type. In these cells, Smo inhibition resulted in decreased expression of vimentin, an intermediate filament protein expressed in mesenchymally derived cells and cells undergoing epithelial mesenchymal transition [63]. The association between Hh signaling

and epithelial mesenchymal transition through downregulation of E-cadherin, a calcium-dependent cell to cell adhesion protein, has also been reported [64]. The correlation between Hh signaling and MMP-9 was identified to increase invasiveness of pancreatic ductal adenocarcinoma cells [65]. In the case of prostate cancer, prostate fibroblasts have demonstrated Smo-mediated Hh signaling resulting in increased proliferation and dedifferentiation in adjacent epithelium [66]. Mounting evidence demonstrates that perlecan and syndecans modulate sonic hedgehog signaling during both development and neoplasia, in particular in prostate cancer by directly binding sonic hedgehog and promoting its interaction with Ptch [67,68]. Furthermore, the activity of heparanase was shown to modulate hedgehog signaling through degradation of heparin sulfate glycosaminoglycans in the pathogenesis of medulloblastoma [69].

The initial link between Hh signaling and cancer came with the discovery that a mutation in *Ptch* was responsible for Gorlin syndrome. Gorlin syndrome, also referred to as nevoid basal cell carcinoma syndrome or basal cell nevus syndrome, is a rare, autosomal-dominant genetic disorder characterized by rampant cancerous and noncancerous tumor formation in various tissues, including the skin, cerebellum and soft tissue [70-72]. Following this discovery, several mouse models for Hh pathway activation were developed and studies in these mice demonstrated that constitutive Hh signaling activity is sufficient to form basal cell carcinoma and medulloblastoma [73,74]. Additionally, mutations in Hh pathway genes have been associated with sporadic BCC [75,76]. Over 90% of sporadic BCCs have mutations in one allele of *Ptch*, presumably arising from DNA damage sustained by UV radiation [77].

While cyclopamine has served as a valuable tool in basic research and preclinical models, its potential as a therapeutic agent is limited due to poor solubility, acid lability, and the significant potential for off target effects [78]. For this reason, academic and industrial scientists have sought new Smo inhibitors. Several Smo inhibitors with improved stability and potency over cyclopamine have been created, including IPI-926, a semi-synthetic derivative of cyclopamine, and KAAD-cyclopamine, a cyclopamine analog [79,80]. To date, three Smo antagonists have been approved by the United States Food and Drug Administration for clinical use: vismodegib (GDC-0449) developed by Genentech and approved by the FDA in 2012, sonidegib (LDE225) developed by Novartis and approved by the FDA in 2015, and glasdegib (PF-04449913) developed by Pfizer and approved by the FDA in 2018 [81-83]. The molecular structures of the above mentioned compounds are shown in **Figure 1.4**. Both vismodegib and sonidegib are highly effective treatments for advanced basal cell carcinomas that are not amenable to surgical removal, and vismodegib was also reported to induce rapid but transient regression of metastatic medulloblastoma [84]. Glasdegib is approved for use in combination with low-dose cytarabine for the treatment of newly-diagnosed acute myeloid leukaemia in patients aged ≥ 75 years or those who have comorbidities that preclude use of intensive induction chemotherapy. However, these successes have been coupled with emerging challenges. As in the medulloblastoma case, chemoresistance occurs with a frequency that correlates with tumor grade [85,86]. Smo mutations contribute to many of these relapses; however, genomic alterations

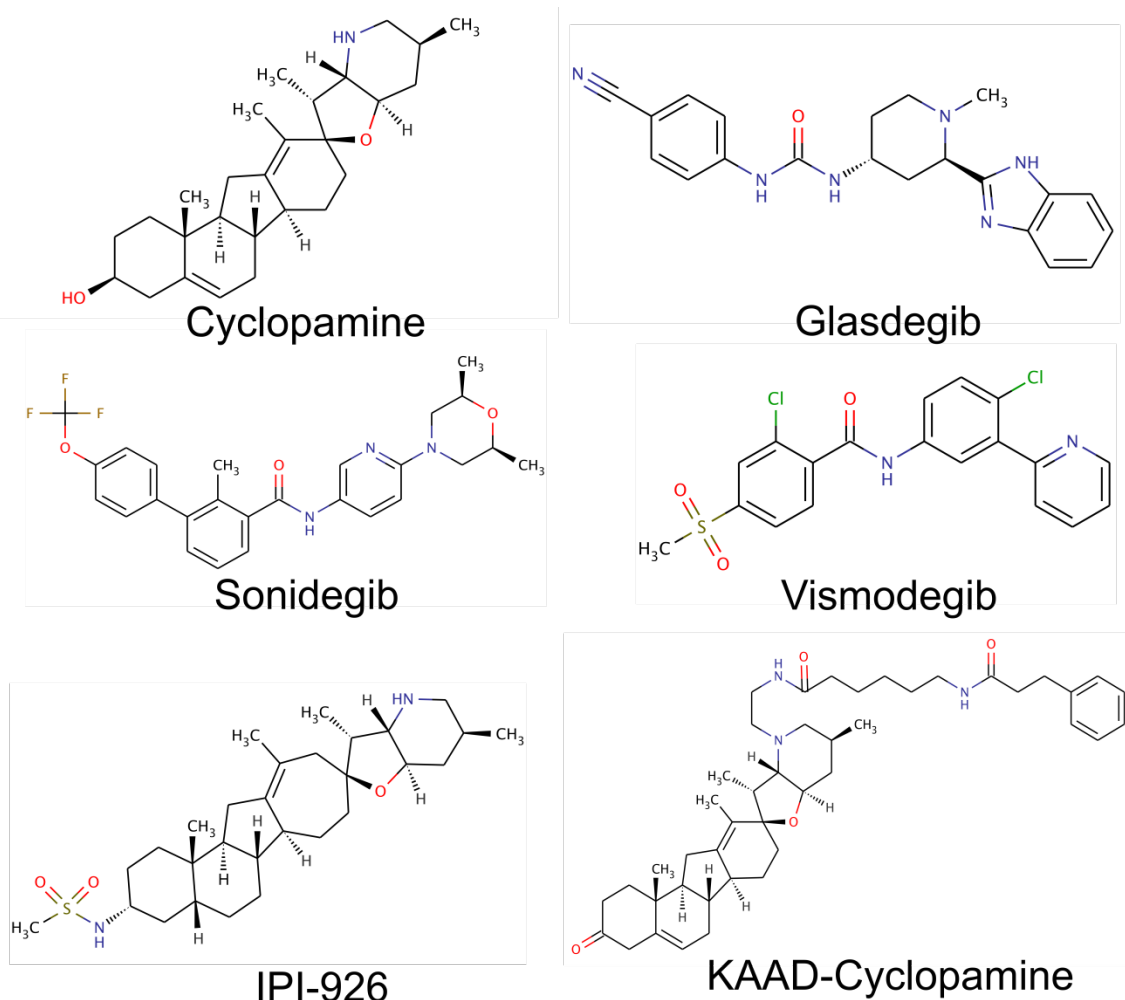


Figure 1.4. Molecular structures of synthetic and natural Smo antagonists. Vismodegib, sonidegib and glasdegib are FDA approved Smo inhibitors.

involving downstream signaling components such as SUFU and GLI2 have been observed as well. In addition, systemic Smo blockade can cause on-target side effects, including hair loss, taste sensation deficits, and muscle cramps, and vismodegib and cyclopamine have been reported to activate noncanonical Smo functions [87,88]. Overcoming these limitations through next-generation Smo inhibitors, alternative delivery methods, and/or new Hh pathway-targeting strategies will be necessary to complete the clinical vision initiated by cyclopamine.

1.4 Overview of the Genus *Veratrum* and Biological Activity of *Veratrum*

Alkaloids

Veratrum is a genus of perennial, flowering plants in the family *Melanthiaceae* with widespread distribution across the Northern Hemisphere and are endemic to temperate and subarctic portions of Europe, Asia and North America [89]. Eleven *Veratrum* species grow in North America. Several species of the *Veratrum* genus, such as *V. album*, *V. californicum*, *V. viride* and *V. nigrum*, are poisonous to humans and animals, and the principal toxic components are steroid alkaloids. More than 100 different alkaloids have been identified from *Veratrum* spp and have been categorized into jervanine, vertranine, cevanine, verazine and solanidine types according to their carbon framework (see **Figure 1.5**). Among the many different steroidal alkaloids, two broad groups have been isolated from *Veratrum* spp: those featuring the typical cyclopentanophenanthrene skeleton of cholesterol containing a 6-6-6-5 ring system (sometimes referred to as the *Solanum* alkaloids) and those which have a C-nor-D-homosteroidal skeleton featuring a 6-6-5-6 ring system. Alkaloids of this latter group are commonly referred to as *Veratrum* alkaloids and were some of the first steroidal alkaloids ever characterized. Within the *Solanum* alkaloids, there are two further classes, those of the verazine type featuring a distinct imine containing ring and those of the solanidine type in which the nitrogen containing ring has become fused to the rest of the cyclic system. The *Veratrum* alkaloids can be further divided into distinct structural groups: the veratranine, jervanine, and cevanine types. The veratranine group is defined by the presence of an aromatic D-ring, whereas alkaloids of the jervanine type feature a tetrahydrofuran E-ring linking the amine containing F-ring to the D-ring through a spiro-

connection at C-17 (see **Figure 1.2** for the carbon numbering scheme). Cevanine alkaloids are distinct from the other two classes of *Veratrum* alkaloids in that they have a six-membered E-ring. Additionally, cevanine alkaloids are highly hydroxylated in *Veratrum* plants, with 7–9 atoms of oxygen, and feature α -ketol and hemiketal (an alcohol and ether attached to the same carbon) linkages between C-4 and C-9 of the A and B rings respectively. **Figure 1.5** shows C-nor-D-homo and cyclopentanophenanthrene skeletons, along with the steroidal alkaloid type and representative structures.

The first Hh pathway inhibitor to be identified was the plant-derived steroidal alkaloid, cyclopamine, which binds directly to the transmembrane helices of Smo and blocks cellular responses to Hh signaling [43-46]. However, additional molecular targets for cyclopamine have been identified. Cyclopamine exhibited growth inhibition of various human breast cancer cells independently of Smo, suggesting inhibitory activity to other molecular targets unrelated to the Hh signaling pathway [90]. In human erthroleukemia cells, cyclopamine was found to inhibit cell proliferation and induced apoptosis through COX-2 overexpression via PKC activation and NF- κ B pathway inhibition [91]. Moving away from cancer, cyclopamine has also been shown to be a potent and selective inhibitor of human respiratory syncytial virus (hRSV) transcription

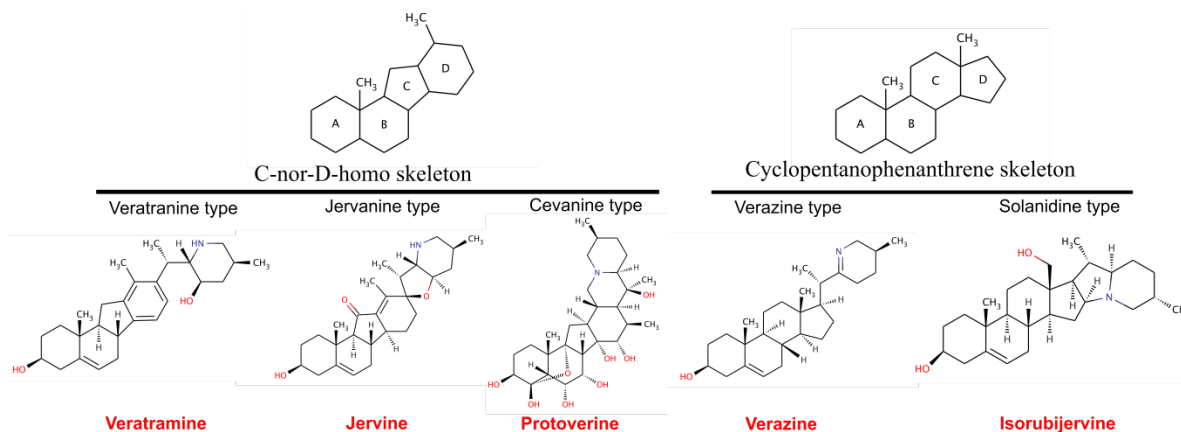


Figure 1.5. Molecular skeletons of C-nor-D-homo and cyclopentanophenanthrene steroidal alkaloids. Species of the genus *Veratrum* produce two broad classes of steroidal alkaloids: the Solanum alkaloids, which feature the classic cyclopentanophenanthrene ring structure and the *Veratrum* alkaloids, which feature a rearranged C-nor-D-homosteroidal ring structure in the C-ring is five membered and the D-ring is six membered. Representative structures of the five categories of steroidal alkaloids: jervanine, veratrine, cevanine, verazine and solanidine, are shown.

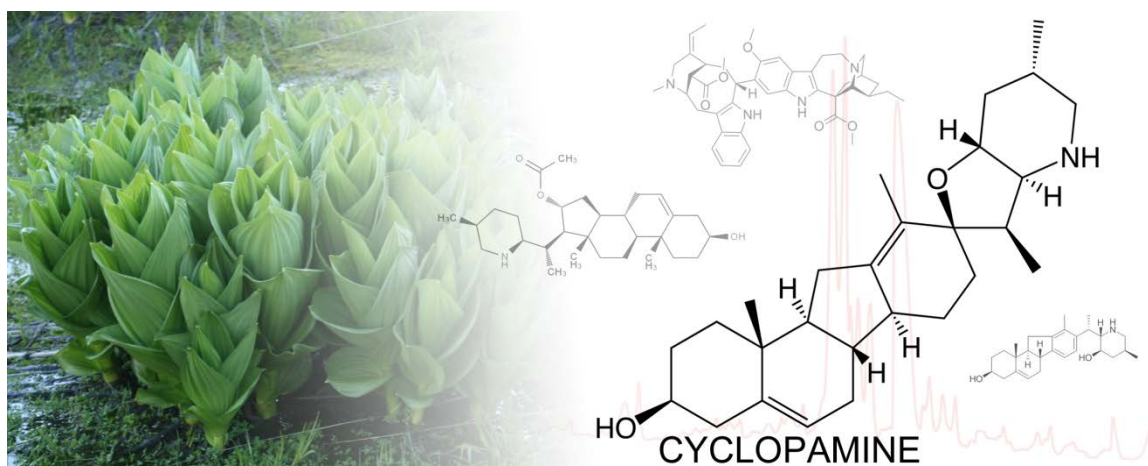
in vitro and *in vivo* [92]. It specifically impairs the function of the hRSV RNA-dependent RNA polymerase complex by reducing expression levels of the viral antitermination factor M2-1. Cyclopamine has also been shown to induce apoptosis by inhibiting PCA3 in human prostate cancer cells [93]. Additionally, cyclopamine has been shown to sensitize tumor necrosis factor (TNF)-related apoptosis-inducing ligand (TRAIL) resistant gastric cancer cells to TRAIL by increased expression of death receptor 5 via endoplasmic reticulum (ER) stress induced by reactive oxygen species, and increased proteasome degradation of survivin, a negative regulator of apoptosis [94].

Veratramine occurs in various *Veratrum* species, including *V. album*, *V. grandiflorum*, *V. viride*, and *V. californicum* [89]. Veratramine has been shown to be effective in lowering blood pressure, antagonizing Na⁺ channel activity, and also potentially serotonin (5-HT) agonist activity, acting on presynaptic 5-HT neurons [95-

97]. The administration of veratramine induces generalized tremors, myoclonus, hind-limb abduction, backward gait, and Straub tail, similar to the 5-HT syndrome in mice. Veratramine has also been shown to be a potent modulator of the transcription factor activator protein-1 (AP-1), which regulates a variety of protein-encoding genes, and participants in many cellular functions, including proliferation, transformation, epithelial to mesenchymal transition, and apoptosis [98]. Isorubijervine occurs in various *Veratrum* species, including *californicum*, *viride*, *album* and *taliense* [89,99]. Isorubijervine has been shown to exhibit strong cardiovascular toxicity in mice, and have been demonstrated to block voltage-gated sodium channels Nav1.3-1.5, specifically expressed in cardiac tissue [99]. Recently, seven new veratranine-type alkaloids were isolated from *V. taliense* and evaluated for their analgesic activity using an acetic acid induced writhing model in mice [100]. *V. taliense* has been used in traditional Chinese medicine for pain and inflammation. Veratridine, a cevanine-type steroidal alkaloid isolated from the rhizomes of *V. album* activates voltage-gated Na⁺ channel by blocking their inactivation, thereby prolonging the opening of the channel and the action potential, and augmenting the contractions to cardiac stimulation [101]. The alkaloid alters the gating and permeability properties of Na⁺ current, and the main symptoms of veratridine toxicity include severe nausea, bradycardia, hypotension, difficulty breathing, salivation, and muscle weakness [102]. Additional notable examples of cevanine alkaloids include zygadenine, germine, protoverine and veracevine, all of which lead to similar physiological effects as veratridine when ingested, including hypotension, bradycardia and apnea [89]. These symptoms are referred to as the Bezold–Jarisch reflex.

The *Veratrum* alkaloids are diverse, as are their biological activities. I anticipate that *Veratrum* alkaloids will continue to be investigated as chemical probes for scrutinizing biological mechanisms, and serving as inspiration for drug development. Steroidal alkaloids are inherently biologically relevant because their molecular scaffolds have complex structures containing abundant chiral centers, making them valuable lead compounds for drug discovery as their molecular targets and mechanisms of action continue to be elucidated.

CHAPTER TWO: CYCLOPAMINE BIOACTIVITY BY EXTRACTION METHOD
FROM *VERATRUM CALIFORNICUM*



Picture 1. Graphical abstract for “Cyclopamine bioactivity by extraction method from *Veratrum californicum*”

2.1 Foreword

The following chapter was published in the journal *Bioorganic and Medicinal Chemistry* in 2016 [103]. The purpose of this manuscript was to correlate the extraction efficiency of cyclopamine from *Veratrum californicum* by eight different methods to the bioactivity of the cyclopamine to inhibit Hedgehog signaling, given that extraction techniques may isomerize the alkaloid resulting in diminished bioactivity. Bioactivity assessment was performed by Shh-Light II cells using the Dual-Glo® Luciferase Assay System. These results correlated for the first time alkaloid recovery efficiency from biomass to steroidal alkaloid inhibition of the Hh pathway. This investigation assessed the limits associated with alkaloid recovery and identified an optimal method to obtain the highest yield of active cyclopamine.

2.2 Abstract

Veratrum californicum, commonly referred to as corn lily or Californian false hellebore, grows in high mountain meadows and produces the steroidal alkaloid

cyclopamine, a potent inhibitor of the Hedgehog (Hh) signaling pathway. The Hh pathway is a crucial regulator of many fundamental processes during vertebrate embryonic development. However, constitutive activation of the Hh pathway contributes to the progression of various cancers. In the present study, a direct correlation was made between the extraction efficiency for cyclopamine from root and rhizome by eight methods, and the associated biological activity in Shh-Light II cells using the Dual-Glo® Luciferase Assay System. Alkaloid recovery ranged from 0.39-8.03 mg/g, with ethanol soak determined to be the superior method to obtain biologically active cyclopamine. Acidic ethanol and supercritical extractions yielded degraded or contaminated cyclopamine with lower antagonistic activity towards Hh signaling.

2.3 Introduction

Veratrum californicum (*V. californicum*), a plant that is rich in steroidal alkaloids, is native to moist, high elevation regions in the western United States [104,89]. Of these alkaloids, cyclopamine has been studied for its effect as a teratogen through antagonism of the Sonic Hedgehog (Shh) signaling pathway, which is principally active during fetal development [40,44,45,105-107]. Inhibition of Shh signaling has gained recent interest due to the discovery that aberrant pathway activation is significant in the progression of over twenty cancers including prostate, gallbladder, pancreatic, and basal cell carcinoma [54,62,64-66,89,108]. Active drug development in this field has either used the structure of cyclopamine as a model from which to develop new cancer chemotherapeutics, as in the case of vismodegib developed by Genentec, or has synthetically altered the natural product, as was done by Infinity Pharmaceuticals to make IPI-926, a drug candidate that

has undergone phase two clinical trials for treatment of recurrent head and neck cancers [80,109,110].

Continued development of Shh inhibitors may increase demand for harvesting *V. californicum* as a natural source of cyclopamine, primarily from roots and rhizomes. Preliminary studies to extract cyclopamine from *V. californicum* were performed by soaking the biomass in benzene for 36 hours [35]. The extraction efficiency of benzene was improved by switching from soaking the biomass for long periods of time to employing Soxhlet reflux [111]. Additional efforts to reduce extraction time and improve product yield include microwave assisted extraction, or alternatively, deglycosylation of cycloposine prior to collection of cyclopamine [112-114].

Chandler et al. took advantage of the high solubility of alkaloids in ethanol and the improved extraction efficiency using Soxhlet to obtain nearly three-fold increase in the amount of cyclopamine as compared to traditional benzene extraction [114]. While higher yields were achieved by ethanol extraction, it was not determined if the collected cyclopamine retained biological activity. Cyclopamine has been reported to degrade to veratramine or inactive isomers under acidic, aqueous conditions [39,115]. Literature and patent review provided no comprehensive investigation to correlate extraction efficiency to the potency of Shh inhibition.

In the current study, the total yield and biological activity of cyclopamine recovered from *V. californicum* root and rhizome using eight extraction techniques was correlated directly to alkaloid activity. Extractions were performed by Soxhlet reflux with benzene, Soxhlet reflux with ethanol in acidic, neutral, and alkaline conditions, ethanol soak, benzene soak, supercritical fluid, and ethanolic microwave assisted extraction (MAE).

Cyclopamine was isolated by high performance liquid chromatography (HPLC), and biological activity was tested using Shh-Light II cells.

2.4 Materials and Methods

2.4.1 Extraction of Cyclopamine

Solvents and Reagents: Extraction solvents, 95% EtOH, benzene, HCl, and NH₄OH were purchased from Fisher Scientific (Pittsburgh, Pennsylvania). HPLC mobile phase consisted of 18 MΩ H₂O and HPLC grade trifluoroacetic acid (TFA), formic acid and acetonitrile (>99% purity, Fisher Scientific). Alkaloid standards for cyclopamine and veratramine were purchased from Logan Natural Products (Logan, Utah), and additional cyclopamine was purchased from LC Laboratories (Woburn, Massachusetts) and Alfa Aesar (Ward Hill, Massachusetts).

Obtaining and Preparing Biomass: A complete specimen of *V. californicum* was harvested at an elevation of 2134 m (~7000 ft), from a northwest facing slope, growing in a moist meadow near the Elk Meadows trail at Bogus Basin Mountain Resort, located in the Boise National Forest, Idaho. The leaf and stalk of the plant were separated from the rhizome and roots, and all plant parts were cut into smaller pieces to fit into quart size Ziploc bags. The sealed bags were placed in a cooler on a bed of ice for transportation. The biomass was collected at a late stage in the plant's life cycle; the plant had noticeable brown edges along its leaves and top indicating annual deterioration of above ground material in preparation for winter. Within two hours and upon arrival in the lab, the roots and rhizomes were chopped into 2 cm segments and dried for 14 hrs. using a LabConco Freezone 4.5 freeze drying unit, followed by storage at -20 °C. Prior to usage, the frozen biomass was again lyophilized to ensure dryness, flash frozen in liquid nitrogen, and

ground to a fine powder by mortar and pestle. The homogenized biomass from the same plant was used to perform each of the following extraction methods in triplicate.

Soxhlet Reflux (Ethanol and Benzene): Approximately 2.0 g of pulverized biomass was packed inside a 25 mL cellulose thimble, which was placed into a Soxhlet column, and fitted with a 500 ml round bottom flask containing 150 ml of either ethanol or benzene. The Soxhlet reflux was maintained for 6 hrs. After 6 hrs., the reflux solvent turned a dark amber color, and assumed a syrup-like consistency upon solvent reduction by rotary evaporation.

Soak Extraction (Ethanol and Benzene): Approximately 2.0 g of pulverized biomass was added to a 250 ml round bottom flask followed by 150 mL of ethanol or benzene. The resultant slurry was sonicated for 30 min. and then stirred for 24 hrs. on a stir plate. The amber extract was vacuum filtered through 0.45 μm Whatman filter paper.

Supercritical Fluid Extraction: A tight coil of copper wire was placed inside a 15 mL Falcon tube with a handle to help lower the coil. The wire was lowered leaving a 1 mL gap between the coil and the bottom of the tube. Two grams of biomass were packed firmly on top of the copper coil. Dry ice was ground into a powder and packed to the top of the tube. The cap was firmly sealed and the entire tube was submerged in warm tap water. The reaction was considered complete when solid and liquid CO_2 were no longer present and bubbles ceased to appear in the submersion tank. Dry ice was added an additional three times to ensure complete extraction. The biomass and filtrate were rinsed with ethanol to remove residue from the tube. Ethanol fractions were combined for later chemical analysis.

Microwave Extraction: Microwave assisted extraction method was performed on 2.0 g pulverized biomass using 50 mL of 67% ethanol and 33% water (v/v). Sodium carbonate (15 g/L) was added to ensure alkaline conditions (pH 10). The microwave assisted extraction was performed using a CEM MARS 5 system. The reaction vessel was heated from room temperature to 120 °C over three minutes. The temperature was held at 120 °C for three minutes using a power of 100 W. A subsequent 20 min. cool-down period resulted in a solution temperature of less than 55 °C. The solution was transferred to a 250 mL round bottom flask and evaporated to a volume of approximately 10 mL using a rotary evaporator (35-50 °C), followed by vacuum filtration to obtain the concentrated extract.

Crude Product Preparation: The crude extract obtained from each method was dissolved in 10 mL of ethanol, and the solution was warmed and sonicated to achieve complete dissolution. Addition of NH₄OH achieved alkaline solvent conditions of pH >10. The aqueous solution was added directly to a supported liquid extraction (SLE) column (Chem Elut, Agilent, Santa Clara, California) and allowed to adsorb for 10 min., followed by elution of alkaloids with chloroform (3×10 mL) using a vacuum manifold set to a pressure of 2 mbar. The chloroform fractions were combined, filtered, and evaporated to dryness. All samples were dissolved in 1 mL ethanol as a mixture of alkaloids.

2.4.2. Purification, Quantification, and Qualitative Analysis of Cyclopamine from Extracts

Cyclopamine Purification: HPLC was used to purify cyclopamine from the alkaloid mixture using a Dionex UltiMate[®] 3000 uHPLC system coupled to a diode array detector

(DAD) and an automated fraction collector. A semi-preparative Agilent Zorbax SB-C₁₈ column (9.4 × 250 mm, 5 μm) was used to achieve separation. The mobile phase was 0.1% TFA in water (Buffer A) and acetonitrile (Buffer B) with a flow rate of 3.0 ml/min. The linear gradient method was used to separate alkaloids from the mixture starting at 5% acetonitrile and ending at 90% acetonitrile over 25 min. Cyclopamine isolated by this procedure was stored as a dried solid at -20 °C for use in bioactivity studies and mass spectrometry analysis.

Cyclopamine Quantification: Aliquots of crude alkaloid extracts were used to quantitate cyclopamine content using a charge aerosol detector (CAD), and MSQ Plus mass spectrophotometer equipped with a Thermo Acclaim 120 C₁₈ column (2.1 × 150 mm, 3 μm). Buffer and gradient conditions were the same as stated above, but the flow rate was decreased to 0.3 ml/min. Cyclopamine standard was used to create a calibration curve at concentrations of 0.5, 1.0, 2.5, 5.0 and 10.0 mM with detection recorded by a Corona Veo RS CAD with the power function set to 1.70. The quantity of cyclopamine was determined from the alkaloid mixtures obtained from each extraction method performed in triplicate, and the extraction efficiency and the standard deviation was calculated.

Qualitative Analysis of Cyclopamine: Cyclopamine isolated from each alkaloid mixture was analyzed by mass spectrometry using an ultra-high resolution Quadrupole Time of Flight (QTOF) instrument (Bruker maXis). The electrospray ionization (ESI) source was operated under the following conditions: positive ion mode; nebulizer pressure: 0.8 Bar; flow rate of drying gas (N₂): 4 L/min; drying gas temperature: 200 °C; voltage between HV capillary and HV end-plate offset: 3000 V to -500 V; mass range

was set from 80 to 1000 m/z; and the quadrupole ion energy was 4.0 eV. Samples were analyzed by direct infusion with a syringe pump at a flow rate of 240 μ L/hr. Sodium formate was used to calibrate the system in the mass range. Spectra were collected for intact parent ions followed by isolation and fragmentation using collision induced decay MS/MS over a range of collision energies (0-40 eV). Fragmentation patterns were compared to cyclopamine and veratramine standards. Data were analyzed using the Compass Data Analysis software package (Bruker Corporation, Billerica, Massachusetts).

2.4.3. Biological Activity of Purified Extracts

Cell Culture: Shh-Light II cells (JHU-068) were maintained in Dulbecco's Modified Eagle Medium (DMEM) (Gibco) supplemented with 0.4 mg/mL geneticin, 0.15 mg/mL ZeocinTM (Invitrogen), and 10% bovine calf serum. The cells were grown at 37 °C in an atmosphere of 5% CO₂ in air and 100% relative humidity. This mouse embryonal NIH 3T3 cell line contains a stably transfected luciferase reporter with eight copies of the consensus Gli binding site [116]. Cyclopamine samples were dissolved in ethanol and added to DMEM media containing 0.5% bovine calf serum.

Reporter Assay: Shh-Light II cells were seeded in a 96-well plate and grown to complete confluence in the media described above. When cells were confluent, the media was replaced with DMEM supplemented with 0.5% bovine calf serum, and treated with 0.1 ng of N-terminal mouse recombinant Shh (R&D Systems, Minneapolis, Minnesota) dissolved in DMEM, and select cyclopamine treatment. To determine the effect of extraction technique on the biological activity of cyclopamine, the collected material from each of the eight extraction methods and three commercial cyclopamine standards

were used to create treatments that resulted in final concentrations of 5, 1, 0.5, 0.1, or 0 (positive control) μM cyclopamine. In each experiment, the controls and treatment wells contained all vehicles, with a final ethanol concentration of 0.05%. Gli activity in the Shh-Light II cell line was assayed 48 hrs. after treatment with Shh protein and selected compounds using the Dual-Luciferase Reporter Assay System (Promega, Madison, Wisconsin). The Gli-activity was measured by luminescence emitted from cells using a BioTek Synergy H1m Microplate reader. Each experiment was performed thrice.

2.5 Results and Discussion

HPLC chromatograms for crude extracts representative of each of the eight extraction methods are shown in **Figure 2.1**. When necessary, crude samples were spiked with standard to definitively identify the peak corresponding to cyclopamine. Alkaloids typically found in *V. californicum* are shown in **Figure 2.2**. Each extraction technique yielded a unique array of compounds with differing concentrations of alkaloids in relation to the amount of cyclopamine. The complex sample matrices influence the elution time of cyclopamine as compared to the isolated standard, so peak verification was necessary for correct identification.

Soxhlet reflux with ethanol was found to be optimal when the extraction time was allowed to proceed for 6 hours (data not shown). This time was determined by testing the extraction efficiency at six points: 1, 2, 4, 6, 8 and 24 hours. As extraction time was allowed to increase there was a corresponding increase in extracted cyclopamine, which achieved a maximum at 6 hrs. after which cyclopamine quantity was observed to decrease. It was assumed that prolonged exposure to elevated temperatures degraded cyclopamine, but the nature of the degradation was not investigated.

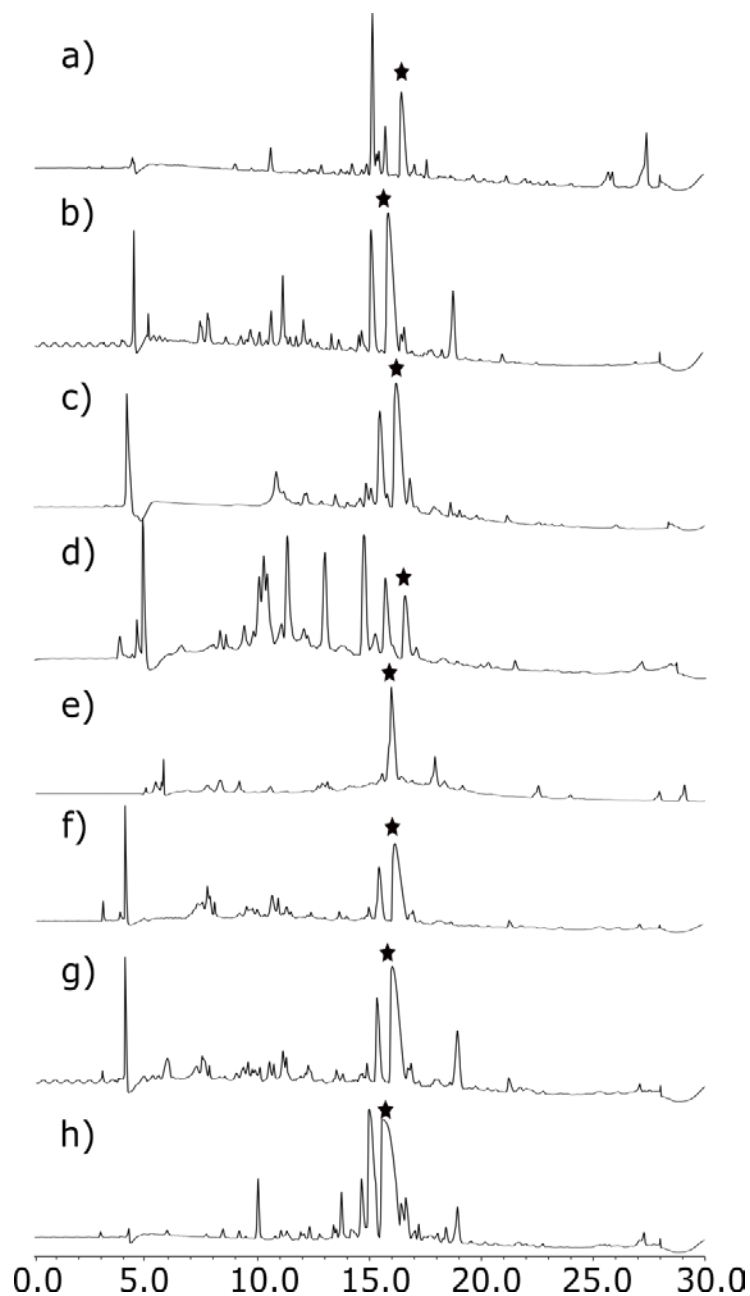


Figure 2.1. Chromatograms for alkaloid mixtures collected over a 30 minute run time. All chromatograms are shown over the same intensity range (y-axis), and the isolated peak is indicated by asterisks. Extraction conditions are as follows: a) benzene soak, b) ethanol soak, c) microwave assisted, d) supercritical CO₂, e) acidic ethanol Soxhlet, f) alkaline ethanol Soxhlet, g) neutral ethanol Soxhlet, and h) benzene Soxhlet.

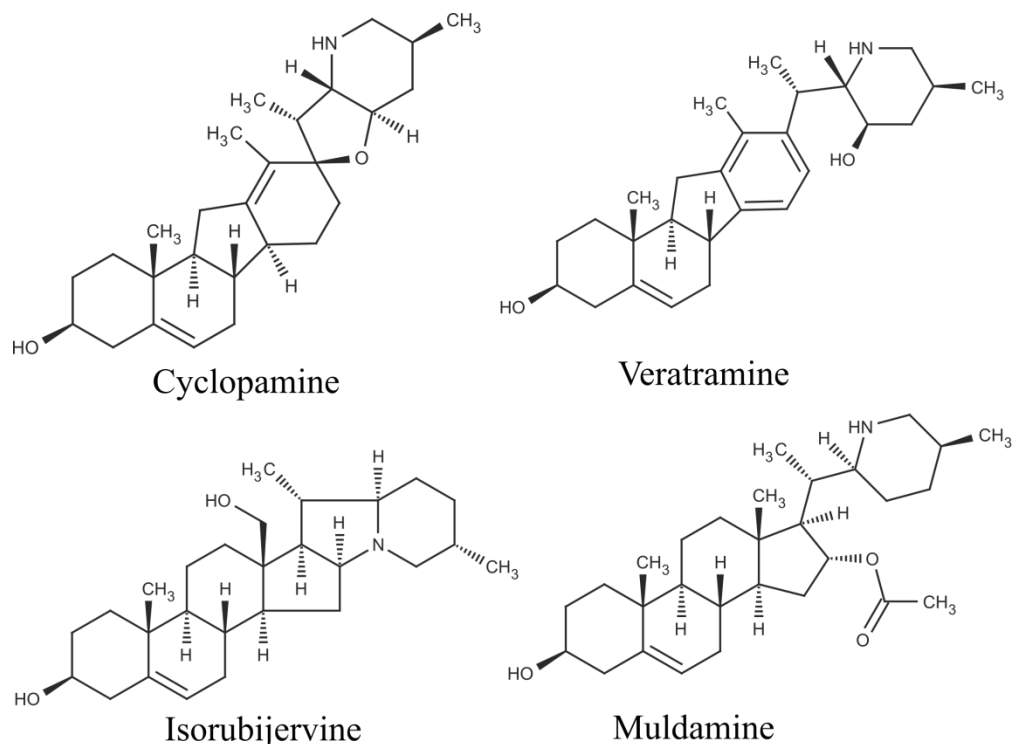


Figure 2.2. Molecular structures of steroidal alkaloids present in *V. californicum*. Shown are cyclopamine, veratramine, isorubijervine and muldamine.

Cyclopamine from each extraction technique was quantified from crude samples by HPLC-CAD, and a standard curve generated from commercially available cyclopamine ($R^2 = 0.9972$). The concentration of cyclopamine in crude alkaloid extracts was determined and the efficiency of the cyclopamine extraction was calculated as a function of dry material from which it was extracted. The cyclopamine extraction results are summarized in **Table 1**. **Table 1** shows the mg of cyclopamine extracted per g of initial biomass. Each extraction was repeated in triplicate, and the standard deviation of the yield is shown. The percent recovery relative to ethanol soak extraction is shown for

Table 1. Comparison of extraction efficiency and corresponding bioactivity of cyclopamine. Recovery is reported as mg of alkaloid per g of biomass used.

Extraction Method	Average (mg/g)	Standard Deviation (mg/g)	Relative % Recovery	Relative Gli-Reporter Activity at 0.1 μ M
Ethanol Soak	8.03	0.13	100.0	40.45 \pm 8.49
Benzene Soak	0.39	0.18	4.9	42.68 \pm 2.74
Benzene Sox	0.95	0.32	11.8	45.17 \pm 7.63
Ethanol Sox	0.75	0.14	9.3	57.10 \pm 7.29
Ethanol Sox (acidic)	0.11	0.02	1.4	91.10 \pm 5.98*
Ethanol Sox (basic)	0.73	0.11	9.1	40.14 \pm 8.61
Supercritical	0.66	0.10	8.2	90.40 \pm 6.50*
Microwave	1.19	0.53	14.8	65.16 \pm 8.63

*Statistically lower bioactivity than cyclopamine standard.

comparison between extraction methods, because recovery from ethanol soak was superior to all other methods. The activity of cyclopamine isolated by each extraction technique to inhibit Hh signaling at 0.1 μ M is also shown, where comparable high inhibition was observed for ethanol and benzene soak, and Soxhlet under conditions of benzene solvent or alkaline ethanol, and poor bioactivity was measured for acidic ethanol Soxhlet and supercritical fluid extraction methods. In **Table 1**, the acidic ethanol Soxhlet and supercritical extracts are indicated in bold font and by an asterisks to show reduced biological activity compared to the cyclopamine standard, which measured at 58.08 \pm 7.51 percent reduction in Gli-reporter activity at 0.1 μ M cyclopamine treatment.

The amount of recovered cyclopamine by ethanol soak was substantially greater than that obtained by other techniques, yielding 8.03 mg/g, compared to 0.39 to 1.19 mg/g. Based on literature precedent, it is likely that prolonged ethanol exposure results in deglycosylation of cycloposine to cyclopamine, while simultaneously providing a mild solvent condition that prevents cyclopamine degradation [112]. The acidic ethanol Soxhlet extraction yielded virtually no detectable cyclopamine of the correct m/z. Despite this, as indicated in **Figure 2.1**, the major peak in the acidic ethanol Soxhlet extraction was collected and evaluated for inhibitory activity towards Hh signaling.

All extraction methods yielded a white, amorphous powder upon isolation except the acidic ethanol Soxhlet and supercritical extraction methods. These methods yielded brown and tan powders, respectively. Cyclopamine has been reported to degrade to veratramine or isomerize under acidic conditions, resulting in reduced bioactivity [39,115]. Therefore, it was anticipated that extraction by Soxhlet reflux using acidic ethanol as the solvent, would yield a product of diminished effectiveness to inhibit Hh signaling. High resolution QTOF MS showed the product obtained under acidic conditions was characterized by an m/z and fragmentation pattern consistent with veratramine [114], with a $[M+H]^+$ peak of 410.304, and major fragmentation peaks of 295.2, 114.1, 183.1, 211.1, 171.1, and 84.1 (**Figure 2.3**).

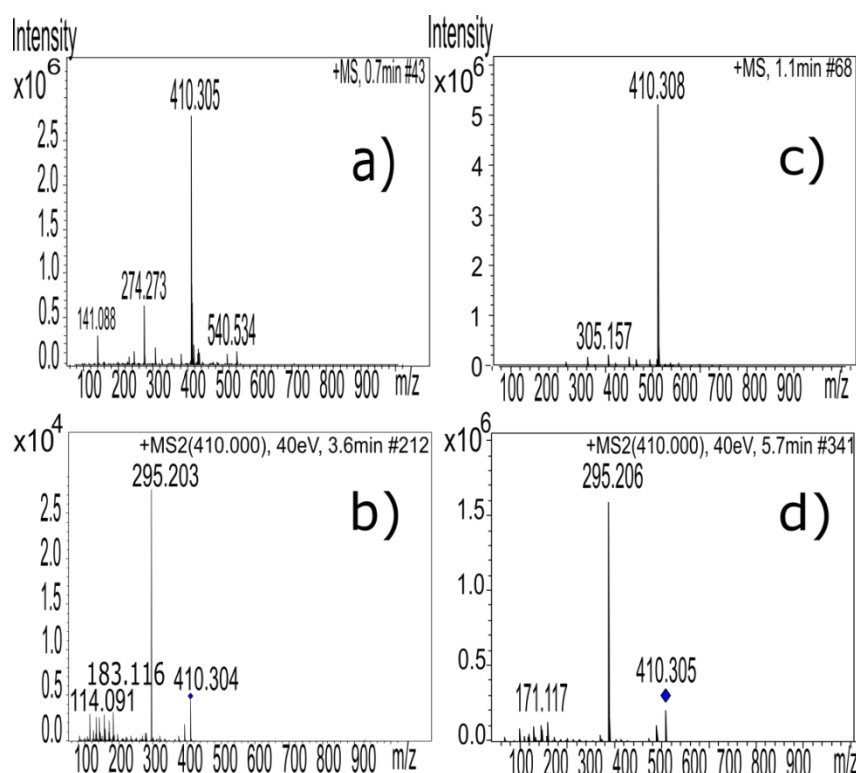


Figure 2.3. Direct comparison of MS and MS/MS of the acidic ethanol Soxhlet isolated product and veratramine standard. a) High resolution MS analysis of acidic ethanol Soxhlet extracted product, and b) MS/MS analysis of isolated ion of m/z of 410.0. c) High resolution MS analysis of veratramine standard, and d) MS/MS analysis of isolated ion of m/z of 410.0.

To confirm that each extraction method yielded biologically active cyclopamine capable of Hh pathway inhibition, the isolated cyclopamine was tested alongside three commercially available cyclopamine standards from different suppliers in a Hh-responsive fibroblast cell line Shh-Light II assay [116]. Extracted cyclopamine from all methods was able to decrease Shh peptide-stimulated Gli reporter activity at a level equivalent to the cyclopamine standards for each concentration tested, except for supercritical CO₂ and acidic ethanol Soxhlet (**Figure 2.4**).

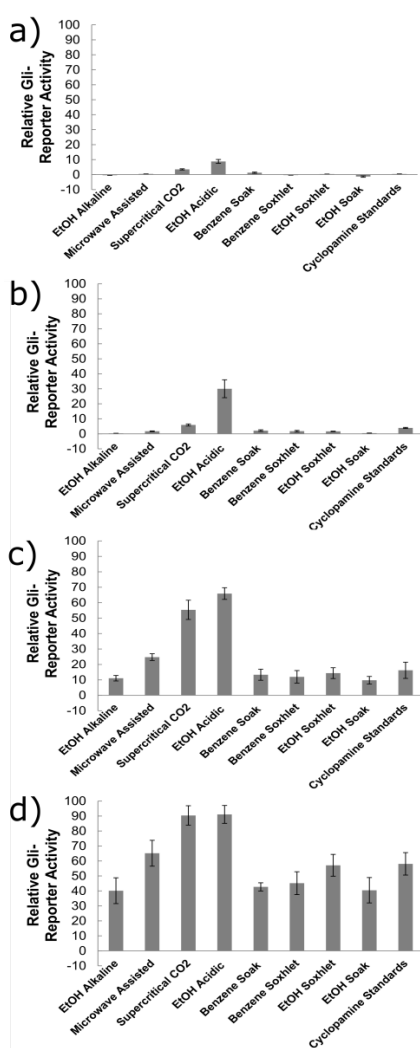


Figure 2.4. Effects of extract on Shh-stimulated Gli-responsive promoter in the Shh-Light II cell line. Shh-Light II cells were treated with various compounds in the presence of 2 $\mu\text{g}/\text{mL}$ mouse recombinant Shh for 48 h. a), b), c), and d) correspond to 5, 1, 0.5, and 0.1 μM cycloamine, respectively, for each extraction method. Experiments were performed in triplicate with standard deviation indicated.

Included in **Figure 2.4** is average of the triplicate trials of the three commercial standards. With the exception of the supercritical CO_2 and acidic ethanol Soxhlet extraction methods, each technique and the standard control resulted in nearly complete (>98%) inactivation of the Shh peptide-stimulated Hh pathway activity at both 5 μM and 1 μM , and an average of $13.5 \pm 5.3\%$ and $49.4 \pm 9.8\%$ of reported activity at 0.5 μM and

0.1 μM , respectively. Based upon the similarities observed in the biological activity, all extraction techniques except the supercritical fluid and acidic ethanol Soxhlet can be presumed to have yielded cyclopamine with chemical and isomeric purity equivalent to that of the three commercial cyclopamine standards tested. The purity of the standards was confirmed to be $>98\%$ by integrating the peak area of the high resolution QTOF MS (see **Figure 2.7**).

Inhibition of Hh signaling was observed in Shh-Light II cells treated with acidic ethanol Soxhlet isolated product, although at considerably decreased potency compared to other extraction techniques and cyclopamine standards. Gli-reporter activity was measured at $8.8\pm 1.3\%$, $30.0\pm 6.0\%$, $65.9\pm 3.8\%$, and $91.1\pm 6.0\%$ for 5, 1, 0.5, and 0.1 μM samples, respectively. To further investigate the identity of this acid degraded product, the inhibitory activity of veratramine standard on Hh signaling in Shh-Light II cells was performed. Inhibition was observed in the cells treated with the standard, but it was markedly less potent than the acid degraded product. The relative Gli-report activity measured at 72.0% for the cells treated with 1 μM veratramine standard, compared to 30.0% activity for cells treated with 1 μM acid degraded product (see **Figure 2.5**).

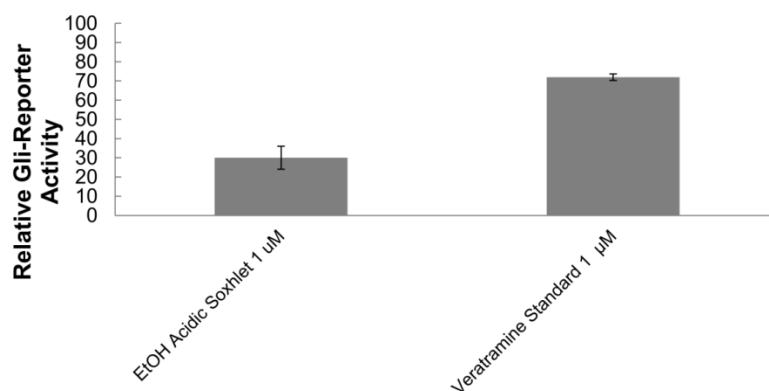


Figure 2.5. Direct comparison of Shh-Light II cells treated with 1 μM veratramine standard, compared to 1 μM acid degraded product from acidic ethanol Soxhlet extraction.

The result displayed in **Figure 2.5** may be due to presence of additional alkaloids in the acidic ethanol extract, such as peaks observed at m/z 540.534, 416.351 and 430.330 as shown in the MS (**Figure 2.3a**), and trace quantities of residual cyclopamine. Veratramine has been reported to be ineffective in blocking hedgehog signaling in chick embryos at 240 nM, but acid treated cyclopamine has been shown to inhibit Hh signaling with a diminished potency in Shh-Light II cells at 1 μ M [45]. These discrepancies could be the result of the disparate techniques and concentrations used to evaluate disruption of Hh signaling. Decreased bioactivity for cyclopamine extracted by supercritical fluid was also observed. The high resolution QTOF MS of this sample showed a veratramine contaminate, as evidenced by a $[M+H]^+$ of 410.3. Veratramine in the supercritical extract was observed in each of the triplicate trials, indicating the crude sample matrix from this extraction technique made the separation and isolation of pure cyclopamine less efficient on the semi-preparative C_{18} HPLC column. In the acidic ethanol Soxhlet extractions spiked with cyclopamine standard, there are clearly distinct peaks observed for veratramine and cyclopamine (**Figure 2.6**). This is not the case for the supercritical fluid extraction, indicating that the unique constituents of the crude supercritical fluid extract made collection of cyclopamine independent of veratramine more difficult. However, it is not immediately clear why this phenomenon is observed. From integration of MS peaks, the supercritical extract yielded cyclopamine that was 79.4% pure, with the remainder of

the mixture being primarily veratramine (Figure 2.7).

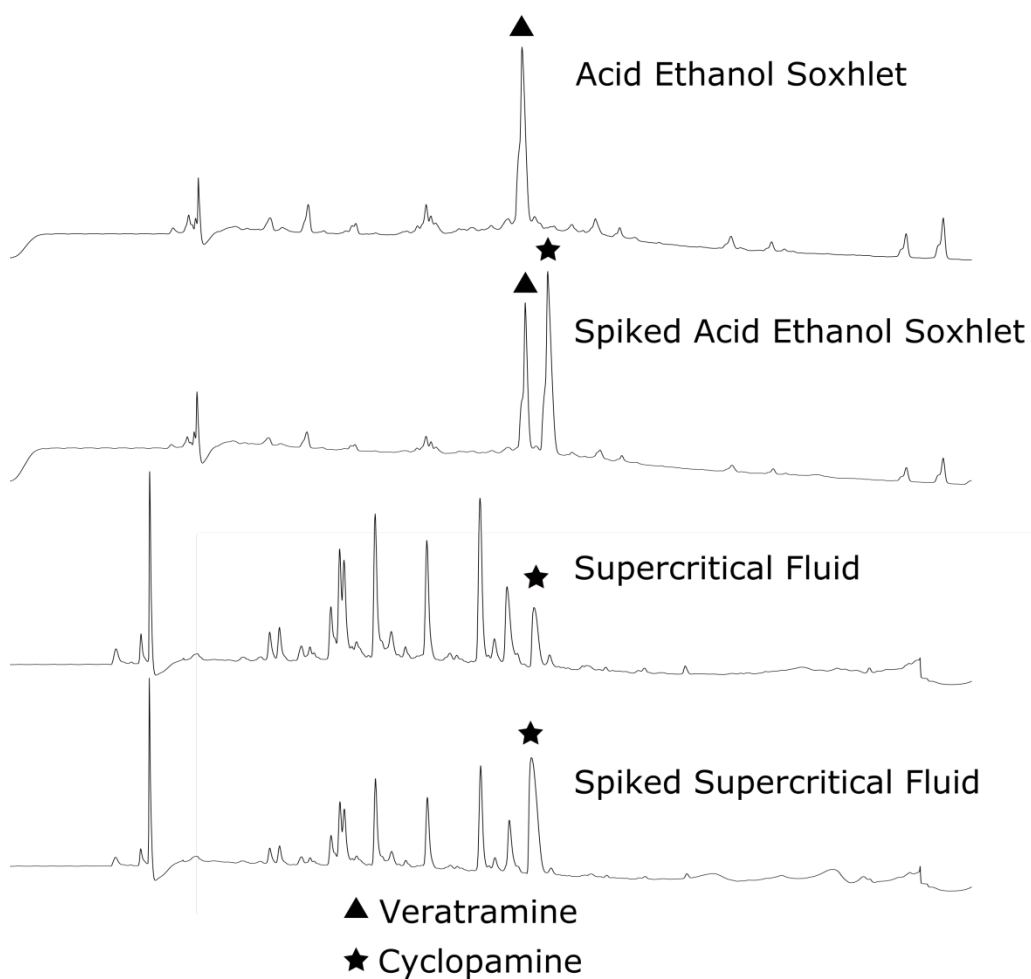


Figure 2.6. Comparison of acidic ethanol Soxhlet extraction and supercritical fluid extraction spiked with cyclopamine standard. Distinct peaks observed for veratramine and cyclopamine are observed in the acidic ethanol extraction, but not the supercritical fluid extraction.

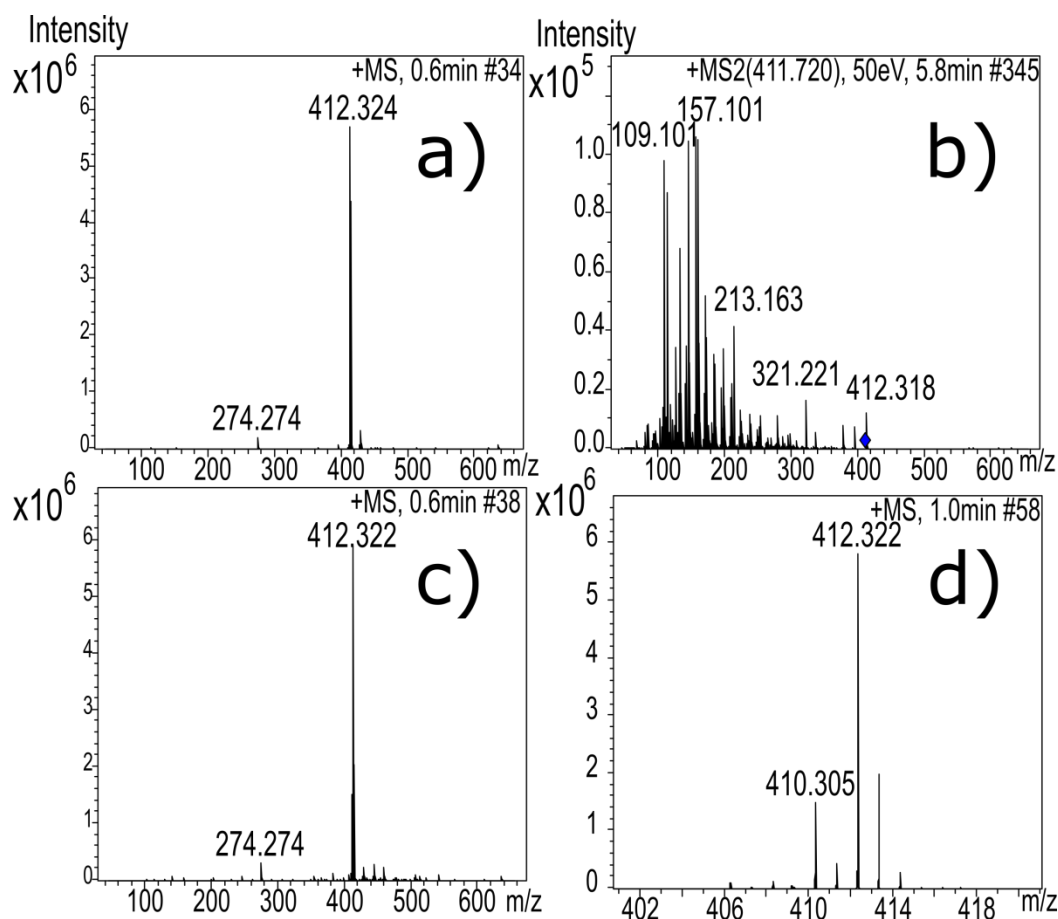


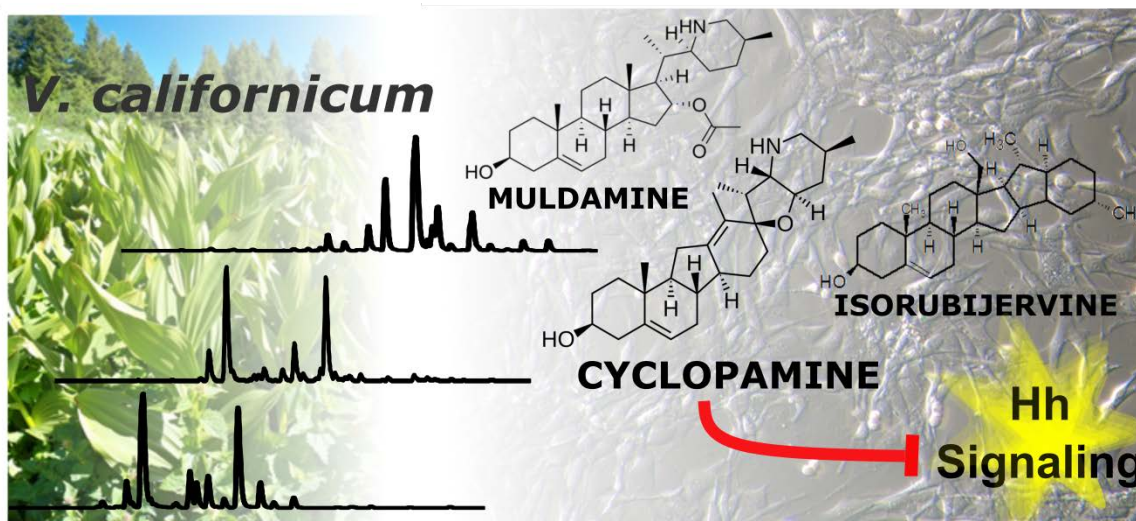
Figure 2.7. MS analysis of cyclopamine standards and collected from supercritical fluid extraction. a) and c) show confirmation of cyclopamine purity from commercial standards, and b) MS/MS fragmentation of cyclopamine collected by collision induced decay (CID). CID was collected at 50eV. d) shows direct injection of cyclopamine collected from supercritical extraction. The presence of veratramine observed at m/z 410.3 indicates a mixture of alkaloids.

2.6 Conclusion

Most of the extraction techniques evaluated in this study yielded cyclopamine with purity that is comparable to commercially available sources, as demonstrated in Hh signaling inhibition assay. The ethanol soak method yielded substantially higher quantities of cyclopamine compared to the other methods. Acidic ethanol Soxhlet extraction caused cyclopamine to degrade. The degradation product is suspected to be veratramine, although it demonstrated Hh inhibition at considerably increased potency

compared to commercially available veratramine standard. Veratramine was also present in the supercritical fluid extract because the separation method comprised of HPLC mobile phase and semi-preparative C₁₈ column were not well enough refined to completely separate these closely related chemical species. The identity of the unique assortment of alkaloids resulting from each extraction technique warranted further investigation, as did the precise chemical nature of the acid degraded product.

CHAPTER THREE: NATIVE *V. CALIFORNICUM* ALKALOID COMBINATIONS
INDUCE DIFFERENTIAL INHIBITION OF SONIC HEDGEHOG SIGNALING



Picture 2. Graphical abstract for “Native *V. californicum* alkaloid combinations induce differential inhibition of Sonic hedgehog signaling”

3.1 Foreword

The following chapter is based on a manuscript published in the journal *Molecules* in 2018 [117]. The purpose of the manuscript was to present the most comprehensive quantitative and qualitative analysis of ethanolic extracts of aerial plant (stem and leaf) and compare the bioactivity using Shh-Light II cells to alkaloids in the root/rhizome. The paper went on to describe the evaluation of known *Veratrum californicum* steroidal alkaloids, at the ratio identified by plant part, as compared to plant extract for inhibition of Hedgehog signaling inhibition. Finally, mass spectrometry analysis provided evidence that as many as eleven novel alkaloids, present in raw plant

extracts, may contribute to Hedgehog signal inhibition. The bioactivity was assessed by Shh-Light II cells using the Dual-Glo® Luciferase Assay System. The current investigation identified alkaloids suspected to be Hedgehog signaling inhibitors for isolation and bioactivity assessment.

3.2 Abstract

Veratrum californicum is a rich source of steroidal alkaloids such as cyclopamine, a known inhibitor of the Hedgehog (Hh) signaling pathway. Here we provide a detailed analysis of the alkaloid composition of *V. californicum* by plant part through quantitative analysis of cyclopamine, veratramine, muldamine and isorubijervine in the leaf, stem and root/rhizome of the plant. To determine if additional alkaloids in the extracts contribute to Hh signaling inhibition, we replicated the concentrations of these alkaloids observed in extracts using commercially available standards and compared the inhibitory potential of the extracts to alkaloid standard mixtures using Shh-Light II cells. Alkaloid combinations enhanced Hh signaling pathway antagonism compared to cyclopamine alone, and significant differences were observed in the Hh pathway inhibition between the stem and root/rhizome extracts and their corresponding alkaloid standard mixtures, indicating that additional alkaloids present in these extracts are capable of inhibiting Hh signaling.

3.3 Introduction

The Hedgehog (Hh) signaling pathway plays a vital role in embryonic development [6,75]. In mammals, the Hh signaling pathway consists of the secreted ligands Sonic hedgehog (Shh), Desert hedgehog (Dhh) and Indian hedgehog (Ihh); the transmembrane receptor proteins Patched (Ptch1 and Ptch2), the transmembrane signal transducer Smoothed (Smo), and the Gli transcription factors (Gli1, Gli2, Gli3) [15]. In

the absence of Hh ligands, Ptch1 prevents the translocation of Smo to the primary cilia, thereby inhibiting the nuclear localization of Gli and suppressing transcriptional activity.

Upon binding of Hh ligands to Ptch1, Smo suppression is abolished and downstream pathway activity proceeds, resulting in nuclear translocation and activation of Gli.

Although the Hh ligand proteins all act as morphogens and have similar physiological effects, each Hh ligand performs specialized functions due to the spatial and temporal differences in their expression [16]. The Shh signaling pathway is a major regulator of various processes, including cell differentiation and proliferation, and tissue polarity [6,118]. Inhibition of Shh signaling is widely researched because aberrant Shh signaling is a hallmark of many cancers [54,89,108]. This has been reported in many cancers, including prostate, gallbladder, pancreatic, and basal cell carcinoma [62,65,66]. Basal cell carcinoma (BCC) is the most common human cancer and is driven predominantly by the hyper activation of the Hh pathway [75,85,119]. For this reason, a significant number of BCC patients experience a clinical benefit from vismodegib (Erivedge®), a Smo inhibitor approved by the US Food and Drug Administration (FDA) to treat metastatic or reoccurring BCC [120]. In phase 2 trials in BCC patients, a majority experienced clinical benefit with vismodegib treatment that included 30% of metastatic BCC patients demonstrating a 30% decrease in visible tumor dimension, and 64% experiencing stable tumor size. In patients with locally advanced BCC, 43% showed a 30% decrease in visible tumor dimension, and 38% demonstrating stable tumor size. However, developed resistance to vismodegib in up to 20% of advanced BCC patients within one year of treatment represents a significant limitation [85,121]. Various studies have implicated amino acid mutations in the vismodegib binding-site in Smo as a mechanism underlying

acquired resistance [85,122,123]. Due to adverse side effects and the potential for acquired resistance to vismodegib there is a continued need to investigate novel compounds that target the Hh signaling pathway, and identification of natural products that act as Hh signaling inhibitors continues to be investigated [115,124-126].

Veratrum californicum (*V. californicum*) is native to the western United States and is rich in steroidal alkaloids, including cyclopamine, veratramine, isorubijervine and muldamine [6,24]. Of these alkaloids, the most notorious is cyclopamine, a teratogen antagonist of the Shh signaling pathway [44]. Interest in *V. californicum* arose in the 1950s when unsettling high incidences of craniofacial birth defects in lambs were observed by shepherds in Idaho. Numerous review articles have recounted the history of scientific interest in the *V. californicum*, the efforts undertaken by researchers at the Poisonous Plant Research Laboratory in Logan, UT to identify and validate the causative agents of the observed birth defects, and the chronological order of the isolation and structural elucidation of individual steroidal alkaloids [89,78,103]. However, few reports in the literature have used modern, highly sensitive analytical techniques to examine the full array of steroidal alkaloids in *V. californicum* [114]. Our lab has implemented extraction techniques of the root and rhizome of *V. californicum* aimed at isolating these steroidal alkaloids and characterizing their bioactivity towards Hh signaling using Shh-Light II cell assays [114,103]. In the current study, we used ethanol extraction of the leaves, stems and roots of *V. californicum* to determine if alkaloid ratios in the extract yield synergistic amplification of Hh signaling suppression as compared to traditional single alkaloid activity. The extracts were characterized using liquid chromatography and high resolution electrospray ionization time of flight tandem mass spectrometry, and their

biological activity was tested using Shh-Light II cells. The concentrations of cyclopamine, veratramine, isorubijervine and muldamine were determined, and mixtures of commercially available standards were prepared in the same ratios as found in the extracts derived from the leaf, stem and root/rhizome of *V. californicum*. We sought to test whether well-characterized steroidal alkaloids, at ratios consistent with native plant content, exhibited a synergistic effect to inhibit Hh pathway signaling commensurate with plant extract. Additionally, we sought to determine if additional alkaloids present in the *V. californicum* contribute to Hh signaling inhibition. Earlier investigations of *V. californicum* alkaloids may have failed to identify less abundant alkaloids that are biologically significant and potentially valuable novel Hh pathway signaling antagonists.

3.4 Results

3.4.1 Qualitative Comparison of *V. californicum* Alkaloids by Plant Part

Qualitative variation is observed in the alkaloid composition of *V. californicum* by plant part. The alkaloid profiles of the extracts from the leaf, stem and root/rhizome of *V. californicum* are shown in **Figure 3.1 a-c**. Identification of each alkaloid peak was achieved by high resolution mass spectrometry and verified by elution time compared to commercially available standards. Data for most prominent peaks labelled in **Figure 3.1 a-c** including retention time, m/z, molecular formula (MF) and alkaloid identity are summarized in **Table 2**. Mass spectra showing the m/z for each alkaloid used to estimate molecular formulas listed in **Table 2** are shown in **Figure 3.2**.

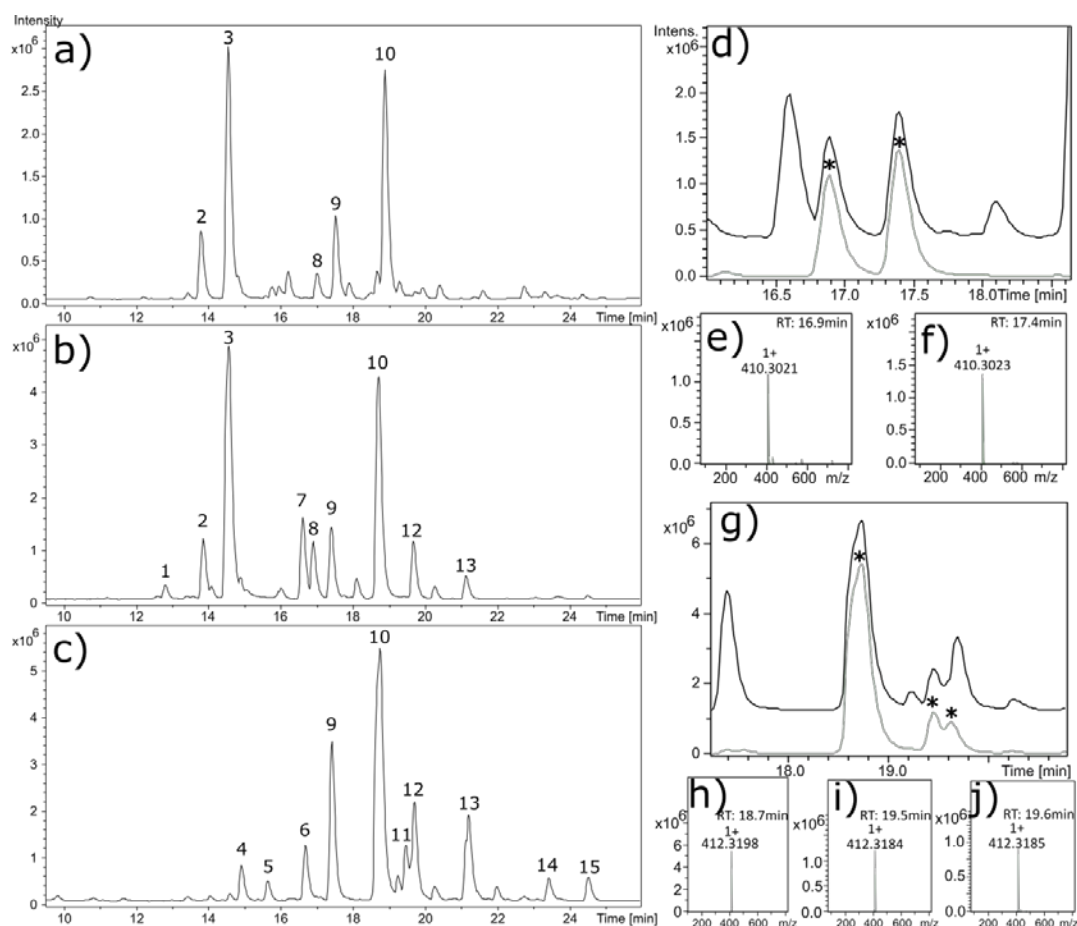


Figure 3.1. Alkaloid chromatograms of *V. californicum* by plant part.

Chromatograms for extracts from the **a)** leaf, **b)** stem, and **c)** root/rhizome of *V. californicum*. Common and unique alkaloids identified by MS are observed in each extract. Labelled peaks correspond to the data summarized in **Table 2**. Extracted ion chromatograms (EIC) are shown in **d)** and **g)** demonstrating the presence of veratramine and cyclopamine isomers in stem and root/rhizome extracts, respectively. The total ion chromatogram is shown in **d)** for the stem extract (black) and EIC (grey) generated using the m/z window 410.3023 ± 0.01 . The mass spectra for the peaks indicated by * in **d)** are shown in **e)** and **f)**. The total ion chromatogram is shown in **g)** for the root extract (black) and the EIC (grey) generated m/z window 412.3186 ± 0.02 . The mass spectra for the peaks indicated by * in **g)** are shown in **h-j)**.

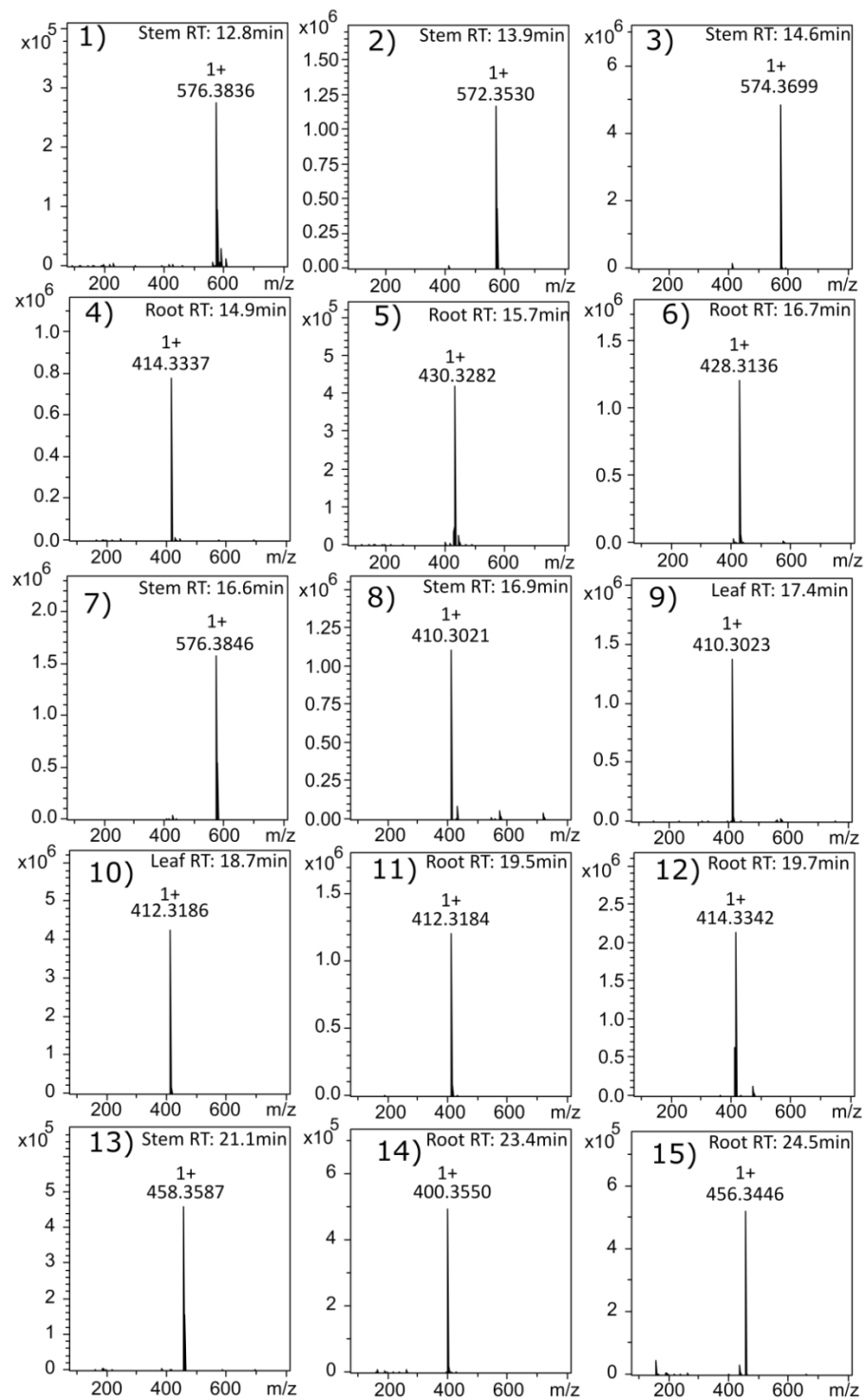


Figure 3.2. Mass spectra data showing the m/z, retention time and source for each alkaloid used to estimate molecular formulas listed in Table 2.

Table 2. Alkaloid list extracted from *V. californicum* leaf, stem and root. Summary data of corresponding to the peaks identified in Figure 3.1 a-c.

Peak	Retention Time (min)	m/z	Molecular Formula	Alkaloid
1	12.8	576.3836	C ₃₃ H ₅₃ NO ₇	N/A
2	13.9	572.3530	C ₃₃ H ₄₉ NO ₇	Veratrosine
3	14.6	574.3699	C ₃₃ H ₅₁ NO ₇	Cycloposine
4	14.9	414.3337	C ₂₇ H ₄₃ NO ₂	N/A ¹
5	15.7	430.3282	C ₂₇ H ₄₃ NO ₃	N/A
6	16.6	428.3136	C ₂₇ H ₄₁ NO ₃	N/A
7	16.7	576.3846	C ₃₃ H ₅₃ NO ₇	N/A
8	16.9	410.3021	C ₂₇ H ₃₉ NO ₂	Veratramine
9	17.4	410.3023	C ₂₇ H ₃₉ NO ₂	N/A ²
10	18.7	412.3186	C ₂₇ H ₄₁ NO ₂	Cycloamine
11	19.5	412.3184	C ₂₇ H ₄₁ NO ₂	N/A ³
12	19.7	414.3342	C ₂₇ H ₄₃ NO ₂	Isorubijervine
13	21.1	458.3587	C ₂₉ H ₄₇ NO ₃	Muldamine
14	23.4	400.3550	C ₂₇ H ₄₅ NO	N/A
15	24.5	456.3446	C ₂₉ H ₄₅ NO ₃	N/A

Cycloamine (Peak 10, m/z 412.3186) and veratramine (Peak 9, m/z 410.3023) were observed in extracts from each of the three plant parts. Alkaloids present in extracts from both the stem and leaf include cycloposine (Peak 3, m/z 574.3699) and veratrosine (Peak 4, m/z 572.3530), which are glycosylated cycloamine and veratramine, respectively. Peak 1 is a glycosylated alkaloid observed only in stem extract, with an m/z of 576.3836, corresponding to molecular formula C₃₃H₅₃NO₇. In the stem and root/rhizome extracts, isorubijervine (Peak 12, m/z 414.3342) and muldamine (Peak 13, m/z 458.3587) are both observed.

Peaks 4, 5, 6, 14 and 15 in **Figure 3.1c** correspond to unique alkaloids present only in the root/rhizome extract. These alkaloids have m/z of 414.3337, 430.3282, 428.3136, 400.3550 and 456.3446 and correspond to the estimated molecular formulas of $C_{27}H_{43}NO_2$, $C_{27}H_{43}NO_3$, $C_{27}H_{41}NO_3$, $C_{27}H_{45}NO$ and $C_{29}H_{45}NO_3$, respectively. Potential cyclopamine isomers were observed in the root extract, with a m/z consistent with cyclopamine observed to elute with three distinct retention times. **Figure 3.1g** shows the extracted ion chromatogram (EIC) for cyclopamine generated using the m/z window 412.3186 ± 0.02 , and the corresponding mass spectra are shown in **Figure 3.1h-j**. **Figure 3.1d** shows the EIC for veratramine using the m/z window 410.3023 ± 0.01 , and the corresponding mass spectra are shown in **Figure 3.1e-f**.

3.4.2 Quantitative Analysis of *V. californicum* Alkaloids

Quantification of cyclopamine, veratramine, isorubijervine and muldamine in alkaloid extracts were determined using charged aerosol detection and calibration curves generated from commercially available standards, with values of R^2 greater than 0.99. Extractions were performed three times, and alkaloid concentrations are shown by plant part in **Table 3** as mg of each alkaloid extracted per g of initial biomass \pm the standard deviation of the concentration observed in triplicate quantities. The quantity of cyclopamine was determined to be 0.21 ± 0.02 mg/g, 3.23 ± 0.16 mg/g, and 7.38 ± 0.08 mg/g for the leaf, stem and root/rhizome, respectively.

Table 3. Quantification of cyclopamine, veratramine, muldamine and isorubijervine by plant part. Alkaloid quantities are reported as mg of alkaloid per g of plant biomass.

Plant Part	Cyclopamine	Veratramine	Muldamine	Isorubijervine
Leaf	0.21 \pm 0.02	0.09 \pm 0.01	Not Detected	Not Detected

Stem	3.23±0.16	1.33±0.13	0.36±0.06	1.00±0.08
Root/Rhizome	7.38±0.08	3.07±0.14	3.47±0.23	2.92±0.09

3.4.3 Bioactivity Evaluation of Combined Standards and Plant Extracts

Alkaloid standard mixtures were created using commercially available standards in the same ratios as observed in the three plant parts. HPLC was used to validate that the alkaloid standard mixtures matched the concentrations of the ethanolic extract, as is shown for the root/rhizome extract and root standard mixture in **Figure 3.3**. The

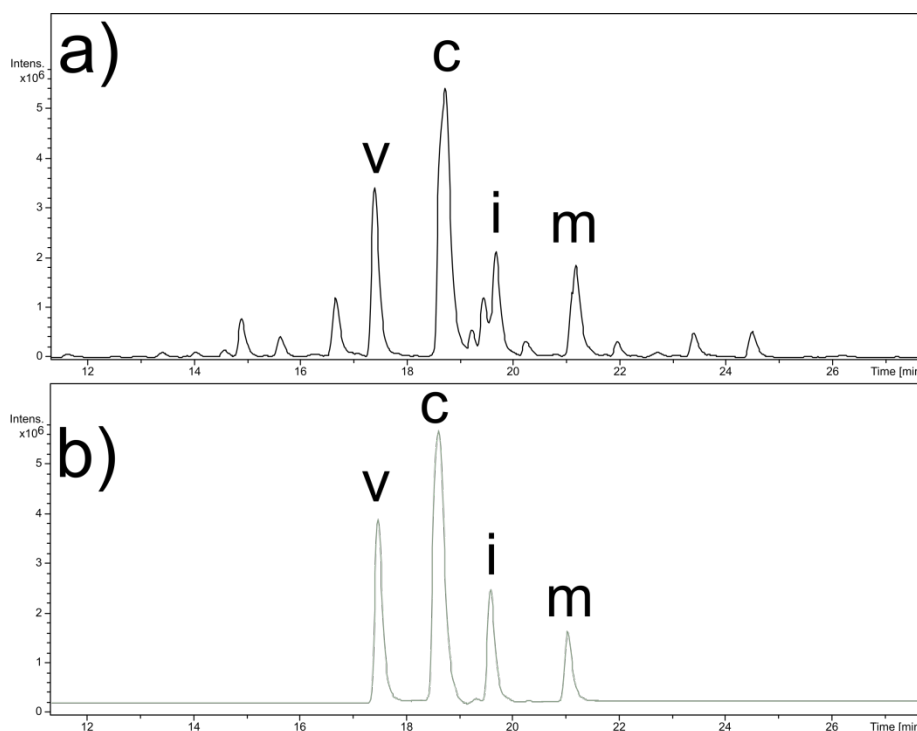


Figure 3.3. HPLC Comparison of ethanolic root extract with root standard mixture. a) ethanolic root extract and b) the root standard mixture, with each commercially available alkaloid indicated as follows: v, veratramine; c, cyclopamine; i, isorubijervine; and m, muldamine. Comparison of the HPLC chromatograms illustrates the quantitative similarity in the concentrations of the alkaloids for which commercial standards are available. Differences in bioactivity between these samples are due to the additional alkaloids present in the extract.

bioactivity of these alkaloid standard mixtures were quantified using Shh-Light II cells, and compared to cyclopamine alone at the same concentration, and to *V. californicum* extracts derived from leaf, stem, and root/rhizome of the plant. The treatment conditions evaluating Hh signaling inhibition in Shh-Light II cells are summarized in **Table 4** with extracts and alkaloid standard mixtures normalized to cyclopamine concentrations of 0.5 and 0.1 μM , referred to as “high concentration” and “low concentration” treatments

Table 4. Bioactivity treatment conditions for Shh-Light II cell assay.

Treatment Condition	Cyclopamine (μM)	Veratramine (μM)	Muldamine (μM)	Isorubijervine (μM)
Cyclopamine High	0.5	0	0	0
Leaf Standards High	0.5	0.2	0	0
Stem Standards High	0.5	0.2	0.15	0.05
Root Standards High	0.5	0.2	0.2	0.2
Cyclopamine Low	0.1	0	0	0
Leaf Standards Low	0.1	0.04	0	0
Stem Standards Low	0.1	0.04	0.03	0.01
Root Standards Low	0.1	0.04	0.04	0.04
Leaf Standards High - Cyc	0	0.2	0	0
Stem Standards High - Cyc	0	0.2	0.15	0.05
Root Standards High - Cyc	0	0.2	0.2	0.2

herein. The results of the biological assays are shown in **Figure 3.4**. There is no significant difference between cyclopamine, the alkaloid standard mixtures, and the plant extracts at high concentration treatments shown in **Figure 3.4a**. In the low concentration treatments shown in **Figure 3.4b**, there is no significant difference observed between cyclopamine standard, and the leaf standard mixture or the leaf extract, indicating that the addition of 0.04 μM veratramine in the standard mixture did not enhance Hh signaling inhibition. No difference is observed between the leaf extract at low concentration and the corresponding combined standard cocktail.

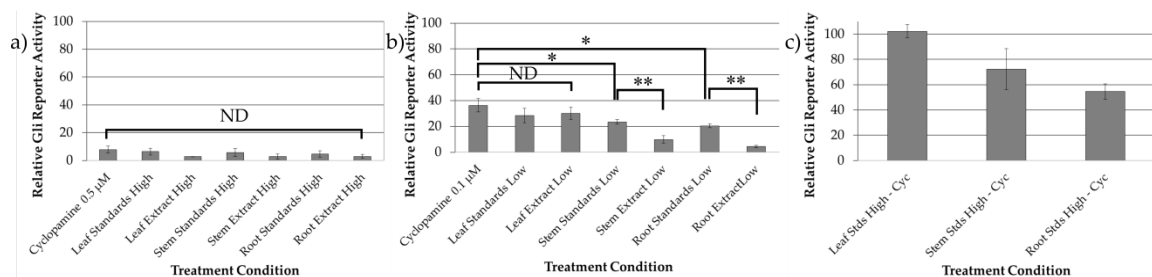


Figure 3.4. Bioactivity data for cyclopamine alone, the alkaloid standard mixtures and the plant extracts at a) high concentration (0.5 μM) and b) low concentration (0.1 μM). No significant difference was observed between treatment conditions at high concentration. Statistically noteworthy differences were observed in the low concentration treatments, and * indicates $P < 0.05$, and ** indicates $P < 0.01$. The inhibitory activity of veratramine, isorubijervine and muldamine in the absence of cyclopamine in the same concentrations as the high concentration treatment conditions is shown in c).

The alkaloid standard mixtures of the stem and root/rhizome samples were significantly different ($P < 0.05$) than cyclopamine alone at the same concentration, with relative Gli-reporter activity determined to $23.56 \pm 1.86\%$ and $20.59 \pm 1.50\%$ for the stem and root/rhizome, respectively, compared to $36.31 \pm 5.13\%$ for 0.1 μM cyclopamine. The inhibitory activity of these compounds was tested in the absence of cyclopamine in the same concentrations as the high concentration treatment conditions, and the results are shown **Figure 3.4c**. No Hh inhibition was shown for the leaf standards mixture minus cyclopamine (0.2 μM veratramine), indicating that veratramine does not inhibit the Hh signaling pathway. Modest Hh inhibition was demonstrated for the stem and root/rhizome standard mixtures minus cyclopamine, indicating that isorubijervine and muldamine demonstrate Hh antagonism.

There is a significant difference ($P < 0.01$) between the stem and root/rhizome extracts and their corresponding alkaloid standard mixtures, indicating that additional alkaloids present in the extracts are capable of inhibiting Hh signaling.

3.5 Discussion

The current investigation sought to achieve three objectives. The first was to provide a detailed analysis of the alkaloid composition of *V. californicum* based on plant part by performing a quantitative comparison of the alkaloids present in the leaf, stem and root/rhizome of the plant. The second was to evaluate the potential synergistic activity of cyclopamine, veratramine, isorubijervine and muldamine at ratios consistent with alkaloids present in three plant parts, and determine if the alkaloid combinations resulted in more effective Hh pathway antagonism than cyclopamine alone. The third was to determine if additional alkaloids present in the extracts contribute to Hh signaling inhibition by comparing the inhibitory potential of the plant extracts to alkaloid standard mixtures with identical concentrations of cyclopamine, veratramine, isorubijervine and muldamine.

Qualitative differences were observed in the alkaloid composition of *V. californicum* by plant part. Using high resolution mass spectrometry, we identified alkaloids that have previously been unreported for *V. californicum*. The molecular formula and mass of Peak 1 is consistent with that expected for glycosylated isorubijervine or etioline. Glycosylated etioline has previously been reported to be present in the root of *Solanum spirale* [127]. Additional investigation would be required to determine this definitely. Etioline is an intermediary in the biosynthetic pathway of cyclopamine, and its presence in the extract would not be surprising [89]. Peak 4, observed in only in the root/rhizome extract has a m/z and predicted molecular formula consistent with etioline. In this study, potential cyclopamine isomers (see **Figure 3.1g**) were observed in the root/rhizome extract analyzed by LC-MS. One of these potential

cyclopamine isomers may be dihydroveratramine, which has previously been identified in *Veratrum album* by Wilson, et al. [128]. However, the relative retention time between dihydroveratramine and cyclopamine observed by Wilson, et al. does not support this conclusion, because dihydroveratramine (RT: 13.66 min) was observed to elute prior to cyclopamine (RT: 15.09 min), whereas the purported cyclopamine isomer observed in this study elutes after cyclopamine (see **Table 2**) under similar HPLC conditions. No naturally occurring isomers of cyclopamine have been previously observed in *V. californicum*.

In Shh-Light II cells using the Dual-Glo® Luciferase Assay System, we evaluated the inhibition of Hh signaling of cyclopamine alone, combinations of alkaloid standards, and the inhibitory potential of extracts from each plant part. As shown in **Figure 3.4a**, there is no significant difference between cyclopamine, the alkaloid standard mixtures, and the plant extracts at high concentration treatments. There are trends that indicate enhanced inhibition of alkaloid standard mixtures and extracts compared to cyclopamine alone, but these do not amount to statistically significant differences. This result may be due to low levels of Gli reporter activity observed in each treatment. However, as demonstrated in **Figure 3.4b**, we determined that at the low concentration conditions, addition of muldamine, veratramine and isorubijervine enhance Hh signaling inhibition significantly in comparison to cyclopamine as demonstrated by the stem and root/rhizome standard mixtures. Addition of veratramine to cyclopamine does not enhance Hh signaling inhibition as demonstrated by the leaf standard mixture compared to cyclopamine alone. By replicating concentrations of cyclopamine, veratramine, isorubijervine and muldamine observed in plant extracts using commercially available

standards and comparing the inhibitory potential of the plant extracts to alkaloid standard mixtures, we determined that additional alkaloids present in the crude stem and root/rhizome extracts inhibit Hh signaling. The alkaloids present in the leaf extract include cycloposine, veratrosine, cyclopamine, veratramine, and the potential veratramine isomer labeled Peak 8 in **Figure 3.1**. No difference is observed between the leaf extract at low concentration and the corresponding combined standard mixture. This indicates that cycloposine, veratrosine and Peak 8 do not contribute to Hh signaling inhibition in this model system. However, it has been proposed that hydrolysis of the glycosidic linkage in glycosylated alkaloids during digestion contributes to the teratogenic effects of *V. californicum* alkaloids when consumed by foraging sheep [38]. Furthermore, no significant difference is observed between cyclopamine alone, the leaf standard mixture or the leaf extract, indicating that the addition of 0.04 μM veratramine in the standard mixture, or the additional alkaloids present in the leaf extract did not enhance Hh signaling inhibition. We observed a significant difference between the alkaloid standard mixtures of the stem and root/rhizome samples to that of cyclopamine, indicating the addition of veratramine, isorubijervine and muldamine enhance Hh inhibition. However, the modest enhancement of Hh inhibition seems to be additive rather than synergistic, with the addition of these alkaloids providing more, albeit weakly inhibitory effects. No Hh inhibition was demonstrated for 0.2 μM veratramine in the leaf standard minus cyclopamine treatment, indicating veratramine does not inhibit the Hh signaling pathway. This corroborates feeding trials in which veratramine was shown to cause teratogenic malformations in sheep distinct from the cyclopia, such as hypermobility of the knee joints leading to bow-legged lambs unable to stand [129]. The stem and root/rhizome

standard mixtures containing veratramine, isorubijervine and muldamine indicate that muldamine and/or isorubijervine inhibit the Hh pathway. Muldamine has been shown to result in craniofacial defects in hamsters in feeding studies that may be attributed to interruption of normal Hh signaling [105]. Further investigation to isolate, characterize, and assess the bioactivity of individual, less abundant alkaloids present in the stem and root/rhizome extracts is underway.

3.6 Materials and Methods

3.6.1 Chemicals and Solvents

Cyclopamine was purchased from Alfa Aesar (Ward Hill, MA), veratramine was purchased from Abcam Biotechnology Company (Cambridge, United Kingdom), and isorubijervine and muldamine were purchased from Logan Natural Products (Plano, TX). Extraction and purification solvents, 95% ethanol, ammonium hydroxide and chloroform were purchased from Fisher Scientific (Pittsburgh, Pennsylvania). High performance liquid chromatography (HPLC) mobile phases included 0.1% formic acid and HPLC grade acetonitrile (>99% purity, Fisher Scientific).

3.6.2 Sample Extraction and Preparation

A complete specimen of *V. californicum* was harvested in the Boise National Forest, Idaho at an elevation of 2134 m. The leaf, stem and roots/rhizomes of the plant were separated, and all plant parts were cut into smaller pieces to fit into quart size sealable bags. The specimens were placed in a cooler on a bed of ice for transportation. The biomass was collected at a late stage in the plant's life cycle; the plant had noticeable brown edges along its leaves and top indicating annual deterioration of above ground material in preparation for winter. Within two hours and upon arrival in the lab, the plant

material was chopped into 2 cm segments and dried for 14 hrs. using a LabConco Freezone 4.5 freeze drying unit, followed by storage at -20 °C. The biomass was flash frozen in liquid nitrogen, and pulverized into a fine powder using a mortar and pestle. Approximately 2.0 g of powdered biomass was added to a 250 mL round bottom flask followed by 100 mL of 95% ethanol. The resultant slurry was sonicated for 1 hr. and then agitated for 24 hrs. on a stir plate. The biomass was removed by vacuum filtration (Whatman filter paper, 0.45 µm), and solvent removed by rotary evaporation. The dried crude extract was dissolved in 10 mL of ethanol, and the solution was warmed to 40 °C and sonicated to achieve complete dissolution. Addition of 35% aqueous ammonia achieved alkaline solvent conditions (pH ≥10). The aqueous alkaline solution was added directly to a supported liquid extraction (SLE) column (Chem Elut, Agilent, Santa Clara, California) and allowed to adsorb for 10 min., followed by elution of alkaloids with chloroform (3×10 mL) using a vacuum manifold set to a pressure of 2 mbar. The chloroform fractions were combined, filtered, and evaporated to dryness. All samples were dissolved in 1 mL ethanol as a mixture of alkaloids.

3.6.3 Alkaloid Quantification

The concentrations of cyclopamine, veratramine, isorubijervine and muldamine in alkaloid extracts were determined by Thermo Scientific UltiMate 3000 HPLC equipped with a Corona Veo RS charge aerosol detector (CAD) and MSQ Plus mass spectrometer (MS). HPLC separation of alkaloids was achieved using a Thermo Acclaim 120 C₁₈ column (2.1 × 150 mm, 3 µm), and mobile phases consisting of 0.1% formic acid (v/v) in water (Buffer A) and 0.1% formic acid (v/v) in acetonitrile (Buffer B) with a flow rate of 0.3 ml/min. A linear gradient method beginning at 95% Buffer A and 5% Buffer B, up to

60% Buffer B over a 25 min. run time achieved desired separation of alkaloids from the extracts. Cyclopamine, veratramine, isorubijervine and muldamine standards were used to create a calibration curve at concentrations of 0.1, 0.5, 1.0, 5.0 and 10.0 mM with detection recorded by a CAD with the power function set to pA 1.70. The quantity of these alkaloids were determined from the alkaloid mixtures obtained from the leaf, stem and root extracts in triplicate.

3.6.4 Alkaloid Identification

In order to identify the steroidal alkaloids in *V. californicum* leaf, stem and root/rhizome extracts, samples were analyzed by HPLC-MS, where the mass spectrometer was an ultra-high resolution Quadrupole Time of Flight (QTOF) instrument (Bruker maXis). The electrospray ionization (ESI) source was operated under the following conditions: positive ion mode, 1.2 bar nebulizer pressure, 8 L/min flow of N₂ drying gas heated to a temperature of 200 °C, 3000 V to -500 V voltage between HV capillary and HV end-plate offset, mass range set from 80 to 800 m/z, and the quadrupole ion energy at 4.0 eV. Sodium formate was used to calibrate the system in this mass range of 80 to 800 m/z. HPLC separation was achieved using a XTerra MS C₁₈ column, 3.5 µm, 2.1 x 150 mm (Waters, Milford, MA). The flow rate was 250 µL/min. The mobile phases were 5% acetonitrile and 0.1% formic acid in water (Buffer A) and acetonitrile and 0.1% formic acid (Buffer B). The linear gradient method was used to separate analytes starting at 5% Buffer B and increasing to 60% Buffer B over 25 min. A 1 µL sample injection was used. Data were analyzed with the Compass Data Analysis software package (Bruker Corporation, Billerica, Massachusetts).

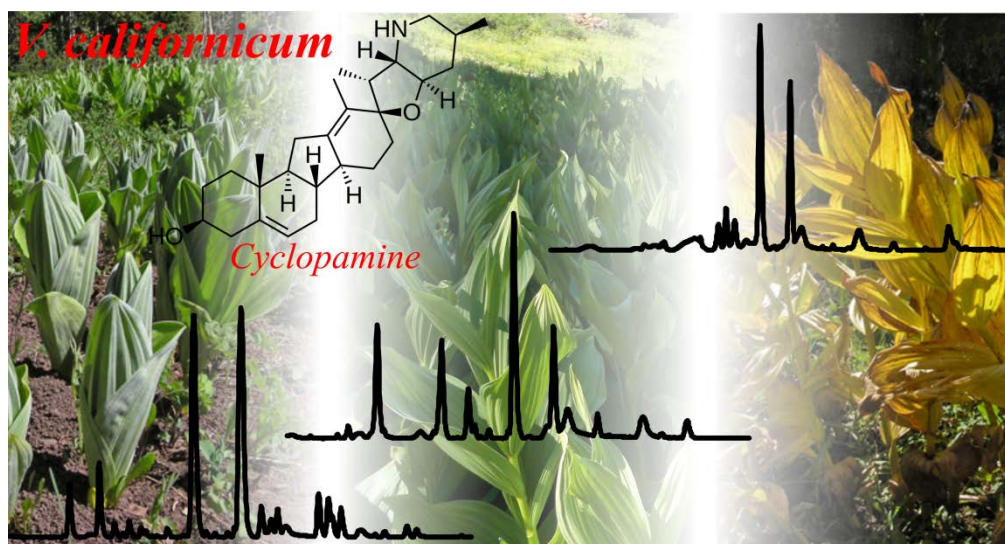
3.6.5 Cell Culture

Shh-Light II cells (JHU-068) were maintained in Dulbecco's Modified Eagle Medium (DMEM) (Gibco) supplemented with 0.4 mg/mL geneticin, 0.15 mg/mL Zeocin™ (Invitrogen), and 10% bovine calf serum. The cells were grown at 37°C in an atmosphere of 5% CO₂ in air and 100% relative humidity. This mouse embryonal NIH 3T3 cell line contains a stably transfected luciferase reporter with eight copies of the consensus Gli binding site [116]. Alkaloid treatment conditions were dissolved in ethanol and added to DMEM media containing 0.5% bovine calf serum.

3.6.6 Biological Assays

Shh-Light II cells were seeded in a 96-well plate and grown to complete confluence in the media described above. When cells were confluent, the media was replaced with DMEM supplemented with 0.5% bovine calf serum, and treated with 0.1 ng of N-terminal mouse recombinant Shh (R&D Systems, Minneapolis, Minnesota) dissolved in DMEM, and select alkaloid treatment. In each experiment, the controls and treatment wells contained all vehicles, with a final ethanol concentration of 0.05%. Gli activity in the Shh-Light II cell line was assayed 48 hrs. after treatment with Shh protein and select compounds using the Dual-Luciferase Reporter Assay System (Promega, Madison, Wisconsin). The Gli-activity was measured by luminescence emitted from cells using a BioTek Synergy H1m Microplate reader. The Gli-activity determined in the biological assay is presented as a relative response ratio (RRR) as described in the Dual-Luciferase Reporter Assay System manual. Each experiment was performed thrice.

CHAPTER FOUR: STEROIDAL ALKALOID VARIATION IN *VERATRUM CALIFORNICUM* AS DETERMINED BY MODERN METHODS OF ANALYTICAL ANALYSIS



Picture 3. Graphical abstract form “Steroidal alkaloid variation in *Veratrum californicum* as determined by modern methods of analytical analysis”

4.1 Foreword

The following chapter is based on a manuscript published in the journal *Fitoterapia* in 2019 [130]. This study was conducted using modern analytical methods and state-of-the-art instrumentation, and presents the ratio of steroidal alkaloids present in the aerial and root/rhizome of *Veratrum californicum* collected from two different growth plots throughout the growth cycle of the plants. This study further identifies the presence of *Veratrum californicum* steroidal alkaloids that have yet to be characterized.

4.2 Abstract

Veratrum californicum is a rich source of steroidal alkaloids, many of which have proven to be antagonists of the Hedgehog (Hh) signaling pathway that becomes aberrant in over twenty types of cancer. These alkaloids first became known in the 1950's due to their teratogenic properties, which resulted in newborn and fetal lambs developing cyclopia as a result of pregnant ewes consuming *Veratrum californicum*. It was discovered that the alkaloids in *V. californicum* were concentrated in the root and rhizome of the plant with much lower amounts of the most active alkaloid, cyclopamine, present in the aerial plant, especially in the late growth season. Inspired by the limitations in analytical instrumentation and methods available to researchers at the time of the original investigation, we have used state-of-the-art instrumentation and modern analytical methods to quantitate four steroidal alkaloids based on study parameters including plant part, harvest location, and growth stage. The results of the current inquiry detail differences in alkaloid composition based on the study parameters, provide a detailed assessment for alkaloids that have been characterized previously (cyclopamine, veratramine, muldamine and isorubijervine), and identify at least six alkaloids that have not been previously characterized. This study provides insight into optimal harvest time, plant growth stage, harvest location, and plant part required to isolate, yet to be characterized, alkaloids of interest for exploration as Hh pathway antagonists with desirable medicinal properties.

4.3 Introduction

Congenital malformations in lambs were observed in alarming frequency during the first half of the 20th century in south-western Idaho, and beginning in 1956 a detailed

study of the malformed lamb problem was undertaken by researchers from the United States Department of Agriculture [131]. The affected lambs were commonly called “monkey-faced,” and were observed to have head deformities that included complete cyclopia, hydrocephalus, harelip, cleft palate, and displacement of the nose. Observations by ranchers with affected animals implicated mountain ranges with altitudes up to 10,000 feet containing alpine meadows used for grazing during the breeding season, typically in early August. Controlled breeding experiments determined the congenital anomaly was not due to genetic factors, and potential environmental elements including an excess or deficiency of nutritional factors, toxic mineral elements, or the presence of poisonous plants were assumed to underlie the observation. Field studies determined that deformities occurred in lambs from ewes that grazed during the latter part of the summer in wet seepage meadows above 6,000 feet in elevation, locations where *Veratrum californicum* is commonly encountered [31]. Subsequent controlled feeding trials of fresh and dried green *V. californicum* reproduced the deformities observed in the field, and validated the teratogenic role of *V. californicum* [33]. Following the confirmation that ingestion of *V. californicum* by pregnant ewes was responsible for the observed malformations, attention was turned toward the isolation and characterization of teratogenic compounds underlying the phenomenon of fetal malformation [34]. The teratogenic material was speculated to be steroidal alkaloids, either in the form of glycosidic derivatives or the parent alkaline. The compound responsible for the cyclopic malformations was found and given the trivial name cyclopamine [132]. Benzene extraction of *V. californicum* root and subsequent separation with paper chromatography revealed eight to ten unique alkaloids. In order to purify adequate

quantities of alkaloids for additional chemical characterization, recrystallization of crude benzene extracts from acetone-water and methanol-water allowed for the enrichment of three alkaloids –veratramine, cyclopamine and an unknown compound designated as alkaloid Q.

Feeding experiments and field observations suggested that significant variation was observed in the teratogenic effect of *V. californicum* on lambs that consumed the plant at differing growth sites and growing periods [133]. The content of cyclopamine as a function of plant part, stage of growth, and growth location was undertaken by Keeler and Binns circa 1970. In their study, benzene soluble steroidal alkaloids were isolated and total alkaloid concentrations were determined by measuring turbidity following treatment with Mayer reagent, and the concentrations of individual alkaloids were assigned based upon densitometry on photographed thin layer chromatography (TLC) plates. The TLC measurements separated three principal benzene soluble alkaloids: cyclopamine, veratramine, and alkaloid Q. The level of cyclopamine varied considerably between collection sites and stage of growth. Generally, it was determined that the concentration of cyclopamine was highest in the early growth season in the leaves, and in the late growing season in the root/rhizome. The structure of alkaloid Q was later elucidated, and was given the trivial name, muldamine [134].

Decades after the observation of the malformed lambs led to the isolation and characterization of cyclopamine, the teratogenic mechanism of cyclopamine was determined to be inhibition of the Hedgehog (Hh) signaling pathway [44]. The Hh signaling pathway is required for proper development of all animals containing bilateral symmetry and guides the formation of hands and feet, the central nervous system, and

most epithelial tissues [16,135-137]. In mammals, the mechanism of the Hh signaling begins with the binding of one of three secreted ligands; Sonic hedgehog (Shh), Desert hedgehog (Dhh) or Indian hedgehog (Ihh) to the transmembrane transporter protein Patched (Ptch) [17]. Ptch, when not bound to one of these Hh ligands, inhibits the seven-transmembrane protein Smoothed (Smo), a G protein-coupled-like receptor. Upon binding with Hh ligands, this inhibition is inactivated, and a signaling cascade originating at Smo begins; the pathway culminates in the activation of the Gli family of zinc-finger transcription factors in vertebrates. The Gli transcription factors (particularly Gli-1 and Gli-2) up-regulate the transcription of Hh target genes, which enhance cellular proliferation and the epithelial-mesenchymal transition [5,138-140]. Although normal to development and several adult somatic processes, Hh signaling has been demonstrated to contribute to the pathogenesis of over twenty cancers, and is exceedingly active in basal cell carcinoma (BCC) [89]. The medicinal properties and potential for discovery of therapeutic compounds, like those found in *V. californicum*, are the reason considerable interest persists in the identification of novel Hh signal inhibitors, including those isolated from natural sources [115,124-125].

Few reports in the literature have used modern, highly sensitive analytical techniques to examine the full array of steroidal alkaloids in *V. californicum*. Our lab has surveyed and optimized steroidal alkaloid extraction conditions and employed state-of-the-art analytical instrumentation leading to identification of less abundant alkaloids present in *V. californicum* extracts [114]. We have also correlated extraction methods with teratogenic properties using Shh-Light II cell assays to determine how isolation of alkaloids using different chemical treatments alters the potency of cyclopamine [103].

Recently, our lab demonstrated that uncharacterized alkaloids present in *V. californicum* inhibit the Hh signaling pathway by comparing commercially available alkaloid standards to alkaloids extracted from plant specimens [117]. We first determined the concentration of four commercially available alkaloids –cyclopamine, veratramine, muldamine and isorubijervine– present in the ethanolic extract of *V. californicum*, replicated the concentration of those alkaloids observed in the crude extract in a cocktail from commercially available standards, and compared the inhibitory effect of crude extracts to the mixture of alkaloid standards. Using Shh Light II cells and a luminescence based assay, significant differences were observed for Hh pathway inhibition between the stem and root/rhizome extracts and their corresponding alkaloid standard mixtures, indicating that uncharacterized alkaloids present in plant extracts contribute to Hh signaling inhibition. In the current study, we quantify the amounts of four steroidal alkaloids –cyclopamine, veratramine, muldamine and isorubijervine– in *V. californicum* as a function of plant part, growth cycle and collection location. The molecular structures of the alkaloids quantified in this study are shown in **Figure 2.2**. In addition to providing quantitative data for these four compounds, we provide a qualitative examination of the chemical diversity of alkaloids present in *V. californicum*. At least six alkaloids with unique molecular weight, molecular formula, and identity are reported, constituting potential drug targets for Hedgehog pathway inhibition.

4.4 Materials and Methods

4.4.1 Materials

Plants were gathered from alpine meadows in the Boise National Forest in 2014 and stored in a freezer. All solvents were purchased from commercial sources and used

without further purification. The solvents used were ethanol (95%), chloroform (HPLC grade), formic acid (MS grade), ammonium hydroxide (30% in water), and acetonitrile (HPLC grade), all obtained from Fischer Scientific (Hampton, NH, USA).

4.4.2 Plant collection

Plants were harvested from two stands of *V. californicum* near the Bogus Basin Mountain Resort, Boise National Forest, Idaho, USA. *V. californicum*, also known as California false hellebore, grows up to 2 m in height, has cornstalk-like stems and has large, broad elliptical leaves [141,142]. Plants were harvested at 6901 feet, elevation (N43 45.719" W 116 05.327") beside the Shindig Trail, and at 7066 feet elevation (N43 45.858" W 116 05.090") beside the Elk Meadows Trail. In each location, three to five full plants were harvested; the rhizome and aerial plant were separated, and transported on ice to the lab. Once in lab, plant parts were diced, followed by drying with a LabConco Freezone 4.5 freeze drying unit (Labconco Corporation, Kansas City, MO, USA), before being stored at -20°C. Plants were harvested on May 23, 2014, July 3, 2014, and September 5, 2014 at both locations.

4.4.3 Biomass preparation

To prepare for extraction, the biomass was removed from the freezer, cut into even smaller pieces (1-2 cm cubes) and placed in a lyophilizer for 24-48 hours to ensure dryness. Once dried the samples were submerged in liquid nitrogen, and crushed to a fine powder by mortar and pestle.

4.4.4 Alkaloid extraction

Approximately 2.0 g of powdered biomass was added to 100 mL of 95% ethanol and the mixture was placed in a sonicator for 30 min, followed by agitation for 24 hrs. on

a stir plate. The plant material was separated from the solvent by vacuum filtration (Whatman filter paper, 0.45 μm), and the solid material discarded. The ethanol was removed by rotary evaporation to yield the crude alkaloids. The alkaloids were dissolved in 10 mL of 95% ethanol, and the solution was warmed to 40 °C and sonicated to achieve complete dissolution. Addition of 35% aqueous ammonia achieved alkaline solvent conditions ($\text{pH} \geq 10$). The alkaline solution was added directly to a supported liquid extraction (SLE) column (ChemElut, Agilent, Santa Clara, CA, USA) and allowed to adsorb for 10 min, followed by elution of alkaloids with chloroform (3×10 mL) using a vacuum manifold set to a pressure of 2 mbar. The chloroform fractions were combined, filtered, and evaporated to dryness. All samples were dissolved in 1 mL of 100% ethanol as a mixture of alkaloids.

4.4.5 Alkaloid Quantification

The concentrations of cyclopamine, veratramine, isorubijervine and muldamine in alkaloid extracts were determined using an UltiMate 3000 uHPLC (Thermo Scientific, Waltham, MA, USA) equipped with a Corona Veo RS charged aerosol detector (CAD) and MSQ Plus mass spectrometer (MS). HPLC separation of alkaloids was achieved using a Thermo Acclaim 120 C_{18} column (2.1×150 mm, 3 μm), and mobile phases consisting of 0.1% formic acid (v/v) in water (Buffer A) and 0.1% formic acid (v/v) in acetonitrile (Buffer B) with a flow rate of 0.3 mL/min. A linear gradient method beginning at 95% Buffer A and 5% Buffer B, up to 60% Buffer B over a 25 min. run time achieved desired separation of alkaloids from the extracts. Cyclopamine (Alfa Aesar, Ward Hill, MA, USA, >99% purity), veratramine (Abcam Biotechnology Company, Cambridge, UK, >98% purity), isorubijervine (Logan Natural Products, Plano, TX, USA,

99% purity) and muldamine (Logan Natural Products, Plano, TX, USA, 99% purity) standards were used to create a calibration curve at concentrations of 0.1, 0.5, 1.0, 5.0 and 10.0 mM with detection recorded by CAD with the power function set to pA 1.70. Calibration curves were generated in triplicate for each alkaloid at each of the five alkaloid concentrations. The quantities of these alkaloids were determined from the alkaloid mixtures obtained from the aerial and root/rhizome extracts in triplicate. Quantification was achieved using an intra-lab validated HPLC method. Limits of detection and limits of quantification were determined from the slope and the standard deviation observed from linear calibration curves.

4.4.6 Alkaloid Identification

To identify the steroidal alkaloids in *V. californicum* aerial and root/rhizome extracts, samples were analyzed by HPLC-MS, where the mass spectrometer was an ultra-high resolution Quadrupole Time of Flight (QTOF) instrument (Bruker maXis, Billerica, MA, USA). The electrospray ionization (ESI) source was operated under the following conditions: positive ion mode, 1.2 bar nebulizer pressure, 8 L/min flow of N₂ drying gas heated to a temperature of 200 °C, 3000 V to -500 V voltage between HV capillary and HV end-plate offset, mass range set from 80 to 800 m/z, and the quadrupole ion energy at 4.0 eV. Sodium formate was used to calibrate the system in this mass range. HPLC separation was achieved using a XTerra MS C₁₈ column, 3.5 μm, 2.1 × 150 mm (Waters, Milford, MA, USA). The flow rate was 250 μL/min. The mobile phases were 5% acetonitrile and 0.1% formic acid in water (Buffer A) and acetonitrile and 0.1% formic acid (Buffer B). The linear gradient method was used to separate analytes starting at 5% Buffer B and increasing to 60% Buffer B over 25 min. A 1 μL sample injection

volume was used. Data were analyzed with the Compass Data Analysis software package (Bruker Corporation).

4.5 Results

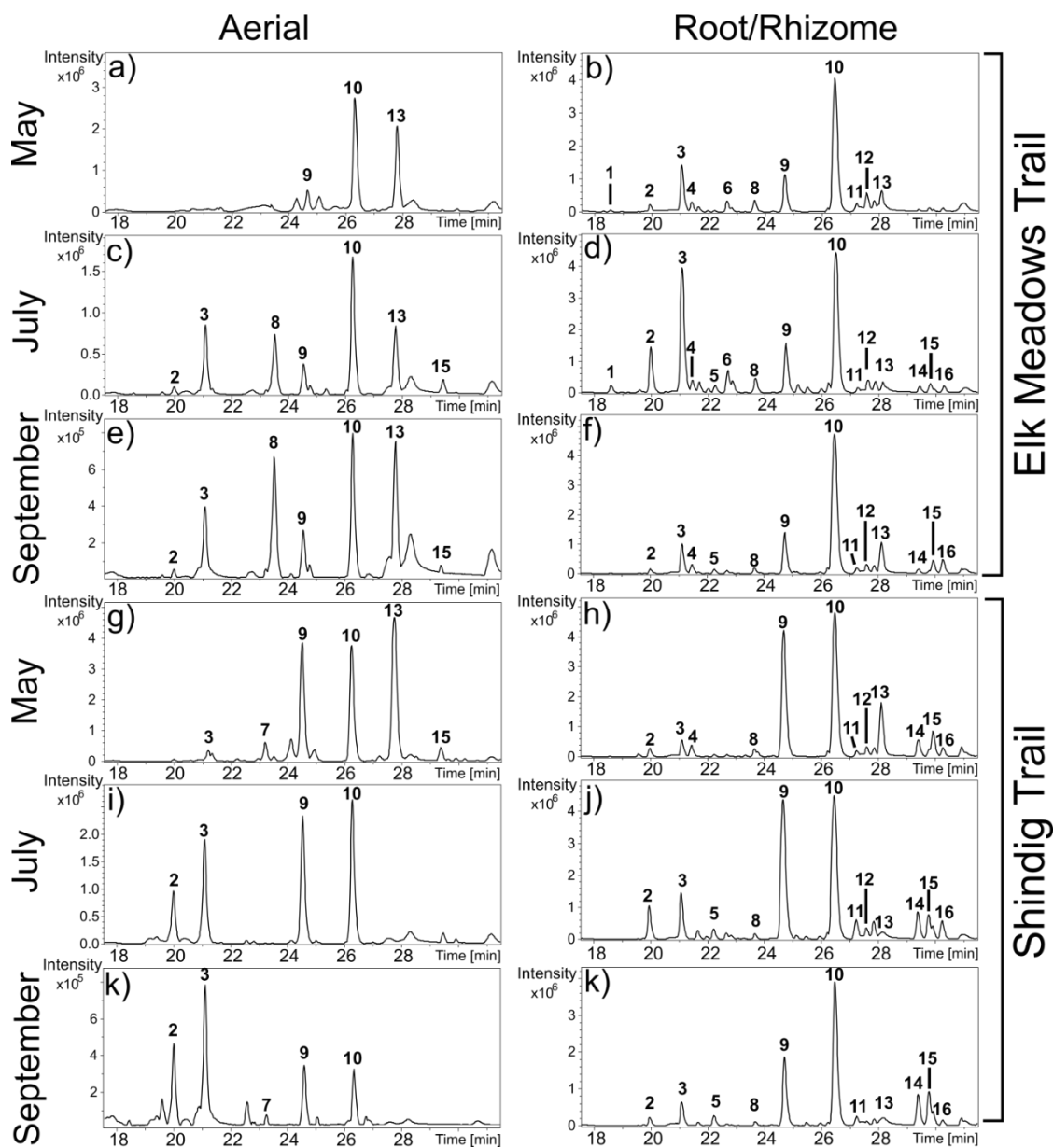


Figure 4.1. Chromatograms of alkaloids extracted from above-ground and below-ground *V. californicum* from two collection sites. Elk Meadows (a-f) and Shindig (g-l) collection sites from aerial and roots/rhizomes of *V. californicum*. Common and unique alkaloids identified by MS are observed in each extract. Labeled peaks correspond to the data summarized in Table 5. The chromatograms displayed were generated as base peak chromatograms from data acquired on a Q-TOF mass spectrometer.

Qualitative variation was observed in the alkaloid composition of *V. californicum* by plant part, growth stage, and harvest location, as shown in the alkaloid profiles of the extracts in **Figure 4.1 a-l**. Identification of each alkaloid peak was achieved by high resolution mass spectrometry and verified by elution time compared to commercially available standards. Data for the peaks labelled in **Figure 4.1 a-l**, including retention time, m/z, molecular formula (MF) and alkaloid identity are summarized in **Table 5**.

Table 5. Summary data corresponding to the peaks identified in Figure 4.1.

Peak	Retention Time (min)	m/z	Estimated Molecular Formula	Alkaloid
1	18.6	576.396	C ₃₃ H ₅₃ NO ₇	N/A
2	20.0	572.365	C ₃₃ H ₄₉ NO ₇	Veratrosine
3	21.1	574.381	C ₃₃ H ₅₁ NO ₇	Cycloposine
4	21.5	414.342	C ₂₇ H ₄₃ NO ₂	Etioline?
5	22.3	430.337	C ₂₇ H ₄₃ NO ₃	Tetrahydrojervine?
6	22.7	574.381	C ₃₃ H ₅₁ NO ₇	N/A
7	23.2	428.320	C ₃₃ H ₅₃ NO ₇	Dihydrojervine?
8	23.6	576.397	C ₃₃ H ₅₃ NO ₇	N/A
9	24.7	410.312	C ₂₇ H ₃₉ NO ₂	Veratramine
10	26.5	412.326	C ₂₇ H ₄₁ NO ₂	Cyclopamine
11	27.2	410.311	C ₂₇ H ₃₉ NO ₂	N/A
12	27.6	412.326	C ₂₇ H ₄₁ NO ₂	N/A
13	28.1	414.343	C ₂₇ H ₄₃ NO ₂	Isorubijervine
14	29.4	416.357	C ₂₇ H ₄₅ NO ₂	22-keto-26-aminocholesterol?
15	29.8	458.370	C ₂₉ H ₄₇ NO ₃	Muldamine
16	30.2	398.347	C ₂₇ H ₄₃ NO	Verazine?

Mass spectra for peaks 1-16 are presented in **Figure 4.3**, showing the retention time and m/z used to estimate molecular formulas provided in **Table 5**. **Figure 4.2** shows quantitative determination of the four common *Veratrum* alkaloids cyclopamine, veratramine, isorubijervine, and muldamine for which commercially available standards were available to obtain calibration curves and accurately determine alkaloid quantity. In general, significantly higher alkaloid concentrations and alkaloid diversity are observed in the root/rhizomes in both locations as compared to the aerial plant. Alkaloid concentration is given as mg alkaloid per g of biomass used for extraction, and the

standard deviation for triplicate sampling is shown. During each collection a minimum of three plant samples were collected and the standard deviation primarily reflects variation in alkaloid concentrations observed between individual plants, and to a lesser extent technical variation in extraction efficiency. The limit of quantification was determined 0.011, 0.011, 0.010 and 0.015 mg/g for cyclophamine, veratramine, muldamine and isorubijervine, respectively; and the limit of detection was determined to be 0.003, 0.003, 0.003 and 0.005 mg/g for cyclophamine, veratramine, muldamine and isorubijervine, respectively.

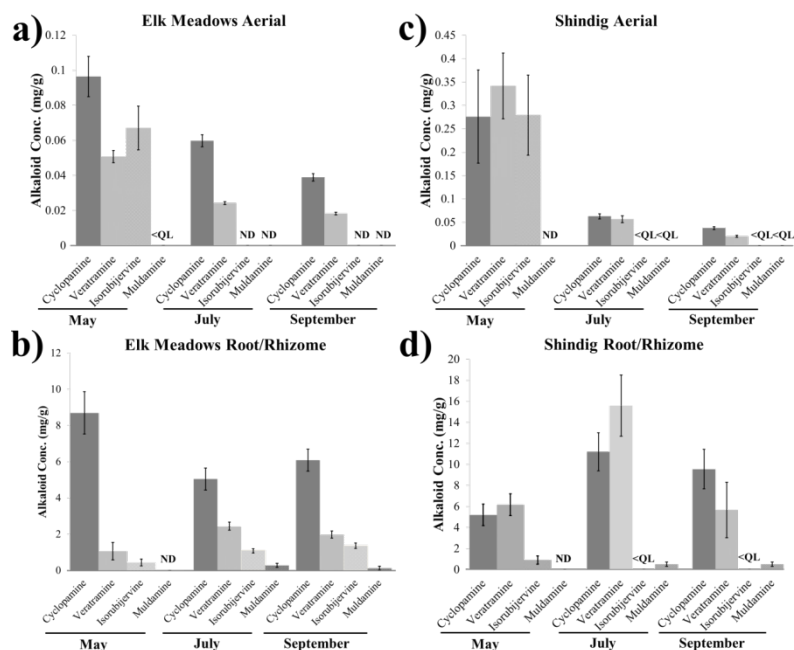


Figure 4.2. Quantification of alkaloids from both harvest sites for aerial and below ground *V. californicum*. Alkaloid concentration is presented as mg alkaloid per g of plant biomass extracted. Significantly higher concentrations were observed in the below ground plant as compared to the aerial plant. Quantification data was generated using charged aerosol detection and calibration curves created from commercially available alkaloid standards.

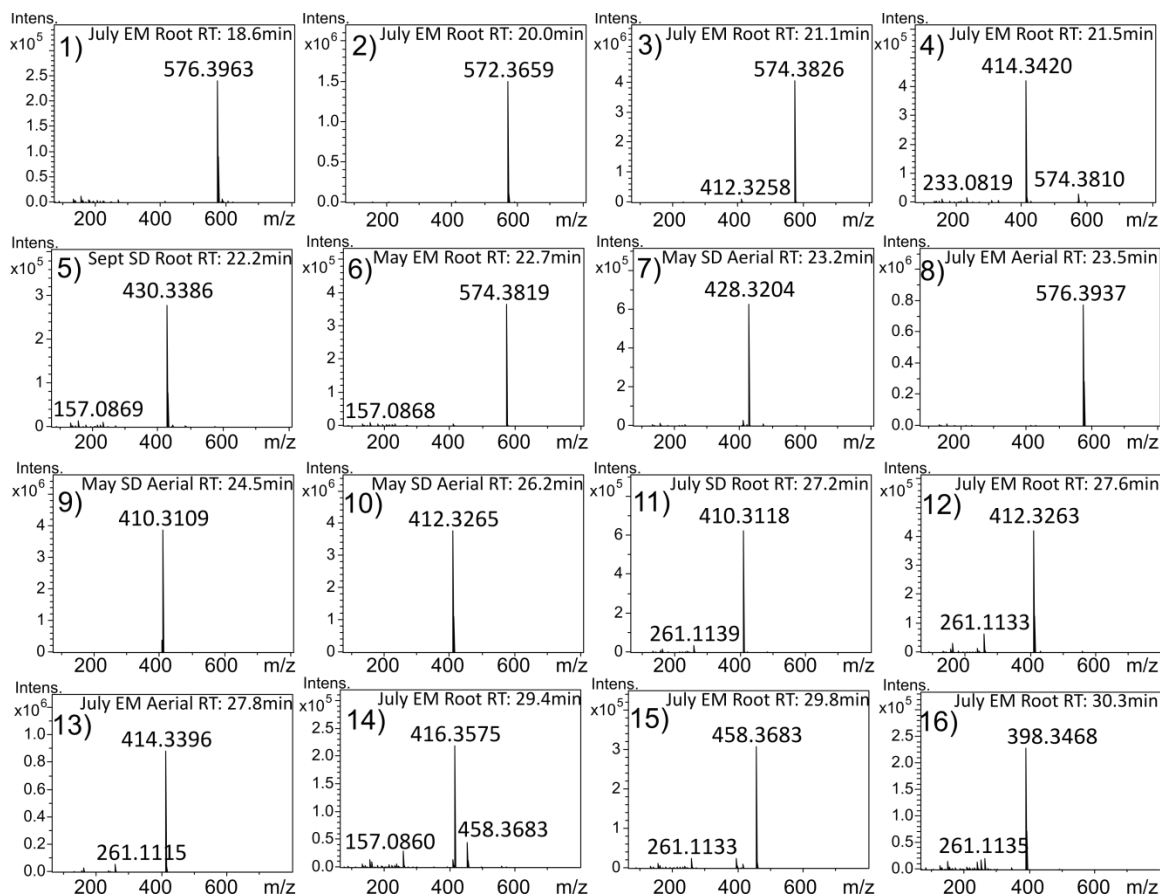


Figure 4.3. Mass spectra from the peaks identified from Figure 4.1 used to generate the data in Table 5. Included is the retention time (R_T) and sample from which the MS data was taken. MS data was acquired using an ultra-high resolution Q-TOF mass spectrometer with mass error <5 ppm.

4.5.1 Root/rhizome alkaloid variation

Specimens collected from the Elk Meadows site showed the highest concentration of cyclopamine in the root/rhizome collected in the early season, May 2014, with 8.69 ± 1.17 mg/g extracted; whereas the July and September collections yielded 4.14 ± 0.50 mg/g and 5.01 ± 0.50 mg/g, respectively. Interestingly, collections from the Shindig site showed the lowest rhizome concentration of cyclopamine in May at 5.20 ± 1.02 mg/g, with significantly higher concentrations observed in July and September, at 11.01 ± 1.02 mg/g and 9.39 ± 1.85 mg/g, respectively. From the Shindig location, a fluctuation in rhizome alkaloid concentration was observed for veratramine similar to that of

cyclopamine, with the highest concentration observed in July at 15.35 ± 2.86 mg/g, and 6.16 ± 1.03 mg/g and 5.57 ± 2.60 mg/g for May and September, respectively. Strangely, the concentration of veratramine was much lower throughout the growth season in the samples collected from Elk Meadows, with the greatest concentration observed in July at 1.98 ± 0.20 mg/g, and 1.06 ± 0.48 mg/g 1.63 ± 0.16 mg/g observed for May and September, respectively.

From both harvest locations, muldamine and isorubijervine were less abundant in the root/rhizome than either cyclopamine or veratramine. From Elk Meadows, isorubijervine was detected above the quantification limit from each sampling period, with the greatest abundance of 1.12 ± 0.12 mg/g in September, and the lowest abundance in May at 0.44 ± 0.19 mg/g. However, from the Shindig location, only the May extract yielded a quantifiable amount of isorubijervine, measured at 0.91 ± 0.39 mg/g. However, qualitative detection of isorubijervine was observed below quantification limit from the Shindig site for both the July and September collection times. From both locations, muldamine was only present above the limit of quantification in the July and September extracts. From Elk Meadows, muldamine was not detected in the May sample, and was determined to be 0.21 ± 0.09 and 0.10 ± 0.08 mg/g for the July and September samples, respectively. The high standard deviation relative to the concentrations determined reflects that observed concentrations varied significantly between plant extracts. For the July extracts, muldamine was only detected above the limit of quantification in two of the three samples analyzed, and only one of three for the September extracts. From Shindig, muldamine was detected in all the extracts, although it was below the limit of detection for May, and July and September yielded 0.48 ± 0.20 mg/g and 0.48 ± 0.42 mg/g,

respectively. Again, concentrations varied considerably between individual plants, with muldamine only detected above the limit of quantification in two of the three samples analyzed for July and one of three for September.

4.5.2 Aerial plant alkaloid variation

In the aerial plant at both harvest locations, the concentration of each alkaloid quantified was highest in May, and was observed to decrease progressively throughout the growth season. For the Elk Meadow location, concentrations of cyclopamine varied from 0.28 ± 0.10 mg/g in May to 0.03 ± 0.00 mg/g in September, while at the Shindig site concentrations varied from 0.10 ± 0.01 mg/g in May to 0.04 ± 0.00 mg/g in September. Veratramine concentrations at the Elk Meadows plot varied between 0.34 ± 0.07 mg/g in May and 0.02 ± 0.00 mg/g in September, and for the Shindig site, veratramine levels were determined to be 0.05 ± 0.00 in May and 0.02 ± 0.00 mg/g in September. Muldamine was either not detected or below the quantification limit in the aerial plant from both locations and during each collection period. Relatively high levels of isorubijervine were detected in the aerial plant in May at both sites, and were determined to be 0.28 ± 0.09 and 0.07 ± 0.01 mg/g for Elk Meadows and Shindig, respectively. These levels were not sustained through the growth season, as all other measurements were below the limit of quantification, or were not detected.

4.6 Discussion

The current investigation sought to explore the diversity of alkaloids from *V. californicum* by plant part, location, and growth stage. In order to provide a detailed analysis of the alkaloid composition of *V. californicum* based on plant part, a quantitative comparison of four alkaloids was performed for –cyclopamine, veratramine,

isorubijervine and muldamine— present in the aerial portion and root/rhizome of the plant. The generation of **Figures 4.1** and **4.2**, and the data presented in **Table 5**, consisted of analysis of 36 separate *Veratrum* samples. For each data point, three independent plant samples were harvested, solvent extracted, and analyzed by HPLC. The harvest sites were within 200 ft elevation difference, and both locations were wet, mucky, and naturally spring fed. Elk Meadows faces west, while Shindig faces east, so sun exposure is different between the two harvest sites.

The magnitude of cyclopamine accumulated in *V. californicum* tissues reported in this study is consistent with recent reports [103,143]. The observation by Augustin et al. that cyclopamine accumulates in the rhizome of the plant during the growth season is consistent with our analysis for the below ground plant at the Shindig location, in which May collections contained 5.20 ± 1.02 mg/g, and September collection yielded 9.39 ± 1.85 mg/g, an increase of ~81% over the growth season. Augustin et al. speculated that this increase, along with higher expression of biosynthetic genes in the below ground plant, indicates that cyclopamine biosynthesis occurs in the underground organs of the plant. However, from the Elk Meadows location, we observed a modest decrease in cyclopamine concentration over the growth season, with the highest value found in May of 8.69 ± 1.17 mg/g, decreasing to 5.01 ± 0.50 mg/g in September, a decrease of ~42%. The reason for the discrepancy in cyclopamine accumulation is unclear. Modest fluctuations were observed in below ground abundance of the other alkaloids analyzed as well. From the Elk Meadows location, veratramine increased over the course of the growth season from a low in May, the highest level observed in July, and then a modest decrease in September. Similarly from the Shindig location the greatest abundance of veratramine

was observed in July. However, the amount of veratramine at this time point was 7.8X greater from the Shindig location compared to the Elk Meadows location, with values of 15.35 ± 2.86 mg/g and 1.98 ± 0.20 mg/g observed from each location, respectively. From the Elk Meadows location, the content of isorubijervine increased slightly over the growth season but remained relatively low, whereas from the Shindig location isorubijervine was only quantifiable from the May collection. Muldamine remained relatively low in abundance from both locations, below or near the quantification and detection limit. In summary, alkaloid abundance and the fluctuations in alkaloid content varied considerably between collection sites. This is consistent with the findings of Keeler and Binns in their original evaluation of alkaloid content by growth stage, and is consistent with the variable teratogenic effect observed in controlled feeding trials [133].

Consistent with prior analysis of *Veratrum* alkaloid content sampled throughout the growth season, the bar graphs detailed in **Figure 4.2** show that aerial alkaloid quantities decrease from early season through late growth phase for the plants [133,143]. This was consistent for both locations and for all of the alkaloids quantified. Plants harvested from Elk Meadows retained ~6% of their original alkaloid content from May to September, while the Shindig aerial plants retained closer to ~27% alkaloid content. However, it is worth noting that while the quantities of cyclopamine and veratramine decreased throughout the growth season, the amount of their glycosylated derivatives – cycloposine and veratrosine– increased throughout the growth season. This suggests conversion to the glycosylated derivatives occurs during the growth season.

Qualitative differences in the alkaloid diversity are observed by plant part. The diversity of alkaloids present in the aerial plant is significantly lower than the alkaloid

diversity of the root and rhizome for the same plants. As is shown in **Figure 4.1** and **Table 5**, mass spectrometry analysis identified 16 molecular ion peaks that yielded estimated molecular formulas consistent with steroidal alkaloids. Using high resolution mass spectrometry and verified by elution time compared to commercially available standards, Peaks 9, 10, 13, and 15 were definitively identified as veratramine, cyclopamine, isorubijervine, and muldamine, respectively (**Figure 4.1**). Peaks 2 and 3 were identified as veratrosine and cycloposine based on the comparison of the accurate and exact mass for these compounds, and the high degree of mass accuracy of our Q-TOF system (mass error <5 ppm). Peak 16, with m/z of 398.347 and predicted molecular formula of $C_{27}H_{43}NO$ is likely verazine, an important intermediate in the cyclopamine biosynthetic pathway [143]. Similarly, Peak 4, with m/z of 414.342 and predicted molecular formula of $C_{27}H_{43}NO_2$ is suspected to be etioline, which is an intermediary in the biosynthetic pathway of cyclopamine, and its presence in the extract is expected [89]. Peak 15, with an m/z of 416.357 and an estimated molecular formula of $C_{27}H_{45}NO_2$ may be the cyclopamine biosynthetic intermediate 22-keto-26-aminocholesterol; definitive determination of this suspected assignment will require additional investigation [143]. Peaks 1 and 8 had the same m/z of 576.396, and estimated molecular formula, $C_{33}H_{53}NO_7$, indicating they may be isomers of one another due to the significantly difference in retention time observed by chromatographic separation. This molecular formula and variation in chromatographic retention time are consistent with glycosylated isorubijervine and etioline. Peaks 5 and 7 have m/z of 430.337 and 428.320, and estimated molecular formulas of $C_{27}H_{43}NO_3$ and $C_{27}H_{41}NO_3$. These may be tetrahydrojervine and dihydrojervine, respectively, as described previously [144].

Additionally, potential isomers of both veratramine and cyclopamine were observed as Peaks 11 and 12, respectively, with identical m/z and estimate molecular formulas, but distinct retention times for each. These compounds may be of significant biological interest, and the isolation and structural characterization of each is currently underway in our laboratory.

4.7 Conclusion

Veratrum californicum is a rich source of steroidal alkaloids including inhibitors of the Hedgehog signaling pathway. Although the two collection sites used in this study were relatively close together and the elevation difference between the two was not significant, quantitative variation in alkaloid amount and qualitative variation in alkaloid diversity were observed between the two sites. Additionally, considerable variation was observed between individual plants, as indicated by the relatively high standard deviation observed between triplicate biological replicates. This study provides insight into optimal harvest time, plant growth stage, harvest location, and plant part required to isolate, yet to be characterized, alkaloids of interest for exploration as Hh pathway antagonists with desirable medicinal properties.

CHAPTER FIVE: PRELIMINARY DATA, FUTURE DIRECTIONS AND CONCLUSION

Natural products have historically been a rich source for medicines to treat human disease, and they continue to play a pivotal role in the fields of chemistry, biology, and medicine [145]. The primary goal of this research was to identify novel alkaloid inhibitors of the Hh signaling pathway. Our lab has used a Shh-Light II cell assay to evaluate the biological activity of numerous individual steroidal alkaloids as antagonists of the Hh signaling pathway (see Figure 5.1). Included in this analysis are the

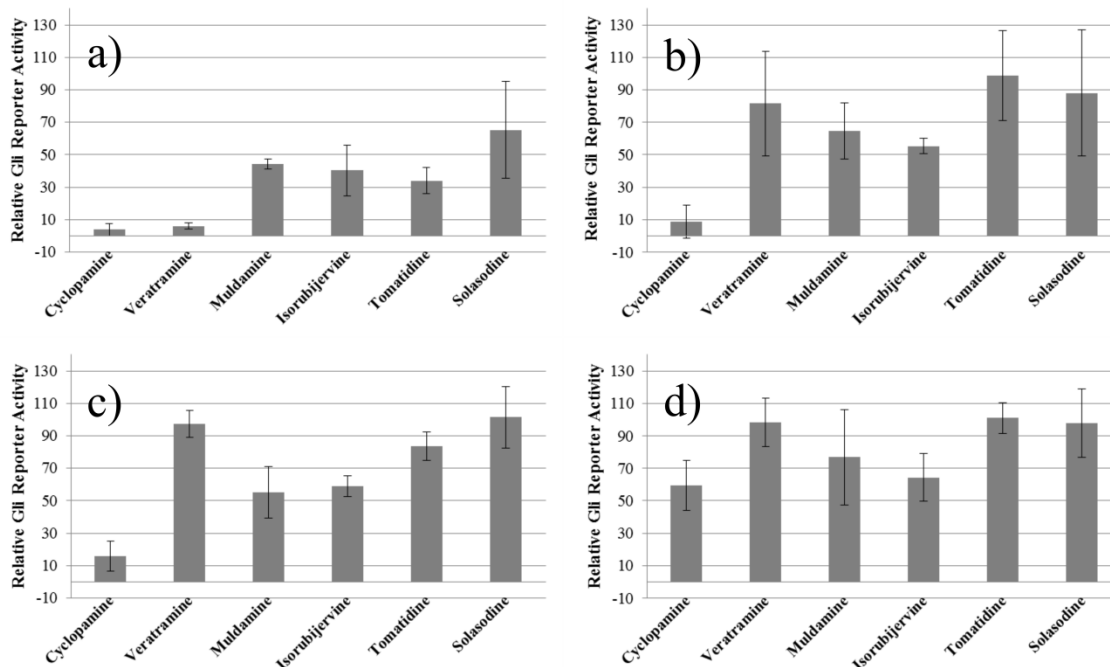


Figure 5.1 Biological activity of individual steroidal alkaloids for Hh signaling inhibition. Steroidal alkaloids cyclopamine, veratramine, muldamine, isorubijervine, tomatidine and solasodine were evaluated in Shh-Light II cells at concentrations a) 5 μ M, b) 1 μ M, c) 0.5 μ M, and d) 0.1 μ M.

previously mention steroidal alkaloids present in *V. californicum* – cyclopamine, veratramine, muldamine and isorubijervine – as well as the structurally similar alkaloids tomatidine and solasodine, both of which are solanidine-type steroidal alkaloids speculated to weakly inhibit Smo [89,116]. The variation in pharmacophore features expressed by *Veratrum* alkaloids that inhibit the protein Smo could be used to develop a more thorough understanding of the molecular features that govern alkaloid-based Smo inhibition. The bioactivity assessment and structural information associated *V. californicum* alkaloids combined with structure activity relationship investigation using the crystal structure of Smo will provide a better understanding of ligand/receptor interactions leading to the emergence of new therapeutic drugs beyond vismodegib, sonidegib, and glasdegib. Pharmacophore analysis and free energy binding calculations using the crystal structure of Smo, coupled with the cell-based assays that have already been undertaken was initially a principal objective of my dissertation research. I believe the combination of wet-lab experimentation coupled with computational prediction of binding affinity is a strategy that will lead to new Smo inhibitors worthy of pursuit by subsequent students in the McDougal laboratory.

Extraction, separation, and mass spectrum identification of six novel alkaloids present in *V. californicum* has been performed. The isolation and biological activity of a cyclopamine isomer offers a promising project for an ambitious student. This isomer is present in the root and rhizome of *V. californicum*, appears at a retention time of 19.4 min and has been designated as Peak 4 (see star over peak) in Figure 5.2a. Isolation and characterization of this alkaloid was pursued because the mass of 412.32 was identical to cyclopamine, and its predicted molecular formula of $C_{27}H_{41}NO_2$ was consistent with

cyclopamine, but the retention time is nearly a minute different than cyclopamine ($R_t=18.7$ min). Based on these data, we hypothesized this alkaloid is an isomer of cyclopamine. MS fragmentation of the target alkaloid (peak 4) is nearly indistinguishable from cyclopamine (Figure 5.3a and b). However, 2D $^1\text{H}/^{13}\text{C}$ heteronuclear single quantum coherence (HSQC) NMR spectra show variation of some proton-carbon chemical shifts when compared to cyclopamine, as shown in the HSQC overlay of the two compounds, Figure 5.3c (cyclopamine in blue, and the unknown isomer in green; overlapping chemical shifts are boxed in red). 2D $^1\text{H}/^{13}\text{C}$ heteronuclear multiple bond correlation (HMBC) spectra have also been obtained, and confirm a divergence of electronic environments for many atoms in each molecule. Bioactivity evaluation of the cyclopamine isomer has demonstrated no significant difference in the inhibitory activity between this novel alkaloid and cyclopamine (see Figure 5.3d). Interestingly, differences in the circular dichroism (CD) spectra indicate that inversion of stereocenters is likely (see Figure 5.3e).

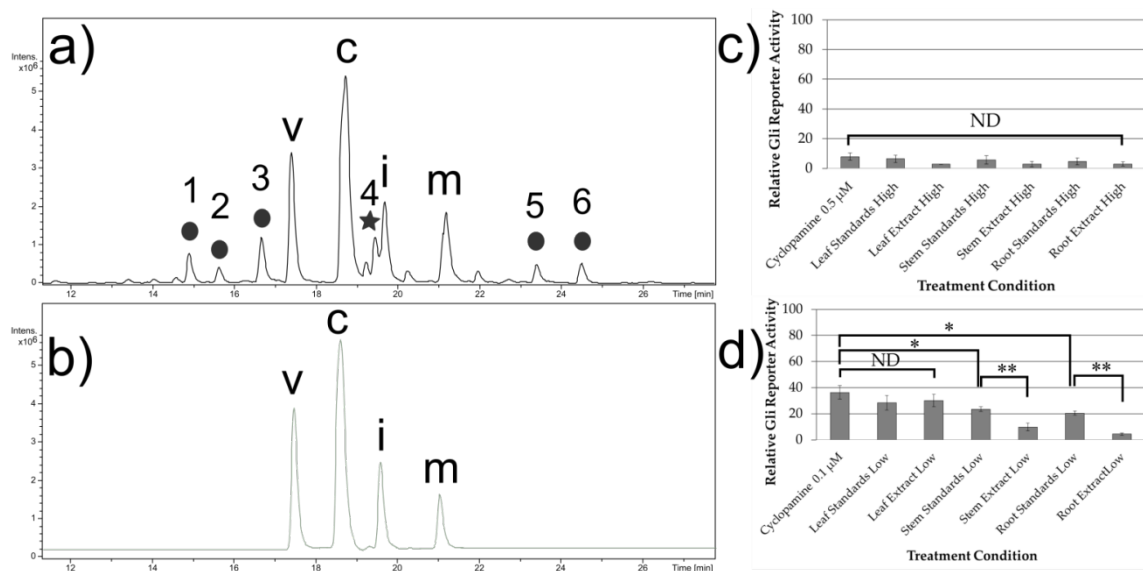


Figure 5.2. Alkaloid chromatogram for biomass extracts from the root/rhizome of *V. californicum*. Common and unique alkaloids identified by MS are observed, with veratramine, cycloamine, isorubijervine and muldamine identified as v, c, i and m, respectively. The star indicates a cycloamine isomer which our lab has isolated and used for bioactivity evaluation, and for which we have begun structure characterization. b) Chromatogram of the alkaloid standard cocktail replicating the concentrations observed in root/rhizome extract. c) and d) Comparison of the biological activity of cycloamine, crude extracts by plant part, and alkaloid standard cocktails emulating the concentrations observed in extracts at c) high (cycloamine, [0.5 μM]) and d) low concentrations (cycloamine, [0.1 μM]). No statistically significant difference was observed at higher alkaloid concentrations in c). However, at lower alkaloid concentrations in d) significant differences were observed, and * indicates $p < 0.05$, and ** indicates $p < 0.01$. Differences in the inhibitory potential of the crude extract of the stem and the root/rhizome and their respective alkaloid standard combinations indicate that additional alkaloids present in the extracts inhibit the Hh signaling pathway.

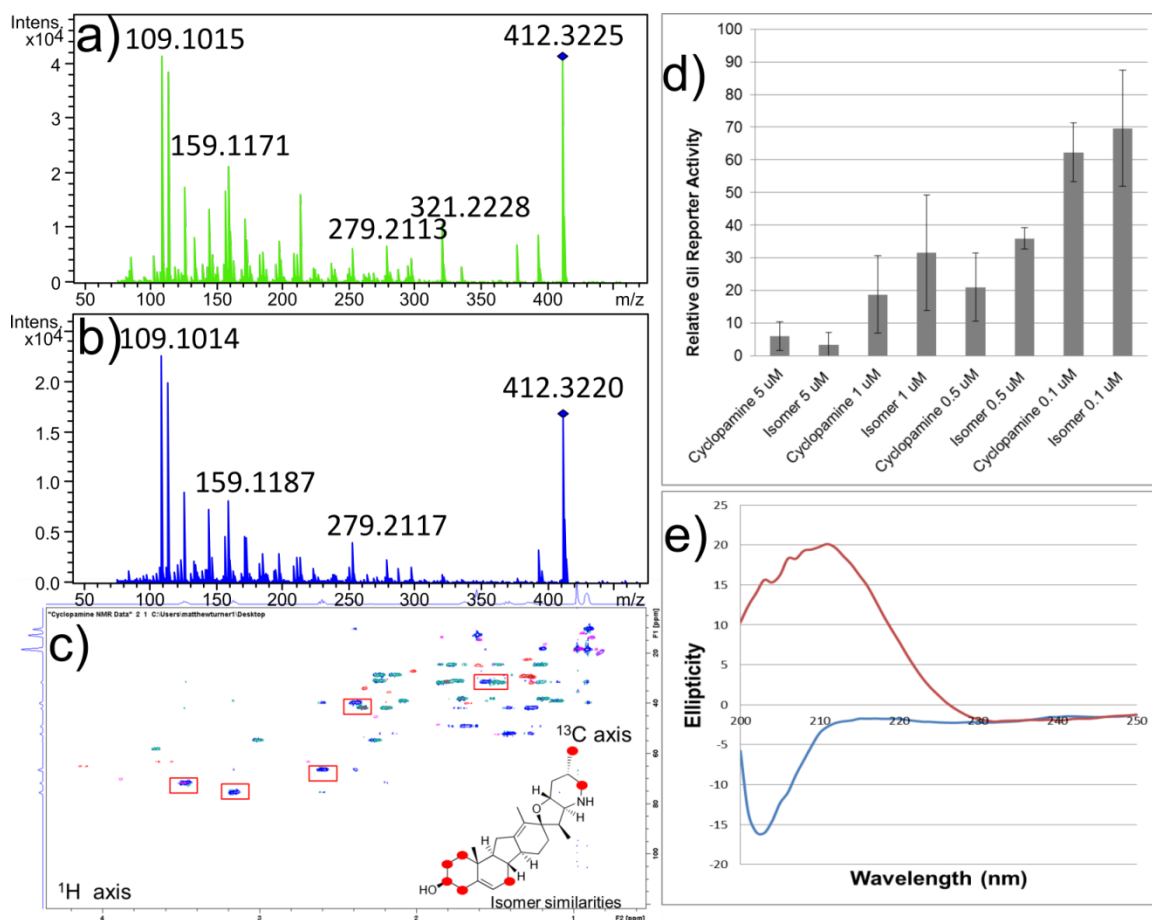


Figure 5.3. Comparison of biological and chemical characteristics of cyclopamine and a potentially novel steroidal alkaloid. MS/MS fragmentation of a) cyclopamine and b) a cyclopamine isomer. MS/MS fragmentation of the two compounds show very similar fragment patterns. c) $^1\text{H}/^{13}\text{C}$ HSQC overlay of cyclopamine (blue) and the cyclopamine isomer (green). Proton-carbon chemical shifts shared by the two compounds are boxed in red, and the corresponding protonated carbon atoms are indicated by red dots on the chemical structure of cyclopamine. d) Biological activity data of cyclopamine and the isomer in Shh Light II cell assay, showing there is no significant difference between the inhibitory potential of the two compounds. e) CD spectra of cyclopamine (blue) and the isomer (red). The discrepancy in the sign of the signal from 220-200 nm indicates there may be differences in the stereochemistry in absolute configuration of the two compounds.

Lastly, inclusion of additional model systems beyond the use of Shh-Light II cells to analyze the effects of *Veratrum* alkaloids would greatly benefit this project. Although Shh-Light II cells provide valuable data and are relatively easy cells to work with, the data obtained from these cells is myopic and only directly relevant to Hh signaling.

Extension of alkaloid analysis to basal cell carcinoma cells would offer direct cancer relevance. Analysis of gene expression changes using PCR or proteomic alterations following alkaloid treatment might yield additional information regarding the mechanisms underlying the genetic basis of basal cell carcinoma. Further exploration of promising alkaloid antagonists of Hh pathway inhibition within a zebrafish model will extend our findings to an organismal model system to address more complex physiological interactions. Furthermore, this may indicate additional molecular targets for *Veratrum* alkaloids beyond Hh signaling that could provide novel avenues for continued research.

REFERENCES

- 1) Nüsslein-Volhard C, Wieschaus E. Mutations affecting segment number and polarity in *Drosophila*. *Nature* **1980**, 287, 795–801. DOI: 10.1038/287795a0
- 2) Lee JJ, von Kessler DP, Parks S, Beachy PA. Secretion and localised transcription suggests a role in positional signalling for products of the segmentation gene hedgehog. *Cell* **1992**, 70: 777–789. DOI: 10.1016/0092-8674(92)90264-d.
- 3) Mohler J, and Vani K. Molecular organisation and embryonic expression of the hedgehog gene involved in cell–cell communication in segmental patterning in *Drosophila*. *Development* 1992, 115: 957–971. DOI:
- 4) Tabata T, Eaton S, Kornberg TB. The *Drosophila* hedgehog gene is expressed specifically in posterior compartment cells and is a target of engrailed regulation. *Genes & Dev.* **1992**, 6: 2635–2645. DOI: 10.1101/gad.6.12b.2635
- 5) Ingham PW. Hedgehog signaling in animal development: paradigms and principles. *Genes & Dev.* **2001**, 15, 3059–3087. DOI:10.1101/gad.938601.
- 6) Rimkus T, Carpenter R, Qasem S, Chan M, Lo HW. Targeting the Sonic Hedgehog Signaling Pathway: Review of Smoothed and GLI Inhibitors. *Cancers*, **2016**, 8, 22. doi:10.3390/cancers8020022.
- 7) Guan Z, Dong B, Huang C, Hu X, Zhang Y, Lin C. Expression patterns of genes critical for SHH, BMP, and FGF pathways during the lumen formation of human salivary glands. *J Mol Histol.* **2019**; 50: 217-227 DOI: 10.1007/s10735-019-09819-x.
- 8) Babu D, Fanelli A, Mellone S, Muniswamy R, Wasniewska M, Prodam F, Petri A, Bellone S, Salerno MC, Giordano M. Novel GLI2 mutations identified in patients with Combined Pituitary Hormone Deficiency (CPHD): Evidence for a

- pathogenic effect by functional characterization. *Clin Endocrinol* **2019**; *90*: 449-456 DOI: 0.1111/cen.13914.
- 9) Hashimoto H, Jiang W, Yoshimura T, Moon KH, Bok J, Ikenaka K. Strong sonic hedgehog signaling in the mouse ventral spinal cord is not required for oligodendrocyte precursor cell (OPC) generation but is necessary for correct timing of its generation. *Neurochem Int* **2018**; *119*: 178-183. DOI: 10.1016/j.neuint.2017.11.003
 - 10) Petrova R, Joyner AL. Roles for Hedgehog signaling in adult organ homeostasis and repair. *Development* **2014**; *141* (18): 3445-57. DOI: 10.1242/dev.083691.
 - 11) Ihrle RA, Shah JK, Harwell CC, et al. Persistent Sonic Hedgehog Signaling in Adult Brain Determines Neural Stem Cell Positional Identity. *Neuron* **2011**, *71*:250–262. DOI: 10.1016/j.neuron.2011.05.018
 - 12) Brownell I, Guevara E, Bai CB, et al. Nerve-Derived Sonic Hedgehog Defines a Niche for Hair Follicle Stem Cells Capable of Becoming Epidermal Stem Cells. *Cell Stem Cell* **2011**, *8*:552–565. DOI: 10.1016/j.stem.2011.02.021
 - 13) Peng YC, Levine CM, Zahid S, et al. Sonic hedgehog signals to multiple prostate stromal stem cells that replenish distinct stromal subtypes during regeneration. *Proc Natl Acad Sci USA*, **2013**, *110*:20611–20616. DOI: 10.1073/pnas.1315729110
 - 14) Li S, Wang M, Chen Y, et al. Role of the Hedgehog Signaling Pathway in Regulating the Behavior of Germline Stem Cells. *Stem Cells Intern.* **2017**: 1–9. DOI: 10.1155/2017/5714608
 - 15) Finco I, Lapensee CR, Krill KT, Hammer GD. Hedgehog Signaling and Steroidogenesis. *Annu. Rev. Physiol.* **2015**, *77*: 105–129. DOI:10.1146/annurev-physiol-061214-111754.
 - 16) Varjosalo M, Taipale J. Hedgehog: functions and mechanisms. *Gene Dev*, **2008**, *22*: 2454–2472. DOI:10.1101/gad.1693608.

- 17) Marigo V, Tabin CJ. Regulation of patched by sonic hedgehog in the developing neural tube. *Proc Natl Acad Sci USA*, **1996**, *93*: 9346-9351. DOI: 10.1073/pnas.93.18.9346
- 18) Bellusci S, Furuta Y, Rush MG, Henderson R, Winnier G, Hogan BL. Involvement of Sonic hedgehog (Shh) in mouse embryonic lung growth and morphogenesis. *Development*, **1997**, *124*: 53-63.
- 19) Hardcastle Z, Mo R, Hui CC, Sharpe PT. The Shh signalling pathway in tooth development: Defects in Gli2 and Gli3 mutants. *Development*, **1998**, *125*: 2803-2811.
- 20) Litingtung Y, Lei L, Westphal H, Chiang C. Sonic hedgehog is essential to foregut development. *Nat Genet*, **1998**, *20*: 58-61.
- 21) St-Jacques B, Dassule HR, Karavanova I, Botchkarev VA, Li J, Danielian PS, McMahon JA, Lewis PM, Paus R, McMahon AP. Sonic hedgehog signaling is essential for hair development. *Curr Biol*, **1998**, *8*: 1058-1068.
- 22) Vortkamp A, Lee K, Lanske B, Segre GV, Kronenberg HM, Tabin CJ. Regulation of rate of cartilage differentiation by Indian hedgehog and PTH-related protein. *Science*, **1996**, *273*: 613-622.
- 23) Bitgood MJ, Shen L, McMahon AP: Sertoli cell signaling by Desert hedgehog regulates the male germline. *Curr Biol*, **1996**, *6*: 298-304.
- 24) Buglino JA, Resh MD. Hhat is a palmitoylacyltransferase with specificity for N-palmitoylation of sonic hedgehog. *J Biol Chem*, **2008**, *283* (32): 22076-22088.
- 25) Chen MH, Li YJ, Kawakami T, Xu, SM, Chuang PT. Palmitoylation is required for the production of a soluble multimeric Hedgehog protein complex and long-range signaling in vertebrates. *Genes Dev*. **2004**, *18*: 641-659.

- 26) Rietveld A, Neutz S, Simons K, Eaton S. Association of sterol- and glycosylphosphatidylinositol linked proteins with *Drosophila* raft lipid microdomains. *J Biol Chem*, 1999, **274**: 12049–12054.
- 27) Briscoe J, Théron P P. The mechanisms of Hedgehog signaling and its roles in development and disease. *Nat. Rev. Mol. Cell Biol.* **2013**, *14*: 416–429.
- 28) Ingham PW, Placzek M. Orchestrating ontogenesis: variations on a theme by sonic hedgehog. *Nat. Rev. Genet.* **2006**, *7*: 841–850.
- 29) Katoh Y, Katoh M. Hedgehog target genes: Mechanisms of carcinogenesis induced by aberrant Hedgehog signaling activation. *Curr Mol Med* **2009**, *9*(7): 873-886. DOI: 10.2174/156652409789105570
- 30) Binns W, James LF, Shupe JL. Cyclopan-type malformation in lambs. *Arch. Environ. Health* **1962**, *5*: 106–108.
- 31) Binns W, James LF, Shupe JL, Everett G. A congenital-type malformation in lambs induced by maternal ingestion of a range plant *Veratrum californicum*. *Am. J. Vet. Res.* **1963**, *24*: 1164–1175.
- 32) James LF. Teratological research at the USDA-ARS Poisonous Plant Research Laboratory. *J. Nat. Toxins*, **1999**, *8*: 63–80.
- 33) Binns W, Shupe JL, Keeler RF, James LF. Chronological evaluation of teratogenicity in sheep fed *Veratrum californicum*. *J Am Vet Med Assoc* **1965**, *147*: 839-842.
- 34) Keeler R, Binns W. Chemical compounds of *Veratrum californicum* related to congenital ovine cyclopan malformations: extraction of active material. *Exp Biol Med.* **1964**, *116*:123–127.
- 35) Keeler R, Binns W. Teratogenic compounds of *Veratrum californicum* (Durand) I. Preparation and characterization of fractions and alkaloids for biologic testing. *Can J Biochem.* **1966**, *44*:819–828.

- 36) Masamune T, Mori Y, Takasugi M, Murai A, Ohuchi S, Sato N, Katsui N. 11-Deoxojervine, a new alkaloid from *Veratrum* species. *Bull. Chem. Soc. Jpn.* **1965**, 38: 1374–1378.
- 37) Keeler R. Teratogenic compounds of *Veratrum californicum* (Durand)—VI. The structure of cyclopamine. *Phytochemistry.* **1969**, 8:223–225.
- 38) Keeler R. Teratogenic compounds of *Veratrum californicum* (Durand) VII. The structure of the glycosidic alkaloid cycloposine. *Steroids.* **1969**, 13:579–588.
- 39) Keeler R. Teratogenic compounds of *Veratrum californicum* (Durand) X. Cyclopia in rabbits produced by cyclopamine. *Teratology.* **1970**, 3:175–180.
- 40) Keeler R, Binns W. Teratogenic compounds of *Veratrum californicum* (Durand) V. Comparison of cyclopean effects of steroidal alkaloids from the plant and structurally related compounds from other sources. *Teratology* **1968**, 1:5–10.
- 41) Bryden MM, Perry C, Keeler RF. Effects of alkaloids of *Veratrum californicum* on chick embryos. *Teratology*, **1973**, 8: 19-25.
- 42) Brown D, Keeler R. Structure-activity relation of steroid teratogens. 2. N-substituted jervines. *J Agric Food Chem.* **1978**, 26:564–566.
- 43) Chiang C, Litingtung Y, Lee E, Young KE, Corden JL, Westphal H, Beachy PA. Cyclopia and defective axial patterning in mice lacking Sonic hedgehog gene function. *Nature* **1996**, 383: 407-413.
- 44) Cooper MK, Porter JA, Young KE, Beachy PA. Teratogen-Mediated Inhibition of Target Tissue Response to Shh Signaling. *Science* **1998**, 280: 1603-1607.
- 45) Incardona JP, Gaffield W, Kapur RP, Roelink H. The teratogenic *Veratrum* alkaloid cyclopamine inhibits Sonic hedgehog signal transduction. *Development*, **1998**, 125: 3553-3562.
- 46) Chen JK, Taipale J, Cooper MK, Beachy PA. Inhibition of Hedgehog signaling by direct binding of cyclopamine to Smoothed. *Genes Dev* **2002**, 16: 2743-2748.

- 47) Weierstall U, James D, Wang C, White TA, Wang D, Liu W, Spence JC, et al. Lipidic cubic phase injector facilitates membrane protein serial femtosecond crystallography. *Nat. Commun.*, **2014**, 5: 3309.
- 48) Merchant JL. Hedgehog signaling in gut development, physiology and cancer. *J Physiol* **2012**, 590: 421-432.
- 49) Bertrand FE, Angus CW, Partis WJ, Sigounas G. Developmental pathways in colon cancer: Crosstalk between WNT, BMP, Hedgehog and Notch. *Cell Cycle* **2012**, 11: 4344-4351.
- 50) Niu Y, Li F, Tang B, Shi Y, Hao Y and Yu P. Clinicopathological correlation and prognostic significance of sonic hedgehog protein overexpression in human gastric cancer. *Int J Clin Exp Pathol* **2014**, 7: 5144-5153.
- 51) Kai K, Aishima S and Miyazaki K. Gallbladder cancer: Clinical and pathological approach. *World J Clin Cases* **2014**, 2: 515-521.
- 52) Nigam A. Breast cancer stem cells, pathways and therapeutic perspectives. *Indinan J Surg* **2013**, 75: 170-180.
- 53) Choi YH: The effects of sonic hedgehog signaling pathway components on non-small cell lung cancer progression and clinical outcome. *World J Surg Oncol* **2014**, 12: 268.
- 54) Ok CY, Singh RR, Vega F. Aberrant activation of the hedgehog signaling pathway in malignant hematological neoplasms. *Am J Pathol* **2012**, 180: 2-11.
- 55) Irvine DA, Copland M. Targeting hedgehog in hematologic malignancy. *Blood*, **2012**, 119: 2196-2204.
- 56) Pietrobono S, Gagliardi S, Stecca B. Non-canonical Hedgehog Signaling Pathway in Cancer: Activation of GLI Transcription Factors Beyond Smoothed. *Front. Genetics*, **2019**, 10:556. DOI: 10.3389/fgene.2019.00556
- 57) Barakat MT, Humke EW, Scott MP. Learning from Jekyll to control Hyde: Hedgehog signaling in development and cancer. *Trends in Molecular Med* **2010**, 16 (8): 337-348. DOI: 10.1016/j.molmed.2010.05.003.

- 58) Hahn H, Wicking C, Zaphiropoulos PG, Gailani MR, Shanley S, Chidambaram A, Vorechovsky I, Holmberg E, Uden AB, Gillies S, Negus K, Smyth I, Pressman C, Leffell DJ, Gerrard B, Goldstein AM, Dean M, Toftgard R, Chenevix-Trench G, Wainwright B, Bale AE. Mutations of the human homolog of *Drosophila* patched in the nevoid basal cell carcinoma syndrome. *Cell* **1996**, *85*: 841–8517
- 59) Pazzaglia S, Tanori M, Mancuso M, Gessi M, Pasquali E, Leonardi S, Oliva MA, Rebessi S, Di Majo V, Covelli V, Giangaspero F, Saran A. Two-hit model for progression of medulloblastoma preneoplasia in Patched heterozygous mice. *Oncogene* **2006**, *25*: 5575–5580. DOI: 10.1038/sj.onc.1209544.
- 60) Varnat, Duquet A, Malerba M, Zbinden M, Mas C, Gervaz P, Ruiz i Altaba A. Human colon cancer epithelial cells harbor active HEDGEHOG-GLI signalling that is essential for tumor growth, recurrence, metastasis and stem cell survival and expansion. *EMBO Mol Med.* **2009**, *1*: 338-351. DOI: 10.1002/emmm.200900039
- 61) Thayer, SP, di Magliano MP, Heiser PW, Nielsen CM, Roberts DJ, Lauwers GY, Qi YP, Gysin S, Fernández-del Castillo C, Yajnik V, Antoniu B, McMahon M, Warshaw AL, Hebrok M. Hedgehog is an early and late mediator of pancreatic cancer tumorigenesis. *Nature*, **2003**, *425*: 851–856. DOI: 10.1038/nature02009
- 62) Matsushita S, Onishi H, Nakano K, Nagamatsu I, Imaizumi A, Hattori M, Oda Y, Tanaka M, Katano M. Hedgehog signaling pathway is a potential therapeutic target for gallbladder cancer. *Cancer Sci* **2014**, *105*: 272-280. DOI: 10.1111/cas.12354
- 63) Eriksson JE, Dechat T, Grin B, Helfand B, Mendez M, Pallari HM, Goldman. Introducing intermediate filaments: from discovery to disease. *J Clin Invest* **2009**, *119* (7): 1763–1771. DOI:10.1172/JCI38339.
- 64) Wong CS, Strange RC, Lear JT. Basal Cell Carcinoma. *BMJ* **2003**, *327*: 794-798.
- 65) Onishi H, Kai M, Odate S, Iwasaki H, Morifuji Y, Ogino T, Morisaki T, Nakashima Y, Katano M. Hypoxia Activates the Hedgehog Signaling Pathway in

- a Ligand-Independent manner by Upregulation of Smo Transcription in Pancreatic Cancer. *Cancer Sci* **2011**, *102*(6): 1144-1150. DOI: 10.1111/j.1349-7006.2011.01912.x
- 66) Wilkinson Furic L, Buchanan G, Larsson O, Pedersen J, Frydenberg M, Risbridger GP, Taylor RA. Hedgehog Signaling Is Active in Human Prostate Cancer Stroma and Regulates Proliferation and Differentiation of Adjacent Epithelium. *The Prostate* **2013**, *73*: 1810-1823. DOI: 10.1002/pros.22720.
- 67) Datta S, Pierce M, Datta MW. Perlecan signaling: Helping hedgehog stimulate prostate cancer growth. *Int. J. Biochem. Cell Biol* **2006**, *38*: 1855-1861. DOI: 10.1016/j.biocel.2006.03.022
- 68) Chang SC, Mulloy B, Magee AI, Couchman JR. Two Distinct Sites in Sonic Hedgehog Combine for Heparan Sulfate Interactions and Cell Signaling Functions. *J. Biol. Chem* 2011, *286*(52): 44391-44402. DOI: 10.1074/jbc.M111.285361
- 69) Ridgway LR, Wetzel MD, Machetti D. Heparanase modulates Shh and Wnt3a signaling in human medulloblastoma cells. *Exp. Ther. Med* **2011**, *2*: 229-237. DOI: 10.3892/etm.2010.189
- 70) Gailani,MR, Ståhle-Bäckdahl M, Leffell DJ, Glynn M, Zaphiropoulos PG, Pressman C, Undén AB, Dean M, Brash DE, Bale AE, Toftgård R. The role of the human homologue of *Drosophila* patched in sporadic basal cell carcinomas. *Nat. Genet.* **1996**, *14*: 78–81. DOI: 10.1038/ng0996-78
- 71) Hahn, H. Wicking C, Zaphiropoulos PG, Gailani MR, Shanley S, Chidambaram A, Vorechovsky I, Holmberg E, Unden AB, Gillies S, Negus K, Smyth I, Pressman C, Leffell DJ, Gerrard B, Goldstein AM, Dean M, Toftgard R, Chenevix-Trench G, Wainwright B, Bale AE. Mutations of the human homolog of *Drosophila* patched in the nevoid basal cell carcinoma syndrome. *Cell* **1996**, *85*: 841–851. DOI: 10.1016/s0092-8674(00)81268-4
- 72) Johnson RL, et al. Human homolog of patched, a candidate gene for the basal cell nevus syndrome. *Science* **1996**, *272*: 1668–1671.

- 73) Corcoran RB, Scott MP. A mouse model for medulloblastoma and basal cell nevus syndrome. *J. Neurooncol.* 2001, *53*: 307–318
- 74) Pazzaglia S. et al. Linking DNA damage to medulloblastoma tumorigenesis in patched heterozygous knockout mice. *Oncogene* **2006**, *25*: 1165–1173.
- 75) Xie J, Murone M, Luoh SM, Ryan A, Gu Q, Zhang C, Bonifas JM, Lam CW, Hynes M, Goddard A, Rosenthal A, Epstein EH, de Sauvage FJ. Activating Smoothed mutations in sporadic basal-cell carcinoma. *Nature* **1998**, *391*: 90–92
- 76) Xie J, et al. Mutations of the PATCHED gene in several types of sporadic extracutaneous tumors. *Cancer Res.* **1997**, *57*: 2369–2372.
- 77) Roewert-Huber J. et al. Epidemiology and aetiology of basal cell carcinoma. *Br. J. Dermatol.* **2007**, *157*: 47–5.
- 78) Chen JK. I only have eye for ewe: the discovery of cyclopamine and development of Hedgehog pathway-targeting drugs. *Nat. Prod. Rep.* **2015**, *00*: 1-3. DOI: 10.1039/x0xx00000x
- 79) Chen JK, Taipale J, Young KE, Maiti T, Beachy PA. Small molecule modulation of Smoothed activity. *Proc.Natl. Acad. Sci. U. S. A.*, **2002**, *99*: 14071-14076.
- 80) Tremblay MR, Lescarbeau A, Grogan MJ, Tan E, Lin G, Austad BC, Yu LC, Behnke ML, Nair SJ, Hagel M, White K, Conley J, Manna JD, Alvarez-Diez TM, Hoyt J, Woodward CN, Sydor JR, Pink M, MacDougall J, Campbell MJ, Cushing J, Ferguson J, Curtis MS, McGovern K, Read MA, Palombella VJ, Adams J, Castro AC. Discovery of a Potent and Orally Active Hedgehog Pathway Antagonist (IPI-926) *J. Med. Chem.*, **2009**, *52*: 4400-4418.
- 81) Von Hoff DD, et al. Inhibition of the Hedgehog Pathway in Advanced Basal-Cell Carcinoma. *Engl. J. Med.*, **2009**, *361*: 1164-1172. DOI: 10.1056/NEJMoa0905360
- 82) Doan HQ, Silapunt S, Migden MR. Sonidegib, a novel smoothed inhibitor for the treatment of advanced basal cell carcinoma. *OncoTargets and Therapy.* **2016**, *9*: 5971-5678.

- 83) Hoy SM. Glasdegib: First Global Approval. *Drugs* **2019**, 79(2): 207-213. DOI: 10.1007/s40265-018-1047-7.
- 84) Rudin CM, et al. Treatment of Medulloblastoma with Hedgehog Pathway Inhibitor GDC-0449 N. *Engl. J. Med.* **2009**, 361: 1173-1178.
- 85) Sharpe HJ, Pau G, Dijkgraaf GJ, Basset-Seguín N, Modrusan Z, Januario T, Tsui V, Durham AB, Dlugosz AA, Haverty PM, Bourgon R, Tang JY, Sarin KY, Dirix L, Fisher DC, Rudin CM, Sofen H, Migden MR, Yauch RL, de Sauvage FJ. Genomic analysis of smoothed inhibitor resistance in basal cell carcinoma. *Cancer Cell* **2015**, 27(3):327-341. DOI: 10.1016/j.ccell.2015.02.001.
- 86) Atwood SX, Sarin KY, Whitson RJ, Li JR, Kim G, Rezaee M, Ally MS, Kim J, Yao C, Chang AL, Oro AE, Tang JY. Smoothed variants explain the majority of drug resistance in basal cell carcinoma. *Cancer Cell* **2015** 27(3): 342-353. DOI: 10.1016/j.ccell.2015.02.002.
- 87) Sekulic A, Migden MR, Oro AE, Dirix L, Lewis KD, Hainsworth JD, Solomon JA, Yoo S, Arron ST, Friedlander PA, Marmur E, Rudin CM, Chang AL, Low JA, Mackey HM, Yauch RL, Graham RA, Reddy JC, Hauschild A. Efficacy and safety of vismodegib in advanced basal-cell carcinoma. *N Engl J Med* **2012**, 366(23): 2171-2179. DOI: 10.1056/NEJMoa1113713
- 88) Teperino R, Amann S, Bayer M, McGee SL, Loipetzberger A, Connor T, Jaeger C, Kammerer B, Winter L, Wiche G, Dalgaard K, Selvaraj M, Gaster M, Lee-Young RS, Febbraio MA, Knauf C, Cani PD, Aberger F, Penninger JM, Pospisilik JA, Esterbauer H. Hedgehog partial agonism drives Warburg-like metabolism in muscle and brown fat. *Cell* **2012**, 151(2): 414-426. DOI: 10.1016/j.cell.2012.09.021
- 89) Chandler CM, McDougal OM. Medicinal History of North American *Veratrum*. *Phytochem Rev* **2014**, 13(3): 671-694. DOI: 10.1007/s11101-013-9328-y.
- 90) Zhang X, Harrington N, Moraes RC, Wu MF, Hilsenbeck SG, Lewis MT. Cyclopamine inhibition of human breast cancer cell growth independent of

- Smoothened (Smo). *Breast Cancer Res. Treat.* **2009**, *115*: 505–521. DOI: 10.1007/s10549-008-0093-3
- 91) Ghezalia L, Leger DY, Limami Y, Cook-Moreau J, Beneytout JL, Liagre B. Cyclopamine and jervine induce COX-2 overexpression in human erythroleukemia cells but only cyclopamine has a pro-apoptotic effect. *Exp. Cell Res.* **2013**, *319*: 1043–1053. DOI: 10.1016/j.yexcr.2013.01.014
- 92) B. Bailly, C.-A. Richard, G. Sharma, L. Wang, L. Johansen, J. Cao, V. Pendharkar, D.-C. Sharma, M. Galloux, Y. Wang, R. Cui, G. Zou, P. Guillon, M. von Itzstein, J.-F. Eléouët, R. Altmeyer. Targeting human respiratory syncytial virus transcription antitermination factor M2-1 to inhibit in vivo viral replication *Sci. Rep.* **2016**, *6*: e25806.
- 93) Shaw, G., Price, A.M., Ktori, E., Bisson, I., Purkis, P.E., McFaul, S., Oliver, R.T., Prowse, D.M., 2008. Hedgehog signalling in androgen independent prostate cancer. *Eur. Urol.* *54* (6), 1333–1343.
- 94) Na YJ, Lee DH, Kim JL, Kim BR, Park SH, Jo MJ, Jeong S, Kim HJ, Lee SY, Jeong YA, Oh SC. Cyclopamine sensitizes TRAIL-resistant gastric cancer cells to TRAIL-induced apoptosis via endoplasmic reticulum stress-mediated increase of death receptor 5 and survivin degradation. *Int J Biochem Cell Biol* **2017**, *89*: 147–156. DOI: 10.1016/j.biocel.2017.06.010
- 95) Honerjäger, P. Cardioactive substances that prolong the open state of sodium channels. *Rev. Physiol. Biochem. Pharmacol.* **1982**, *92*: 1–74.
- 96) El Sayed, K.A. Microbial biotransformation of veratramine. *J. Nat. Prod.* **1998**, *61*: 149–151.
- 97) Nagata R, Izumi K. Veratramine induced behavior associated with seotonergic hyperfunction in mice. *Jap J Pharmacol* **1991**, *55*: 129-137. DOI: 10.1254/jjp.55.129
- 98) Bai F, Liu K, Li H, Wang J, Zhu J, Hao P, Zhu L, Zhang S, Shan L, Ma W. Veratramine modulates AP-1-dependent gene transcription by directly binding to programmable DNA. *Nucleic Acids Res.* **2017**, *46*: 546–557.

- 99) Wang G, Rong MQ, Li Q, Liu YP, Long CB, Meng P, Yao HM, Lai R, Luo XD. Alkaloids from *Veratrum taliense* Exert Cardiovascular Toxic Effects via Cardiac Sodium Channel Subtype 1.5. *Toxins* **2015**, 8:1-10. DOI: 10.3390/toxins8010012.
- 100) Li Q, Zhao YL, Long CB, Zhu PF, Liu YP, Luo XD. Seven new veratramine-type alkaloids with potent analgesic effect from *Veratrum taliense*. *J Ethnopharmacol* **2019**, 244: 112137. DOI: 10.1016/j.jep.2019.112137
- 101) Fekete A, Franklin L, Ikemoto T, Rózsa B, Lendvai B, Sylvester Vizi E, Zelles T. Mechanism of the persistent sodium current activator veratridine-evoked Ca^{2+} elevation: implication for epilepsy. *J Neurochem* **2009** 111(3): 745–756. DOI:10.1111/j.1471-4159.2009.06368.x.
- 102) Ulbricht W. Voltage Clamp Studies of Veratridinized Frog Nodes. *J Cell Comp Physiol* **1965**, 66: 91–98. DOI: 10.1002/jcp.1030660516
- 103) Turner MW, Cruz R, Mattos J, Baughman N, Elwell J, Fothergill J, Nielsen A, Brookhouse J, Bartlett A, Malek P, Pu X, King MD, McDougal OM. Cyclopamine bioactivity by extraction method from *Veratrum californicum*. *Bioorg. Med. Chem.* **2016**, 24: 3752–3757. doi:10.1016/j.bmc.2016.06.017.
- 104) McNeal DW, Shaw AD. *Veratrum*. In: Flora of North America Editorial Committee, eds. **2002**. Flora of North America North of Mexico. New York and Oxford. Vol. 26, pp/ 72-76.
- 105) Keeler RF. Teratogenic effects of cyclopamine and jervine in rats, mice and hamsters. *Proc Soc Exp Biol Med* **1975**, 149(1): 302-306.
- 106) Keeler RF. Cyclopamine and related steroidal alkaloid teratogens: Their occurrence, structural relationship, and biological effects. *Lipids* **1978**, 13(10): 708-715.
- 107) Heretsch P, Tzagkaroulaki L, Giannis A. Cyclopamine and Hedgehog signaling: Chemistry, Biology, Medical Perspectives. *Angew Chem Int Ed.* **2010**, 49: 3418-3427. DOI:10.1002/anie.200906967

- 108) Onishi H, Katano M. Hedgehog signaling pathway as a therapeutic target in various types of cancer. *Can. Sci.* **2011**, *102*: 1756–1760. doi:10.1111/j.1349-7006.2011.02010.x.
- 109) ClinicalTrials.gov, Pilot study of cetuximab and the hedgehog inhibitor IPI-926 in recurrent head and neck cancer. <http://clinicaltrials.gov/show/NCT01255800>, 2013 (accessed 1.11.16).
- 110) National Cancer Institute, FDA Approval for Vismodegib. <http://www.cancer.gov/cancertopics/druginfo/fda-vismodegib/>, 2012 (accessed 5.5.2013).
- 111) Oatis JE, Brunsfeld P, Rushing JW, Moeller PD, Bearden DW, Gallien TN, Cooper G. Isolation, purification, and full NMR assignments of cyclopamine from *Veratrum californicum*. *Chem Cent J.* **2008**, *2*(12):1-6.
- 112) Splinter, S.; Kadali, S. U.S. Patent Application 20110160457, 2011.
- 113) Jayatilake, G. S.; Richheimer, S. L. Mann, D.A.; U.S. Patent Application 20100003728, 2010.
- 114) Chandler CM, Habig JW, Fisher AA, Ambrose KV, Jiménez ST, McDougal OM. Improved extraction and complete mass spectral characterization of steroidal alkaloids from *Veratrum californicum*. *Nat. Prod. Commun.* **2013**, *8*(8): 1059-1064.
- 115) Wilson SR, Strand MF, Krapp A, Rise F, Petersen D, Krauss S. Hedgehog antagonist cyclopamine isomerizes to less potent forms when acidified, *J. Pharm. Biomed. Anal.*, **2010**, *52*: 707–713. doi:10.1016/j.jpba.2010.02.017.
- 116) Taipale J, Chen JK, Cooper MK, Wang B, Mann RK, Milenkovic L, Scott MP, Beachy PA. Effects of oncogenic mutations in Smoothed and Patched can be reversed by cyclopamine. *Nature*, **2000**, *406*:1005–1009. doi:10.1038/35023008.
- 117) Turner MW, Cruz R, Elwell J, French J, Mattos J, McDougal OM. Native *V. californicum* alkaloid combinations induce differential inhibition of Sonic Hedgehog signaling. *Molecules* **2018**, *23*:2222 doi: 10.3390/molecules23092222

- 118) Pathi S, Pagan-Westphal S, Baker DP, Garber EA, Rayhorn P, Bumcrot D, Tabin CJ, Blake Pepinsky R, Williams KP. Comparative biological responses to human Sonic, Indian, and Desert hedgehog. *Mech Dev* **2001**, *106*: 107–117. DOI:10.1016/s0925-4773(01)00427-0.
- 119) Oro AE, Higgins KM, Hu Z, Bonifas JM, Epstein EH, Scott MP. Basal Cell Carcinomas in Mice Overexpressing Sonic Hedgehog. *Science*, **1997**, *276*:817–821. DOI:10.1126/science.276.5313.817.
- 120) Lyons TG, O’Kane GM, Kelly CM. Efficacy and safety of vismodegib: a new therapeutic agent in the treatment of basal cell carcinoma. *Expert Opin Drug Saf* **2014**, *13*: 1125–1132. DOI:10.1517/14740338.2014.939952.
- 121) Chang ALS, Oro AE. Initial Assessment of Tumor Regrowth After Vismodegib in Advanced Basal Cell Carcinoma. *Arch. Dermatol* **2012**, *148*: 1324-1325. DOI:10.1001/archdermatol.2012.2354.
- 122) Pricl S, Cortelazzi B, Col, VD, Marson D, Laurini E, Fermeglia M, Licitra L, Pilotti S, Bossi P, Perrone F. Smoothened (SMO) receptor mutations dictate resistance to vismodegib in basal cell carcinoma. *Mol. Oncol* **2014**, *9*:389–397. DOI:10.1016/j.molonc.2014.09.003.
- 123) Yauch RL, Dijkgraaf GJP, Alicke B, Januario T, Ahn CP, Holcomb T, Pujara K, Stinson J, Callahan CA, Tang T, Bazan JF, Kan Z, Seshagiri S, Hann CL, Gould SE, Low JA, Rubin CM, de Sauvage FJ. Smoothened Mutation Confers Resistance to a Hedgehog Pathway Inhibitor in Medulloblastoma. *Science*, **2009**, *326*: 572–574. DOI:10.1126/science.1179386.
- 124) Gao L, Chen F, Li X, Xu S, Huang W, Ye Y. Three new alkaloids from *Veratrum grandiflorum* Loes with inhibition activities on Hedgehog pathway. *Bioorg. Med. Chem. Lett.* **2016**, *26*: 4735–4738. DOI:10.1016/j.bmcl.2016.08.040.
- 125) Khanfar MA, Sayed KAE. The Veratrum alkaloids jervine, veratramine, and their analogues as prostate cancer migration and proliferation inhibitors: biological evaluation and pharmacophore modeling, *Med. Chem. Research*, **2013**, *22*: 4775–4786. DOI:10.1007/s00044-013-0495-6.

- 126) Ma H, Li HQ, Zhang X. Cyclopamine, a Naturally Occurring Alkaloid, and Its Analogues May Find Wide Applications in Cancer Therapy. *Curr. Top. Med. Chem.* **2013**, *13*: 2208–2215. DOI:10.2174/15680266113139990153.
- 127) Ripperger, H. Steroidal alkaloids from roots of *Solanum spirale*. *Phytochemistry* **1996**, *43*:705-707. DOI:10.1016/0031-9422(96)00347-0
- 128) Wilson SR, Strand MF, Krapp A, Rise F, Herstad G, Malterud KE, Krauss S. Hedgehog antagonists cyclopamine and dihydroveratramine can be mistaken for each other in *Veratrum album*. *J. Pharm. Biomed. Anal.*, **2010**, *53*:497–502. DOI:10.1016/j.jpba.2010.05.024.
- 129) Keeler R, Binns W. Teratogenic compounds of *Veratrum californicum* (Durand) III. Malformations of the veratramine-induced type from ingestion of plant or roots. *Proc. Soc. Ex.p Biol. Med.* 1967, *126*: 452–454.
- 130) Turner MW, Rossi M, Campfield V, French J, Hunt E, Wade E, McDougal OM. Steroidal alkaloid variation in *Veratrum californicum* as determined by modern methods of analytical analysis. *Fitoterapia* **2019**, *137*:104281 DOI: 10.1016/j.fitote.2019.104281.
- 131) Binns W, Thacker EJ, Jamers LF, Tuffman WT. A congenital cyclopian-type malformation in lambs. *J Am Vet Med Assoc* **1959**, *134*:180-183.
- 132) Keeler RF. Teratogenic compounds of *Veratrum californicum* (durand)—IV. First isolation of veratramine and alkaloid Q and a reliable method for isolation of cyclopamine. *Phytochem* **1968** *7*:303–306. DOI: 10.1016/s0031-9422(00)86328-1
- 133) Keeler RF, Binns W. Teratogenic compounds of *Veratrum californicum* as a function of plant part, stage, and site of growth. *Phytochem* **1971**, *10*:1765–1769. DOI: 10.1016/s0031-9422(00)86434-1
- 134) Keeler RF . Teratogenic compounds of *Veratrum californicum* (Durand). Structure of muldamine. *Steroids* **1971**, *18*:741–752. DOI:10.1016/0039-128x(71)90033-x
- 135) Echelard Y, Epstein DJ, St-Jacques B, Shen L, Mohler J, McMahon JA, McMahon AP. Sonic hedgehog, a member of a family of putative signaling

- molecules, is implicated in the regulation of CNS polarity. *Cell* **1993**, 75:1417-1430. DOI: 10.1016/0092-8674(93)90627-3
- 136) Krauss S, Concordet J-P, Ingham P. A functionally conserved homolog of the *Drosophila* segment polarity gene *hh* is expressed in tissues with polarizing activity in zebrafish embryos. *Cell* **1993**, 75:1431-1444. DOI: 10.1016/0092-8674(93)90628-4
- 137) Riddle RD, Johnson RL, Laufer E, Tabin C. Sonic hedgehog mediates the polarizing activity of the ZPA. *Cell* **1993**, 75:1401–1416. DOI: 10.1016/0092-8674(93)90626-2
- 138) Lum L, Beachy PA. The Hedgehog response network: sensors, switches, and routers. *Science* **2004**, 304:1755–1759. DOI: 10.1126/science.1098020
- 139) Kasper M, Regl G, Frischauf A-M, Aberger F. GLI transcription factors: Mediators of oncogenic Hedgehog signalling. *European Journal of Cancer* **2006**, 42:437–445. DOI: 10.1016/j.ejca.2005.08.039
- 140) Kiesslich T, Neureiter D. Advances in targeting the Hedgehog signaling pathway in cancer therapy. *Expert Opin Ther Targets* **2012**, 16:151–156. DOI: 10.1517/14728222.2012.652948
- 141) Niehaus TF, Ripper CL, Savage V. “A Field Guide to Southwestern and Texas Wildflowers.” Houghton, Mifflin Company. **1984** Orlando, FL, USA. pp. 10-11.
- 142) Sun Y, White S, Mann D, Adelberg. Photosynthetic characteristics of *Veratrum californicum* in varied greenhouse environments. *J Med Act Plants* **2013**, 20134:134-142 DOI: 10.7275/R5FJ2DQ7
- 143) Augustin MM, Ruzicka DR, Shukla AK, Augustin JM, Starks CM, O’Niel-Johnson M, McKain MR, Evans BS, Barrett MD, Smithson A, Wong GS, Deyholos MK, Edger PP, Pires JC, Leebens-Mack AH, Mann DA, Kutchan TM. Elucidating steroid alkaloid biosynthesis in *Veratrum californicum*: production of verazine in Sf9 cells. *Plant J* **2015**, 82:991–1003. DOI: 10.1111/tpj.12871
- 144) Lee ST, Panter KE, Gardner DR, Green BT, Welch KD, Zhang J, Chang CWT. Development of a monoclonal antibody-based ELISA for the hedgehog inhibitors

cyclopamine and KAAD-cyclopamine. *J Pharm Biomed Anal* **2012**, *66*: 282-286.
DOI: 10.1016/j.jpba.2012.03.043.

- 145) Wang S, Dong G, Sheng C. Structural Simplification of Natural Products. *Chem Rev* **2019**, *119*:4180-4220. DOI: 10.1021/acs.chemrev.8b00504.